Effect of α_2-receptor agonists on the ketamine metabolism in different species assessed by enantioselective capillary electrophoresis

Inauguraldissertation

zur

Erlangung der Würde eines Doktors der Philosophie

vorgelegt der

Philosophisch-Naturwissenschaftlichen Fakultät

der Universität Basel

von

Friederike Andrea Sandbaumhüter

aus Hagen am Teutoburger Wald, Deutschland

Bern, 2017

Genehmigt von der Philosophisch-Naturwissenschaftlichen Fakultät
auf Antrag von

Prof. Dr. Dr. Stephan Krähenbühl
Prof. Dr. Wolfgang Thormann
PD Dr. Manuel Haschke

Basel, den 15. November 2016

Prof. Dr. Jörg Schibler

Dekan

For my parents

and

my sister

Summary

Medication around and during surgery includes a broad range of different drugs. Effects like anesthesia, analgesia, sedation and muscle relaxation are strived. Other drugs can be added in emergency cases or for controlling vital signs like blood pressure or heart rate. Some drugs are able to generate more than one of these effects. For a safe surgery episode, however, polymedication is necessary. On the other hand a lot of side effects and the risk of pharmacokinetic and pharmacodynamic drug drug interactions have to be considered with an increasing number of applied drugs. Most of the pharmacokinetic interactions can be solved by dose adaptation. For that reason it is important to know as much as possible about metabolism, pharmacokinetics and drug drug interactions of the used drugs. In this dissertation the combination of the racemic drug ketamine with anesthetic, analgesic and antidepressive properties and various sedative α_2-receptor agonists was investigated in vitro and in vivo in different species using enantioselective capillary electrophoresis (CE). Enantiomers of ketamine differ in their pharmacologic and toxicologic profiles. The S-enantiomer has a higher affinity towards the N-methyl-d-aspartate-receptor. Both racemic ketamine and S-ketamine are registered as drugs for human and veterinary use.

CE is a high-resolution separation technique that permits the separation and analysis of the stereoisomers of drugs and metabolites in the same run and can thus be used to determine enzyme kinetics, pharmacokinetics and drug drug interactions. In CE a chiral selector like a cyclodextrin is added to the background electrolyte in order to achieve enantioselectivity. Three different assays were developed and/or optimized during this dissertation to describe the interactions between ketamine and the α_2-receptor agonists medetomidine, its active enantiomer dexmedetomidine, detomidine, xylazine and romifidine.

In the first project (Chapter 2) the effect of medetomidine and its active enantiomer dexmedetomidine on the N-demethylation of ketamine to norketamine was analyzed in vitro with canine liver microsomes, human liver microsomes and the single cytochrome P450 enzymes CYP3A12 (canine) and CYP3A4 (human). For CYP3A12 the enzyme kinetics had to be determined first. For racemic ketamine, a substrate inhibition model was found to provide the best fit to the experimental data. For the single ketamine enantiomers, the kinetics could be described with the Michaelis-Menten model. Inhibition of norketamine formation in presence of medetomidine or dexmedetomidine was observed in most of the performed in vitro experiments. The inhibition parameter K_i and IC_{50} were determined for the single

enantiomers of ketamine by using the four-parameter logistic model and the Cheng-Pursoff equation. They are smaller for the formation of R-norketamine.

Decreased norketamine formation under medetomidine comedication was also seen in an in vivo study with Beagle dogs. One group received racemic or single S-ketamine under sevoflurane anesthesia and another after medetomidine sedation. For analyzing the blood samples which were collected between 0 and 900 min after ketamine injection an enantioselective CE microassay was developed and validated (Chapter 3). Besides the advantage that only 50 µL of serum or plasma are needed for analysis it quantifies not only the enantiomers of ketamine and norketamine (as is the case with the assay used in the first project) but also the stereoisomers of 6-hydroxynorketamine (6HNK) and dehydronorketamine (DHNK). Stereoselectivities were detected for 6HNK and DHNK. With the obtained plasma levels the pharmacokinetics of these substances could be described by using two compartment models for ketamine and norketamine enantiomers and single compartment models for 6HNK and DHNK stereoisomers (Chapter 4).

The impact of the four α_2-receptor agonists medetomidine, detomidine, xylazine and romifidine on the ketamine metabolism was assessed in vitro with equine liver microsomes and by calculation of the inhibition parameters for the N-demethylation of ketamine to norketamine (Chapter 5). Veterinarians observed that the recovery quality of horses after anesthesia with ketamine and an α_2-receptor agonist is dependent on the selected α_2-receptor agonist. The four α_2-receptor agonists differ in their activity and selectivity for the α_2-receptor. Medetomidine was found to be the strongest inhibitor, followed by detomidine. The incubation time was extended and 6HNK and DHNK were determined as well. In these experiments the four α_2-receptor agonists exhibited an effect on the formation of all metabolites.

To have a closer look at HNK a new assay was developed which permits the separation of the stereoisomers of four hydroxylated norketamine metabolites and DHNK (Chapter 6). HNK and DHNK stereoisomers are reported to be responsible for antidepressive effects of ketamine. A mixture of sulfated β-cyclodextrin and highly sulfated γ-cyclodextrin was found to be an effective chiral selector for that task. This assay was applied to analyze in vitro and in vivo samples and data obtained revealed differences in the ketamine metabolism of dogs and horses that could hitherto not be assessed.

Abbreviations

ACN	Acetonitrile
AMPA	α-amino-3-hydroxy-5-methyl-4-isoxazolepropionic acid receptor
AUC	Area under the curve
BGE	Background electrolyte
CD	Cyclodextrin
CE	Capillary electrophoresis
c_{max}	Maximal concentration
CL	Clearance
CL_{int}	Internal clearance
CL_{max}	Maximal clearance
CLM	Canine liver microsomes
Conc.	Concentration
CYP	Cytochrome P450
D_0	Drug dose
DHNK	5,6-dehydronorketamine
ELM	Equine liver microsomes
F	Fraction
Fig.	Figure
GC	Gas chromatography
HLM	Human liver microsomes
HK	Hydroxyketamine
HNK	Hydroxynorketamine
HPLC	High-performance liquid chromatography
HS-γ-CD	Highly sulfated γ-cyclodextrin
ID	Inner diameter
IC_{50}	Half maximum inhibition concentration
IST	Internal standard
i.v.	Intravenous
K_a	Autoactivation constant
K_i	Inhibition constant

K_m	Michaelis-Menten constant
LOD	Limit of detection
LOQ	Limit of quantification
mAU	Milli absorbance unit
$MgCl_2$	Magnesium chloride
MRT	Mean residence time
MS	Mass spectroscopy
NADPH	Nicotinamide adenine dinucleotide phosphate
NaOH	Sodium hydroxide
NK	Norketamine
NMDA	N-methyl-d-aspartate
PDA	Photodiode array
psi	Pound per square inch
Rac.	Racemic
Ref.	Reference
rpm	Rounds per minute
R^2	Determination coefficient
RSD	Relative standard deviation
S	Substrate
SD	Standard deviation
S/N	Signal to noise ratio
t_{max}	Time at which maximum concentration is reached
Tris	Tris(hydroxymethyl)-aminomethan
UV	Ultraviolet
$V_{central}$	Volume of central compartment
V_{max}	Maximum reaction velocity
Vss	Distribution volume at steady state
V_{Ti}	Volume of peripher compartment

Table of content

1. Introduction

1.1 Ketamine

The racemic drug ketamine (for chemical structure see Fig. 1) is well-known in human and veterinary medicine. For a long time it was used for anesthesia only. Later the application of ketamine in subanesthetic doses as analgesic and antidepressive drug emerged and it became a drug of abuse [1–5]. Most of its effects are mediated by the N-methyl-d-aspartate (NMDA) receptor. Interactions with opioid, monoaminergic, cholinergic, muscarinic and nicotinic receptors are also reported [1]. Both ketamine enantiomers are active at the NMDA receptor whereas the affinity of the S-enantiomer is four times higher than of the R-form and two times higher than of racemic ketamine [6–8]. Racemic ketamine and the single S-enantiomer are used in human and veterinary medicine. Because of its higher activity S-ketamine can be applied in lower doses which reduces the occurrence of undesired side effects. Not only ketamine itself also its first metabolite, norketamine, which is formed by N-demethylation (Fig. 1) has an affinity to the NMDA receptor [1,9]. R-ketamine showed stronger antidepressive effects than S-ketamine in experiments with mice. Thus, it is assumed that the antidepressive response is independent of NMDA receptor inhibition [9]. For the further metabolites, namely hydroxynorketamine (HNK, Fig. 1) and 5,6-dehydronorketamine (DHNK, Fig. 1), only little effects at the NMDA receptor were found. An inhibition of the α_7-nicotinic acetylcholine receptor was observed instead. Furthermore, 6HNK activates the α-amino-3-hydroxy-5-methyl-4-isoxazolepropionic acid (AMPA) receptor. The interactions at the α_7-nicotinic acetylcholine receptor and AMPA receptor are mainly responsible for the antidepressive effects. At the AMPA receptor (2R,6R)-hydroxynorketamine (RR-6HNK, Fig. 1) is more active than (2S,6S)-hydroxyketamine (SS-6HNK, Fig. 1) [9,10].

Stereoselectivity is not only seen in the receptor affinities of ketamine and its metabolites and thus their effects but also in the metabolism. The metabolism was studied in vivo and in vitro in different species [11–20]. Cytochrome P450 (CYP) enzymes catalyze the metabolic reactions [7,10,11,19,21]. Most members of this enzyme family are located in the liver but they can be found in other tissues as well where the distribution of the isoforms might be different. The first main step is the N-demethylation of ketamine to norketamine. The formation of S-norketamine is dominant. A hydroxylation to hydroxyketamine (HK) is also possible (Fig. 1). Norketamine is hydroxylated very fast to HNK. The hydroxyl group can be added at various positions on the cyclohexanone and the chlorophenyl ring. Hydroxylation at positions 3 to 6 at the cyclohexanone ring leads to a second chiral center in the molecule. Another pathway to HNK is the N-demethylation of HK [7,10,11,19,21]. DHNK is formed via loss of water of 5HNK and/or 6HNK. It is not yet known whether this reaction is also catalyzed by CYP enzymes or occurs by chemical reaction [11,22,23]. DHNK and the hydroxy metabolites were also found in the breath of mice which received ketamine intraperitoneally [24]. Fig. 1 shows the scheme of the ketamine metabolism. In addition to the metabolites presented there, norketamine-N-oxide and other metabolites were mentioned in the literature but not further investigated [11,25–27].

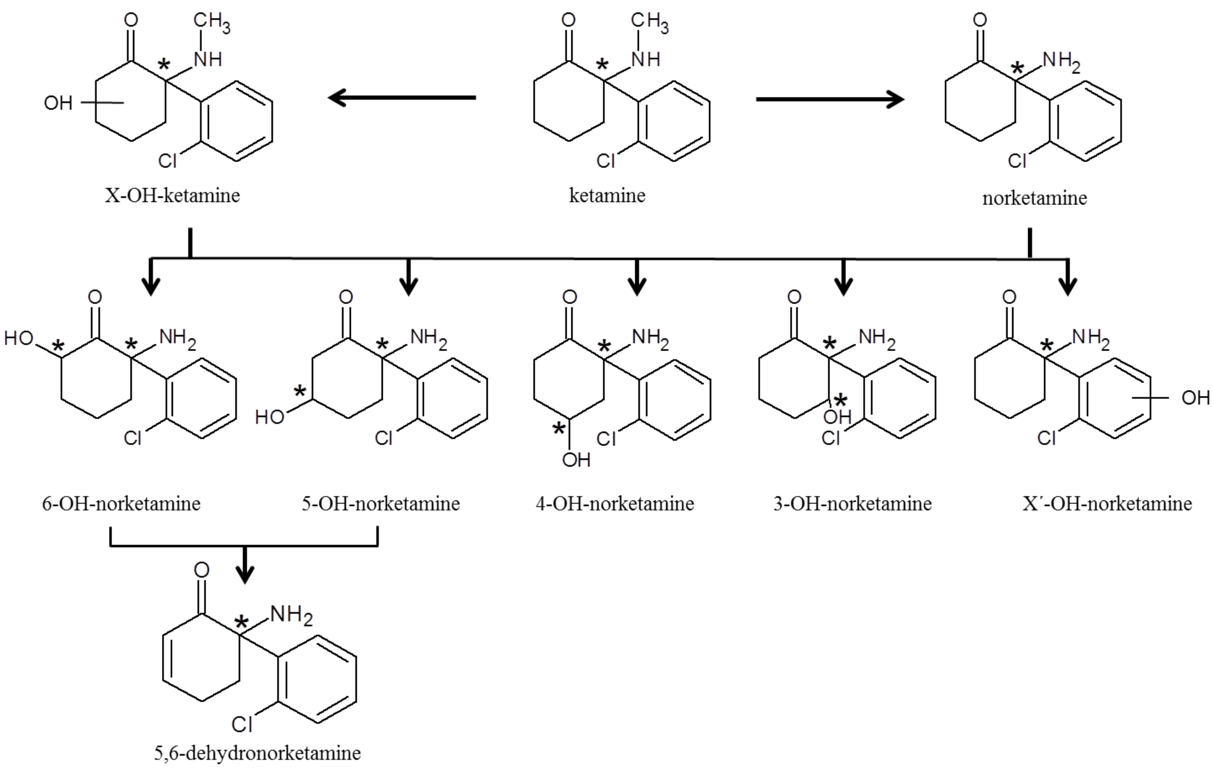

Figure 1: Schematic representation of the main pathways of the ketamine metabolism. Chiral centers are marked with asterisks. X: 3, 4, 5 or 6; X´: 2´, 3´, 4´or 5´.

All described stereoselectivities in pharmacological effects and metabolism hypothesize that also the pharmacokinetics and pharmacodynamics and the interactions with other drugs are affected. In regard to improvement of success and safety in therapy it is important to study the characteristics and the behavior of the enantiomers separately. This requires enantioselective analytical methods for ketamine and its metabolites.

1.2 α_2-receptor agonists

Ketamine is often used in combination with other drugs e. g. α_2-receptor agonists. They can support each other in their therapeutic effects or decrease induced side effects. The risk of pharmacokinetic or pharmacodynamic drug drug interactions increases with the number of applied drugs. Loss of the effect or reaching of toxic concentrations can be the consequence, dependent if inhibitive or inductive interactions take place and if prodrugs are involved. Most of the pharmacokinetic interactions can be solved by dose adaptation. Detailed information about the interactions is necessary to be able to optimize the application of drug combinations.

The first α_2-receptor agonist, clonidine, was developed as an antihypertensive drug for human use. Besides clonidine which is still used, dexmedetomidine, the pharmacologic active enantiomer of medetomidine, brimonidine and tizanidine are registered for human therapy. They can be found as sedatives, anesthesia adjuncts and in the treatment of wide-angle-glaucoma, attention-deficit/hyperactivity disorder and panic disorders [29,30]. The combination with ketamine is only described for dexmedetomidine and is rarely used [31–35].

In contrast, the four sedative α_2-agonists medetomidine, detomidine, xylazine and romifidine which are available in veterinary medicine are all used in daily practice together with ketamine (for chemical structures see Fig. 2). Furthermore, they have anesthetic sparing effects, provide muscle relaxation and show analgesic effects [34]. The combination of ketamine with an α_2-receptor agonist has the advantage of decreasing each other's side effects. Tachycardia, hypertension, salivation and muscular rigidity caused by ketamine are reduced. On the other side ketamine counteracts the risk of bradycardia and hypotension [31–33,37,38]. The α_2-receptor antagonists, atipamezole, tolazoline and yohimbine, are available as reversal agents [29].

The different α_2-recetor agonists differ based on their chemical structures in their selectivity for the α_2-receptor and thus in their sedative and analgesic potency [29,36,39]. Dependent on the selected α_2-receptor agonist in the combination with ketamine veterinarians observe differences in the behavior of horses while recovering after anesthesia [40–43 and observations at the Vetsuisse Zürich].

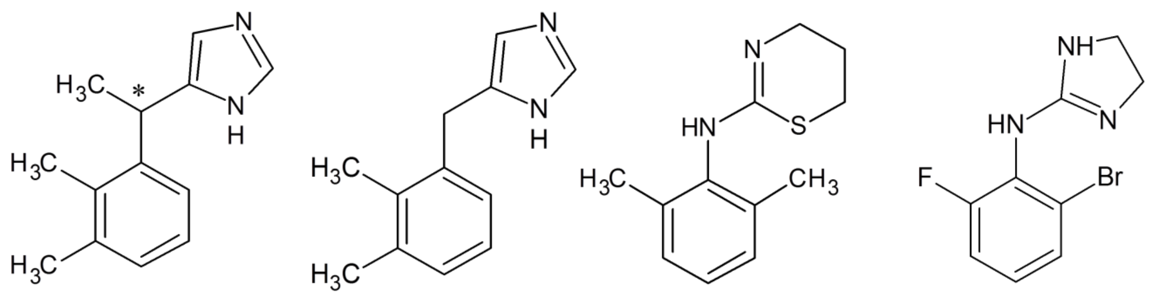

medetomidine detomidine xylazine romifidine

Figure 2: Chemical structures of the α_2-receptor agonists which are used in veterinary practice. The chiral center of medetomidine is marked with an asterisk.

1.3 Enantioselective capillary electrophoresis

Capillary zone electrophoresis (CE) belongs to the family of electrophoretic separation techniques. Charged analytes migrate under the influence of an electric field through a capillary filled with background electrolyte (BGE). The migration velocity of an analyte in the capillary is dependent on the effective electrophoretic mobility of the analyte, the applied electric field and the used BGE. The electrophoretic mobility is determined by charge, size and form of the analyte molecule and also by the characteristics of the background electrolyte (ionic strength, pH, viscosity, presence of buffer additives). In CE, most separations take place in narrow bore fused-silica capillaries with 25 to 75 µm ID. These capillaries typically exhibit a negative surface charge which induces, upon power application, a buffer flow towards the cathode. This flow has a plug profile and its magnitude is dependent on the electric field strength, the pH and composition of the BGE, and is referred to as electroosmotic flow. Detection can be performed on-column with optical (absorbance and fluorescence) or conductivity detectors or at the column end with direct link to ionization and mass spectrometric analysis [44–48]. A schematic representation of a CE instrument is given in Fig. 3.

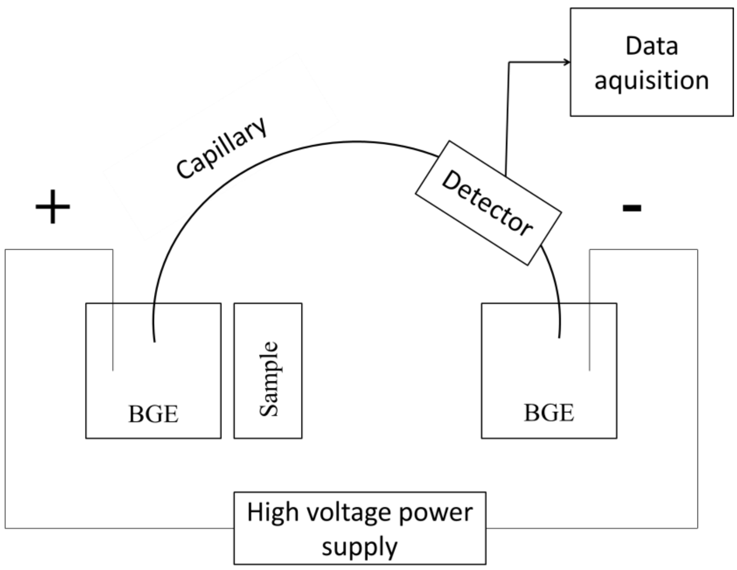

Figure 3: Schematic of a CE instrument

Characteristics of CE are high resolution, short analysis times, robustness and flexibility. Other attractive features are low consumption of chemicals and low costs for capillaries. These aspects paved the way for successful use of CE in chiral analysis. CE has advantages over the chromatographic techniques like HPLC and GC where expensive chiral stationary phases are necessary [53,54]. In order to achieve chiral resolution in CE, small amounts of cyclodextrins, chiral crown ethers, macrocyclic glycopeptide antibiotics, linear oligo- or polysaccharides, proteins or chiral micelle builders are added alone or in combination to the BGE. Different binding affinities of the enantiomers to the chiral selector(s), different migration velocities of the formed complexes and/or differences in migration velocities between the unbound enantiomer and complex induce chiral separation. The separation system can be optimized and adjusted by change of type and concentration of the chiral selector and of the composition of the BGE (pH, ionic strength, additional additives) [44–54].

Enantiomers can strongly differ in their pharmacologic, toxicologic or pharmacokinetic characteristics. Thus, chiral analysis is a crucial part in drug development and quality control, for determination of enantiomeric characteristics and purity. CE is an established and attractive technique for analysis of chiral pharmaceuticals and their metabolites in in vitro, in vivo and environmental samples [49–54]. Chiral CE is listed in the pharmacopoeia europea e. g. for determination of enantiomeric purity for ropivacaine and galantamine and was used in our laboratory for analysis of ketamine and metabolites [11–20,55]. The data presented in this dissertation were obtained with three enantioselective CE-based assays that were developed and optimized for that work [17,20,56, Chapter 6]. Examples of electropherograms which illustrate the high resolution obtained for the stereoisomers of ketamine and metabolites in one run are shown in Fig 4.

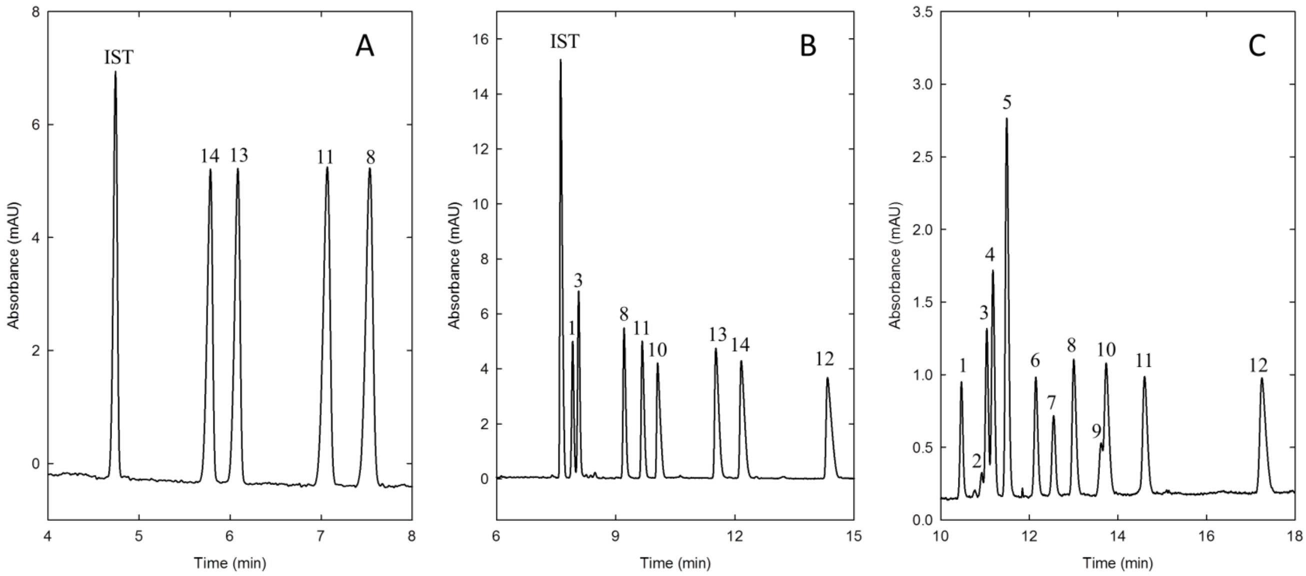

Figure 4: Electropherograms of ketamine and its metabolites obtained with three different CE-based methods. (A) Standards of ketamine and norketamine (2.38 µg/mL/enantiomer) were analyzed with 2 % γ-cyclodextrin as chiral selector (Chapter 2). (B) Standards of 0.01 µg/mL of enantiomer of ketamine, norketamine, 6HNK and DHNK were analyzed with the microassay using 0.66 % highly sulfated γ-cyclodextrin as chiral selector (Chapter 3). (C) A mixture of norketamine, DHNK and four urine fractions of hydroxylated norketamine metabolites were analyzed with an assay based on 5 mg/mL sulfated β-cyclodextrin and 0.1 % highly sulfated γ-cyclodextrin as chiral selector (Chapter 6). Key: 1: RR-6HNK, 2: R-II, 3: SS-6HNK, 4: R-IV, 5: S-II, 6: R-III, 7: S-IV, 8: R-NK, 9: S-III, 10: S-DHNK, 11: S-NK, 12: R-DHNK, 13: R-ketamine, 14: S-ketamine, IST: internal standard lamotrigine (A) and d-(+)-norephedrine (B), respectively.

The importance of in vitro experiments in all stages of drug development is increasing. Interactions with other substances or pharmacokinetics can be predicted. Two enzyme assay modes based on CE are possible. In off-line assays the incubation is performed in a vial and the educts and/or products are analyzed thereafter with CE. In the on-line mode incubation of reactants and the analysis takes place in the capillary. This provides the use of the on-line approach in fully automated high throughput screening systems [57].

1.4 Pharmacokinetic modeling

Pharmacokinetics describe the concentration of a drug as function of time. A drug undergoes the phases of liberation, absorption, distribution, metabolism and elimination. The behavior in all these phases and the resulting concentration levels are important for an effective and safe use. Pharmacokinetics can be analyzed by using non-compartmental or compartmental models. Calculation of pharmacokinetic parameters provides a mean to compare drugs and situations. Modeling requires drug concentrations in the blood from administration until excretion. Enough data points in all parts and especially in the critical parts of the kinetics are inalienable for meaningful results. The concentrations are plotted against the time. The profile gives first information about the behavior and the model which describes the kinetic best. There are one, two or multicompartment models dependent on the distribution between well-perfused and fatty tissues [58–60]. Besides the manual way for calculation of the parameters it is also possible to estimate them with special software packages. In this dissertation the Phoenix WinNonlin 6.4 software was used. On the basis of the input parameters and the chosen pharmacokinetic model the curve and the parameters are calculated [17]. For making conclusions about the relationship between drug concentration and effect also pharmacodynamic data must be considered.

1.5 Goals of the dissertation

The goals of this dissertation were i) to develop analytical methods based on enantioselective capillary electrophoresis to analyze ketamine metabolites in a qualitative and quantitative way on ppb to ppm concentration levels, ii) to assess the stereoselectivity of metabolic pathways of ketamine, and iii) to investigate the influence of the α_2-receptor agonists medetomidine, dexmedetomidine, detomidine, xylazine and romifidine on the formation and elimination of the ketamine metabolites norketamine, 6HNK and DHNK in vitro and in vivo in different species.

Three different enantioselective CE-based assays were developed, optimized and validated (Fig. 4). Sulfated cyclodextrins were chosen as the chiral selector. In contrast to existing methods two of the assays provide not only the qualitative and/or quantitative analysis of ketamine and norketamine enantiomers but also of the stereoisomers of DHNK and different hydroxylated norketamine metabolites, including RR- and SS-6HNK (Fig. 4B and 4C). Furthermore, the aims in method development were to decrease detection and quantification limits and to reduce the amounts of sample and reagents needed for analysis. All assays are based on liquid/liquid extraction of the analytes from the biological matrix prior to analysis of the reconstituted extracts by CE. Details about the assays are given in chapters 2, 3 and 6.

The methods were used to investigate the effects of different α_2-receptor agonists on the ketamine metabolism. Starting with in vitro experiments with human and canine liver microsomes and single CYP enzymes (CYP3A4 and CYP3A12, respectively) the influence of racemic medetomidine was contrasted with the impact of its active enantiomer dexmedetomidine on the N-demethylation of ketamine to norketamine. Inhibition parameters K_i and IC_{50} were determined for the cases with single ketamine enantiomers as substrates in order to compare the effect of interactions. In vitro data are presented in chapter 2.

The in vitro results could be confirmed with blood samples of Beagle dogs which received ketamine under sevoflurane anesthesia or after medetomidine sedation. Pharmacokinetics of ketamine, norketamine, 6HNK and DHNK were elucidated. The data obtained represent the first study with inclusion of 6HNK and DHNK in a pharmacokinetic model. This part of the dissertation offered the opportunity to study pharmacokinetic modeling manually and by using Phoenix WinNonlin 6.4 software. Details about the modeling and the obtained data are described in chapter 4.

Besides medetomidine also detomidine, xylazine and romifidine are used in combination with ketamine in veterinary medicine. The goal of an in vitro study with equine liver microsomes was to compare the effect of all the four α_2-receptor agonists on ketamine metabolism via calculation of the inhibition parameters in order to find evidence for the clinical observations. In practice differences in the behavior of horses while recovering after anesthesia are observed which are dependent on the α_2-receptor agonist used. Data obtained are presented in chapter 5.

Furthermore, with the development of an assay for separation and analysis of the stereoisomers of four hydroxylated norketamine metabolites, differences in the hydroxylation of norketamine between equines and canines could be elucidated. Details of the assay and first results are presented in chapter 6.

Assay developments and analyses of all samples were executed in the Clinical Pharmacology Laboratory of the Institute for Infectious Diseases, University of Bern, Bern, Switzerland. All samples of dogs and horses analyzed in this dissertation stemmed from studies undertaken in the group of Prof. Regula Bettschart-Wolfensberger at Vetsuisse Faculty Zürich, Zürich, Switzerland. The experiments with animals were executed with the permission of the Committee for Animal Experimentation of Canton Zürich, Zürich, Switzerland.

2. Effects of medetomidine and its active enantiomer dexmedetomidine on N-demethylation of ketamine in canines determined in vitro using enantioselective capillary electrophoresis (Electrophoresis 36 (2015) 2703-2712)

Friederike A. Sandbaumhüter[1], Regula Theurillat[1], Wolfgang Thormann[1]

[1] Clinical Pharmacology Laboratory, University of Bern, Bern, Switzerland

2.1 Abstract

Cytochrome P450 (CYP) enzymes catalyze the metabolism of both, the analgesic and anesthetic drug ketamine and the α_2-adrenergic receptor-agonist medetomidine which is used for sedation and analgesia. As racemic medetomidine or its active enantiomer dexmedetomidine are often coadministered with racemic or S-ketamine in animals and dexmedetomidine together with S- or racemic ketamine in humans, drug drug interactions are likely to occur and have to be characterized. Enantioselective CE with highly sulfated γ-cyclodextrin as chiral selector was employed for analyzing in vitro (i) the kinetics of the N-demethylation of ketamine mediated by canine CYP3A12 and (ii) interactions occurring with racemic medetomidine and dexmedetomidine during coincubation with ketamine and canine liver microsomes (CLM), canine CYP3A12, human liver microsomes (HLM) and human CYP3A4. For CYP3A12 without an inhibitor, Michaelis-Menten kinetics was determined for the single enantiomers of ketamine and substrate inhibition kinetics for racemic ketamine. Racemic medetomidine and dexmedetomidine showed an inhibition of the N-demethylation reaction in the studied canine enzyme systems. Racemic medetomidine is the stronger inhibitor for CLM, whereas there is no difference for CYP3A12. For CLM and CYP3A12, the inhibition of dexmedetomidine is stronger for the R- compared to the S-enantiomer of ketamine, a stereoselectivity which is not observed for CYP3A4. Induction is observed at a low dexmedetomidine concentration with CYP3A4 but not with CYP3A12, CLM and HLM. Based on these results, S-ketamine combined with dexmedetomidine should be the best option for canines. The enantioselective CE assay with highly sulfated γ-cyclodextrin as chiral

selector is an effective tool for determining kinetic and inhibition parameters of metabolic pathways.

2.2 Introduction

Multiple drug therapy is common in practice. The combination of the effects of the co-administrated drugs is often connected with pharmacokinetic and/or pharmacodynamic interactions, which lead to a decrease or increase of both the desired effect and the toxicity. The enzymes of the cytochrome P450 (CYP) family, which are mostly located in the liver, are involved in most of the pharmacokinetic interactions. To benefit from the advantages of drug combinations, it is important to have detailed information about the metabolic steps because many pharmacokinetic problems can be solved by dose adaptation. The combination of ketamine and medetomidine (both are chiral compounds, for chemical structures see Fig. 1) is well-known in veterinary medicine. Ketamine is a N-methyl-d-aspartate (NMDA) receptor antagonist with anesthetic, analgesic and in lower concentrations antidepressive effects [1–4]. In addition, ketamine reacts also with opioid, monoaminergic, cholinergic, nicotinergic and muscarinergic receptors [2]. The affinity of the S-enantiomer to the NMDA receptor is two times higher than that of racemic ketamine and four times higher than that of the R-enantiomer [5–7]. Medetomidine is an α_2-adrenergic receptor agonist used for sedation and anesthetic premedication and, because of its anesthetic-sparing effect, it is applied as anesthetic adjuvant [8–15]. Low analgesic and myorelaxation effects have also been observed [10,11]. The S-enantiomer, dexmedetomidine, is the pharmacologically active enantiomer of medetomidine whereas the R-enantiomer, levomedetomidine, is considered to be pharmacologically inactive but is involved in kinetic drug interactions, including the prolongation of the hepatic metabolism of ketamine [10]. Medetomidine and ketamine compensate each other’s side effects. Medetomidine reduces the risk of tachycardia, hypertension and salivation conditioned by ketamine and ketamine decreases the side effects of medetomidine like bradycardia and hypotension [12,13]. Racemic ketamine, S-ketamine and dexmedetomidine are also used in humans. The combination of them is not as popular as for animals, but there are examples described in the literature [10–14].

The main step of the ketamine metabolism is the N-demethylation to the active metabolite norketamine. This pathway is catalyzed by several CYP enzymes and some of these enzymes mediate also other metabolic steps, including hydroxylation of the cyclohexanone ring of ketamine and norketamine [5,6,15–22]. CYP enzymes are also responsible for the metabolism of medetomidine with hydroxylation to hydroxymedetomidine being the main pathway [11]. Thus, coadministration of the two drugs results in a competition for the active sites of the CYP enzymes. Because of this and the fact that medetomidine is able to bind as an imidazole derivate to the heme iron of CYP, what has a negative impact on the CYP enzyme activity, drug drug interactions are likely to occur [10]. In previous work from our laboratory, the N-demethylation pathway of ketamine and hydroxylation of norketamine were studied for different animal species in vivo and in vitro using enantioselective capillary electrophoresis with sulfated β-cyclodextrin as chiral selector [18–20,22–26]. In addition, the role of selected single human CYP enzymes in the ketamine metabolism was studied in vitro [16,27]. As the employed chiral selector showed significant undesired lot-to-lot differences, sulfated β-cyclodextrin was later substituted with highly sulfated γ-cyclodextrin and this selector was applied to the elucidation of the in vitro CYP3A4-catalyzed N-demethylation kinetics of ketamine to norketamine and its inhibition in the presence of ketoconazole [27]. Furthermore, highly sulfated γ-cyclodextrin was successfully employed for the characterization of the kinetics of this pathway in two different on-line capillary formats [28,29].

Ketamine is often coadministered with medetomidine to domestic dogs undergoing anesthesia for surgery [12]. Pharmacokinetics and clinical effects of ketamine [25,30] and medetomidine [31] have been investigated but, to our knowledge, not with coadministration of the two drugs. Furthermore, in vitro investigations with ketamine in presence of canine liver microsomes (CLM) in absence [22] and presence of various inhibitors [19,24] were conducted. The effect of medetomidine on the ketamine metabolism, however, was not studied. The work of Duhamel et al. with CLM revealed that the ortholog of the human CYP3A4, namely CYP3A12 is involved in the metabolism of medetomidine [11] and studies describing the metabolism/pharmacokinetics of ketamine or medetomidine in presence of single canine CYP3A12 were not found in the scientific literature. Thus, the effect of medetomidine on the N-demethylation of ketamine in vitro was studied with an assay based on enantioselective capillary electrophoresis employing highly sulfated γ-cyclodextrin as chiral selector.

The goals of this work were (i) to present the specifications of the assay with highly sulfated γ-cyclodextrin, (ii) to describe the kinetics of the ketamine N-demethylation mediated by canine CYP3A12, (iii) to analyze the effect of racemic medetomidine and dexmedetomidine on the N-demethylation of racemic ketamine, S-ketamine and R-ketamine catalyzed by CLM, canine CYP3A12, human liver microsomes (HLM) and human CYP3A4, and (iv) to determine the inhibition constants for the interaction of S-and R-ketamine with dexmedetomidine for CLM and canine CYP3A12.

2.3 Material and Methods

2.3.1 Chemicals and reagents

Ketamine and norketamine (as hydrochlorides in methanol, 1 mg/mL of the free base) were from Cerilliant (Round Rock, TX, USA) and the single ketamine enantiomers were provided from CU Chemie Uetikon (Lahr, Germany). Lamotrigine was from The Welcome Foundation (London, UK), medetomidine hydrochloride and dexmedetomidine hydrochloride were from Tocris Bioscience, R&D Systems Europe (Abingdon, UK), and highly sulfated γ-cyclodextrin (20 % *w/v* solution) was from Beckman Coulter (Fullerton, CA, USA). Tris and sodium hydroxide were from Merck (Darmstadt, Germany) and potassium dihydrogen phosphate, di-potassium hydrogen phosphate, methanol and phosphoric acid (85 %) were from Fluka (Buchs, Switzerland). Ethylacetate was from AppliChem (Darmstadt, Germany), dichloromethane was from VWR (Leuven, Belgium) and human albumin was from Behringwerke (Marburg, Germany). Canine CYP3A12 (Beagle) + P450 reductase + cytochrome b_5 SUPERSOMES™, human CYP3A4 + P450 reductase + cytochrome b_5 SUPERSOMES™, pooled male CLM (beagle), pooled HLM and nicotinamide adenine dinucleotide phosphate (NADPH) regenerating system solutions A and B were from Corning (product of Gentest, Woburn, MA, USA).

2.3.2 In vitro reaction for kinetic study

After preincubation (3 min; 37 °C) of racemic ketamine, S- or R-ketamine in ten different concentrations ranging from 2.5 to 500 µM per enantiomer with NADPH regenerating system consisting of 1.49 mM $NADP^+$, 3.2 mM glucose-6-phosphate, 0.4 U/mL glucose-6-phosphate dehydrogenase, 2.9 mM $MgCl_2$ and 50 µM sodium citrate in 100 mM potassium phosphate buffer (pH 7.4), the reaction was started by adding 24 pmol CYP3A12 per mL to a final volume of 200 µL. The reaction was stopped after 8 min with 50 µL 2 M NaOH and lamotrigine (2 µg/mL) was added as internal standard prior to extraction. All experiments were performed in duplicates.

2.3.3 In vitro reaction for inhibition study

Different substrates (S-ketamine, R-ketamine, racemic ketamine, 60 µM per enantiomer) were preincubated with NADPH regenerating system (as described in Section 2.2) in 100 mM pH 7.4 potassium phosphate buffer and dexmedetomidine or racemic medetomidine in different concentrations (0, 0.075, 0.15, 0.3, 0.6, 0.9 µM per enantiomer) for 3 min at 37 °C. The incubation was started by adding CLM, HLM (both 0.5 mg protein/ mL), CYP 3A12 or CYP3A4 (both 25 pmol CYP/mL), to a final volume of 200 µL. The reaction was stopped after 8 min by adding 50 µL 2 M NaOH and lamotrigine (2 µg/mL) was added prior to extraction. All experiments were performed in duplicates.

2.3.4 Sample preparation

For the liquid/liquid extraction, 1500 µL of ethylacetate/dichloromethane (25:75 %, *v/v*) was added to the sample. The tubes were closed, shaken for 10 min and centrifuged at 12000 rpm for 5 min. After removing the upper aqueous phase, the organic phase was transferred to a new vial. The organic phase was acidified with 10 µL of 50 mM phosphoric acid to avoid the loss of analytes during evaporation, dried under a stream of air at 37 °C, reconstituted in 150 µL methanol, vortexed and transferred in another vial. After evaporation, the residues were reconstituted in 30 µL of 17.8 mM Tris-phosphate buffer (pH 2.5).

2.3.5 CE instrumentation and analytical conditions

A Proteome Lab PA 800 instrument (Beckman Coulter, Fullerton, CA, USA) equipped with a 50 µm i.d. fused-silica capillary (Polymicro Technologies, Phoenix, AZ, USA) of 45 cm total length (effective length 36 cm) was used. Samples were injected from 0.5 mL polypropylene vials by applying a vacuum of 1 psi for 5 s. A voltage of -20 kV (reversed polarity) was applied. The current was about -68 µA. For inducing a buffer flow towards the anode a positive pressure of 0.2 psi was applied during the entire experiment. Sample storage and capillary cartridge temperatures were set to 20 °C. Analyte detection took place with an on-column UV variable wavelength detector at 195 nm. The running buffer was composed of 17.8 mM Tris, phosphoric acid (pH 2.5) and 2 % highly sulfated γ-cyclodextrin. Fresh running buffer was prepared every day. Before each experiment, the capillary was sequentially rinsed with 0.1 M NaOH (1 min; 20 psi), bidistilled water (1 min; 20 psi) and running buffer (1 min; 20 psi). Quantification of ketamine and norketamine enantiomers was based on an internal calibration using corrected peak areas. Six calibrators with ketamine and norketamine in concentrations between 0.5 and 30 µM of each enantiomer and 3 independent controls containing 1.25, 12.5 and 25 µM of each enantiomer were prepared in human albumin solution (1.0 mg/mL) and, after addition of the internal standard, extracted as described in Section 2.4.

2.3.6 Data analysis

Kinetic and inhibition data were evaluated with SigmaPlot software version 12.5 (Systat Software, San Jose, CA, USA). Statistic tests like paired Student’s t-test and F-test were done with Microsoft Excel (Microsoft, Redmont, WA, USA). With the F-test the fit of various kinetic models for describing the data was tested. The alternative model was accepted, if $p < 0.05$. A p-value < 0.05 in the paired Student’s t-test declared a significant difference of two data sets.

2.4 Results and discussion

2.4.1 Assay characterization

The assay conditions for determination of the enantiomers of ketamine and norketamine were optimized and validated and are based on those described by Portmann et al. [16], Schmitz et

al. [22] and Kwan et al. [27]. The use of highly sulfated γ-cyclodextrin required adaptions, including the change of the internal standard to lamotrigine. Another improvement was the reduction of the final volume of the incubation preparation to 200 µL which has the advantage of employing lower amounts of reagents needed for extraction. Furthermore, the time for sample preparation became shorter because smaller volumes need less time for evaporation. A typical electropherogram with the enantiomers of ketamine, norketamine and medetomidine is shown in Fig. 1A and data obtained after incubation of 60 µM racemic ketamine with CLM without the inhibitor and with 0.3 µM dexmedetomidine are presented in Figs. 1B and 1C, respectively. For assay calibration six calibrators with racemic ketamine and racemic norketamine in concentrations between 0.5 and 30 µM per enantiomer and the internal standard lamotrigine were prepared in human albumin solution (1.0 mg/mL) and extracted as described in Section 2.4. The calibration curves (n=6) were found to be linear with a mean value of the determination coefficient R^2 of 0.9996 for all four compounds (RSD range: 0.031 to 0.046 %) and the RSD values of the slopes ranged between 2.00 and 2.62 %. All mean intercept values were significantly smaller than the responses of the lowest calibrators. For each enantiomer of ketamine and norketamine, the LOQ with a signal/noise ratio of 1/10 was 0.5 µM and the LOD with a signal/noise ratio of 1/3 was 0.2 µM.
Assay control was performed with three independent control samples containing 1.25, 12.50 and 25.00 µM of each ketamine and norketamine enantiomer. The interday and intraday repeatability was analyzed with these control samples. Intraday RSD values (n=6) for the expected amounts were between 1.15 and 5.49 % and for the interday data (n=6) between 1.76 and 6.43 % (Table 1). There is no significant difference between the intraday and interday values, what shows a good repeatability of the method. The recovery was measured in triplicates by using the lowest control sample. For all ketamine and norketamine enantiomers and lamotrigine, recoveries were between 77 and 82 %. This is in agreement with previous data from our laboratory [22,23]. In this assay, the enantiomers of medetomidine appeared between 3 and 4 min and thus did not interfere with the migration of ketamine, norketamine and lamotrigine (Fig. 1A).

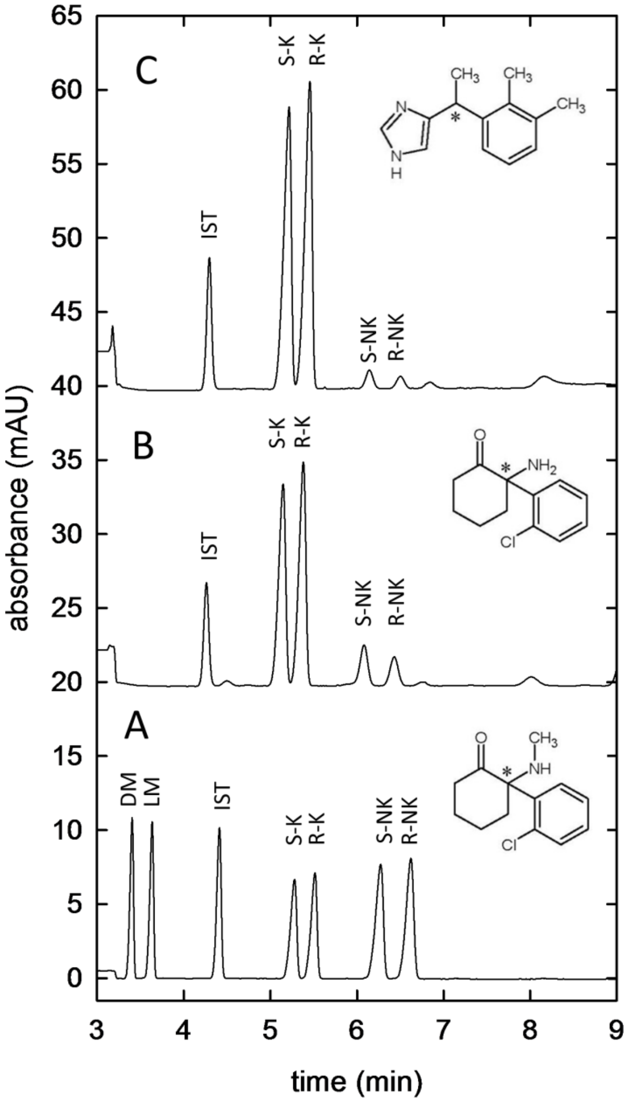

Figure 1. Typical electropherograms of extracts obtained with samples comprising (A) racemic ketamine, norketamine and medetomidine (30 µM each) and human albumin (1.0 mg/mL), (B) 60 µM racemic ketamine incubated with CLM for 8 min, and (C) 60 µM racemic ketamine and 0.3 µM dexmedetomidine incubated with CLM for 8 min. Extraction and CE conditions as described in Sections 2.4 and 2.5, respectively. Data are presented with a y-scale shift of 20 mAU. The inserts in panels A-C depict the chemical structures of ketamine, norketamine and medetomidine, respectively, with asterisks marking the chiral centers. Key: IST: internal standard lamotrigine, S-K: S-ketamine, R-K: R-ketamine, S-NK: S-norketamine, R-NK: R-norketamine, DM: dexmedetomidine, LM: levomedetomidine.

Table 1. Intraday and interday data

Enantiomer	Concentration level (µM)	Intraday data a)		Interday data a)	
		Mean (µM)	RSD (%)	Mean (µM)	RSD (%)
S-ketamine	25.00	24.86	1.15	24.74	2.23
	12.50	12.53	2.50	12.81	2.71
	1.25	1.25	5.49	1.26	3.89
R-ketamine	25.00	24.85	1.33	24.74	1.90
	12.50	12.57	2.63	12.75	2.64
	1.25	1.28	4.05	1.28	5.49
S-norketamine	25.00	23.80	4.74	24.21	2.22
	12.50	12.19	3.59	12.49	3.23
	1.25	1.18	3.06	1.23	5.63
R-norketamine	25.00	23.85	4.57	24.34	1.76
	12.50	12.24	3.43	12.62	2.09
	1.25	1.24	2.60	1.28	6.43

a) Data are based on 6 determinations.

2.4.2 Kinetic study with CYP3A12

The role of different CYP enzymes in the ketamine metabolism was characterized in previous studies [16–23,27]. In analogy to the work with human CYP3A4 [16,24], the focus was on canine CYP3A12 which was previously only used in the qualitative inhibition study of Moessner et al. [24] and in preliminary efforts with ketoconazole and 1-aminobenzotriazole which were both found to be effective inhibitors of its norketamine formation in vitro (unpublished data from our laboratory). Various amounts of racemic ketamine, S-ketamine or R-ketamine were incubated as substrates together with CYP3A12 for 8 min and, after extraction, analyzed with the CE assay. The formation rates of norketamine were plotted against the substrate concentrations and analyzed with different models (Figure 2). For incubation of single enantiomers separately, the formation rates increased and levelled off at a maximum value, i.e. the reaction velocity V_{max} (Fig. 2A). Graphs through the data points were fitted by using nonlinear regression analysis based on the Michaelis-Menten model ($v = (V_{max}\,[S]) / (K_m+[S])$) and the Hill model ($v = (V_{max}\,[S]^n) / (K_a^n+[S]^n)$) and obtained data are presented in Table 2.

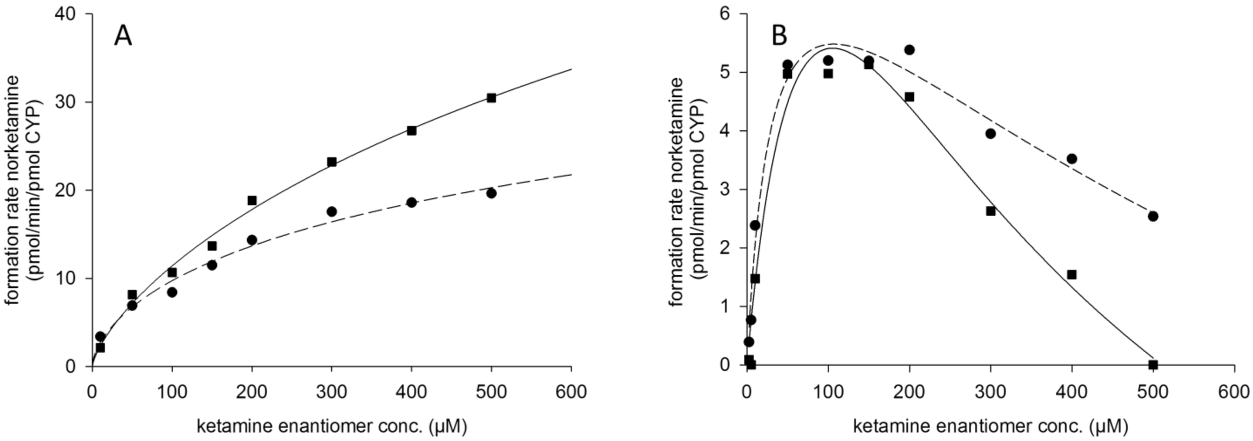

Figure 2. Kinetic data of CYP3A12 catalyzed N-demethylation for incubation of (A) S- and R-ketamine alone and (B) racemic ketamine. The graphs for S-norketamine (filled squares as data points, solid line) and R-norketamine (filled circles as data points, dashed line) represent those obtained with (A) the Michaelis-Menten model and (B) the two-site competition model. All data points are mean of duplicates and line graphs were obtained with consideration of the mean values.

The Michaelis-Menten constant K_m is the substrate concentration at which the reaction velocity is 0.5 V_{max} and it is a measure for the affinity between substrate and enzyme. A small K_m value stands for a high affinity. The autoactivation constant K_a would be equal to K_m, if the Hill coefficient n is 1. Furthermore, the clearance was calculated according to the equation for intrinsic clearance ($CL_{int} = V_{max} / K_m$) and for maximal clearance in consideration to the activation ($CL_{max} = (V_{max} / K_a)\,[|(n - 1)| / n \times (|n -1|)^{1/n}]$) as was the case with CYP3A4 [27]. The calculated values are listed in Table 2. All previously studied enzymes which catalyze the N-demethylation of ketamine followed one of the two kinetic models [16,22,27]. For CYP3A12, with regard to the determination constant R^2 and the result of the F-Test ($p \geq 0.05$) the Michaelis-Menten model was found to be superior for both enantiomers (Table 2). Analysis of the data with the paired Student's t-test revealed a significant difference in the two norketamine formation rates ($p < 0.05$). The formation rate of S-norketamine was found to be higher compared to that of R-norketamine, a result which is in agreement with the data obtained with the human ortholog enzyme CYP3A4 [27]. The same relationship was found to be true for K_m. No difference was noted for the clearance (Table 2). Compared to human CYP3A4, the affinity of the ketamine enantiomers to CYP3A12 was found to be somewhat lower.

Table 2. Kinetic parameters for the CYP3A12 mediated N-demethylation reaction of single ketamine enantiomers[a)]

Model	Parameter	S-ketamine	R-ketamine
Michaelis-Menten	V_{max} (pmol/min/pmol CYP)	52.55 ± 1.91	28.95 ± 2.19
	K_m (µM)	375.4 ± 36.9	188.1 ± 26.5
	R^2	0.994 ± 0.002	0.981 ± 0.004
	Cl_{int} (µL/min/pmol CYP)	0.14 ± 0.01	0.15 ± 0.01
Hill	V_{max} (pmol/min/pmol CYP)	74.20 ± 5.37	32.00 ± 1.27
	K_a (µM)	713.5 ± 31.0	240.2 ± 33.5
	n	0.74 ± 0.14	0.90 ± 0.11
	R^2	0.990 ± 0.009	0.969 ± 0.006
	Cl_{max} (µL/min/pmol CYP)	0.23 ± 0.09	0.19 ± 0.04

a) Data represent mean values ± SD and were obtained with separate incubations of the two enantiomers of ketamine

With incubation of racemic ketamine, a different behavior was observed. For both enantiomers, the norketamine formation rate reached a maximum at a concentration of around 100 µM and decreased continuously with further increase of the substrate concentration (Fig. 2B). There is an inhibition effect on the formation of S- and R-norketamine, which is provoked by the substrate itself. Such data cannot be described by the Michaelis-Menten model or the Hill equation. The data were evaluated with the substrate inhibition model ($v = V_{max} / (1 + K_m / [S] + [S] / K_i)$) and the two-site competition model ($v = (V_{max} ([S] + (\beta[S]^2) / \alpha K_i)) / (K_m + [S](1+K_m/K_i) + [S]^2/\beta K_i)$) [32-36]. These models include an inhibition effect of the substrate at higher concentrations. The inhibition constant K_i describes the affinity between the inhibitor and the enzyme. The two-site competition model considers that a second substrate molecule is able to bind simultaneously at the active site or at a second binding site of the enzyme which is described as a nonproductive or inhibitory site. After binding a second substrate a complex with different kinetic characteristics is developed. The factor α in the equation describes the change in the dissociation in the reaction equilibrium. The rate of metabolism is reduced by the factor β which is a measure for the potency of the inhibition [32–36]. The calculated parameters are presented in Table 3.

Table 3. Kinetic parameters for the CYP3A12 mediated N-demethylation of racemic ketamine [a)]

Model	Parameter	S-ketamine	R-ketamine
Substrate inhibition model	V_{max} (pmol/min/pmol CYP)	540.2 ± 70.6	11.19 ± 2.24
$v = \frac{V_{max}}{1 + \frac{K_m}{[S]} + \frac{[S]}{K_i}}$	K_m (µM)	3825 ± 302	46.24 ± 16.91
	K_i (µM)	1.69 ± 0.30	206.16 ± 32.08
	R^2	0.9315 ± 0.0205	0.9675 ± 0.0078
Two-site competition model	V_{max} (pmol/min/pmol CYP)	25.60 ± 3.47	9.04 ± 1.05
$v = \frac{V_{max} ([S] + \frac{\beta[S]^2}{\alpha K_i})}{K_m + [S]\left(1 + \frac{K_m}{K_i}\right) + \frac{[S]^2}{\beta K_i}}$	K_m (µM)	158.7 ± 52.9	32.85 ± 8.30
	K_i (µM)	287.6 ± 42.0	1010 ± 49
	α	-1.48 ± 0.14	-0.83 ± 0.06
	β	0.82 ± 0.25	0.85 ± 0.01
	R^2	0.9714 ± 0.0002	0.9474 ± 0.0052

a) Data represent mean values ± SD and were obtained with separate incubations of racemic ketamine

The two-site competition model with its highest coefficient of determination R^2 showed the best fits for both enantiomers. Stereoselectivity for the formation rate was also found by using the paired Student's t-test ($p < 0.05$). The stronger substrate inhibition was detected for S-ketamine. It is interesting to note that corresponding data obtained with the human ortholog CYP3A4 revealed Michaelis-Menten kinetics [27]. Data from previous experiments with CLM and racemic ketamine, S-ketamine and R-ketamine as substrates in concentrations up to 1000 µM per enantiomer could be evaluated with the Michaelis-Menten or the Hill model [22]. For the single canine CYP3A12 the same is true for S- and R-ketamine as substrates. With racemic ketamine, however, a substrate inhibition was detected. Comparing the determined kinetic parameters K_m and V_{max} for CYP3A12 with those reported for CLM in [22], it was found that the values for S-ketamine were higher compared to those obtained for R-ketamine for all investigated cases.

2.4.3 Interaction with medetomidine and dexmedetomidine

In veterinary medicine the combination of ketamine and racemic medetomidine or dexmedetomidine is often used. There are also some applications for humans. Dexmedetomidine is the enantiomer of medetomidine with higher pharmacological activity. Although levomedetomidine shows no sedative effect, it plays a role in interaction with the CYP enzymes [10]. The effects of racemic medetomidine and dexmedetomidine on the N-demethylation of ketamine were analyzed for CLM, HLM, canine CYP3A12 and human CYP3A4. The substrate ketamine was added in its racemic form and as single enantiomers in a concentration of 60 µM per enantiomer. The formation rate of S- and R-norketamine without racemic medetomidine and dexmedetomidine and with five different inhibitor concentrations (up to 0.9 µM per enantiomer, which correspond to blood levels attained for sedation and analgesia in canines [31]) was determined with an incubation time of 8 min as described in Section 2.3. The formation rate without inhibitor was set as 100 % and results were expressed in relation to this value. Both, racemic medetomidine and dexmedetomidine were found to inhibit the N-demethylation of ketamine catalyzed by CLM and canine CYP3A12 (Fig. 3). At low inhibitor concentrations, inhibition was noted to be higher for CLM than for CYP3A12. Furthermore, a difference between the influence of racemic medetomidine and dexmedetomidine on the reaction for CLM was observed. The effect of racemic medetomidine is stronger and is more expressed for racemic ketamine (Figs. 3A and 3C).

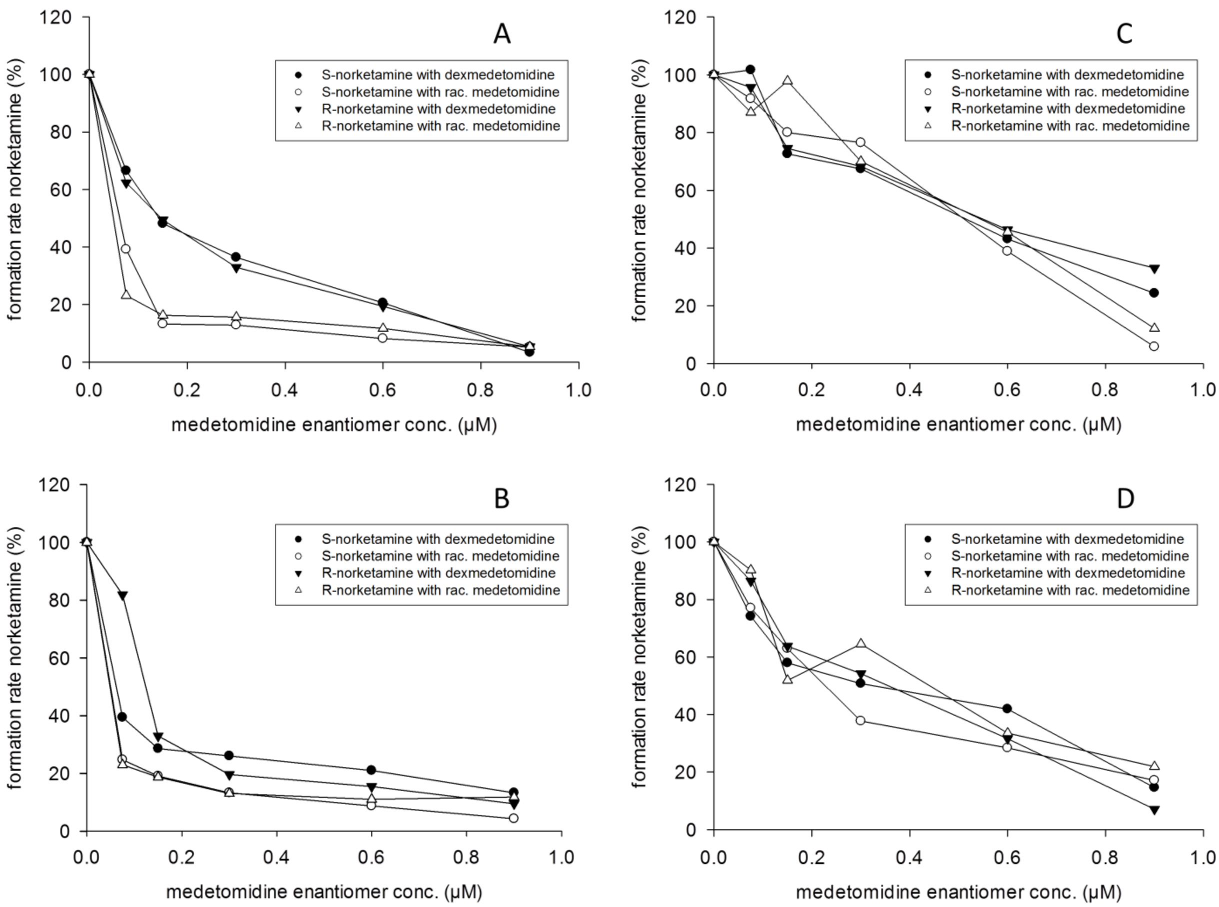

Figure 3. Effect of racemic medetomidine (open symbols) and dexmedetomidine (filled symbols) on ketamine N-demethylation in presence of (A,B) CLM and (C,D) canine CYP3A12. Ketamine was added as (A,C) racemate and (B,D) single enantiomers. The formation of S-norketamine (circles) and R-norketamine (triangles) was determined by CE. The symbols denote means of duplicates.

Experiments with HLM provided similar data (Figs. 4A,4B), which is in agreement with the literature [10]. Kharasch et al. identified levomedetomidine as the stronger inhibitor compared to dexmedetomidine for low inhibitor concentrations. Thus, racemic medetomidine has a higher inhibitive effect and thereby interaction potential than dexmedetomidine alone. For that reason only dexmedetomidine is available for human use.

This phenomenon is not observed for canine CYP3A12 (same inhibition for all inhibitors). Two mechanisms of interaction are possible. As an imidazole derivate medetomidine binds to the heme iron in CYP enzymes [10] and medetomidine is a substrate of CYP enzymes itself [11]. These enzymes play also an important role in the ketamine metabolism. A competition for the active site is thus likely to occur. The substrate with the higher affinity to the active site will block it. The affinity between substrate and enzyme is described by K_m values. K_m values related to CLM, which were found in the literature, confirm the results. A K_m value of 577 nM is reported for medetomidine and CLM [11]. For racemic ketamine and the single enantiomers they are around 23 and 90 times higher, respectively [22]. Thus, medetomidine has the higher affinity to the active site and limits the metabolism of ketamine. There are no K_m values for medetomidine and CYP3A12 in the literature. According to the results described above the affinity of medetomidine to CYP3A12 is also higher than that of ketamine but there is a smaller difference in the affinities.

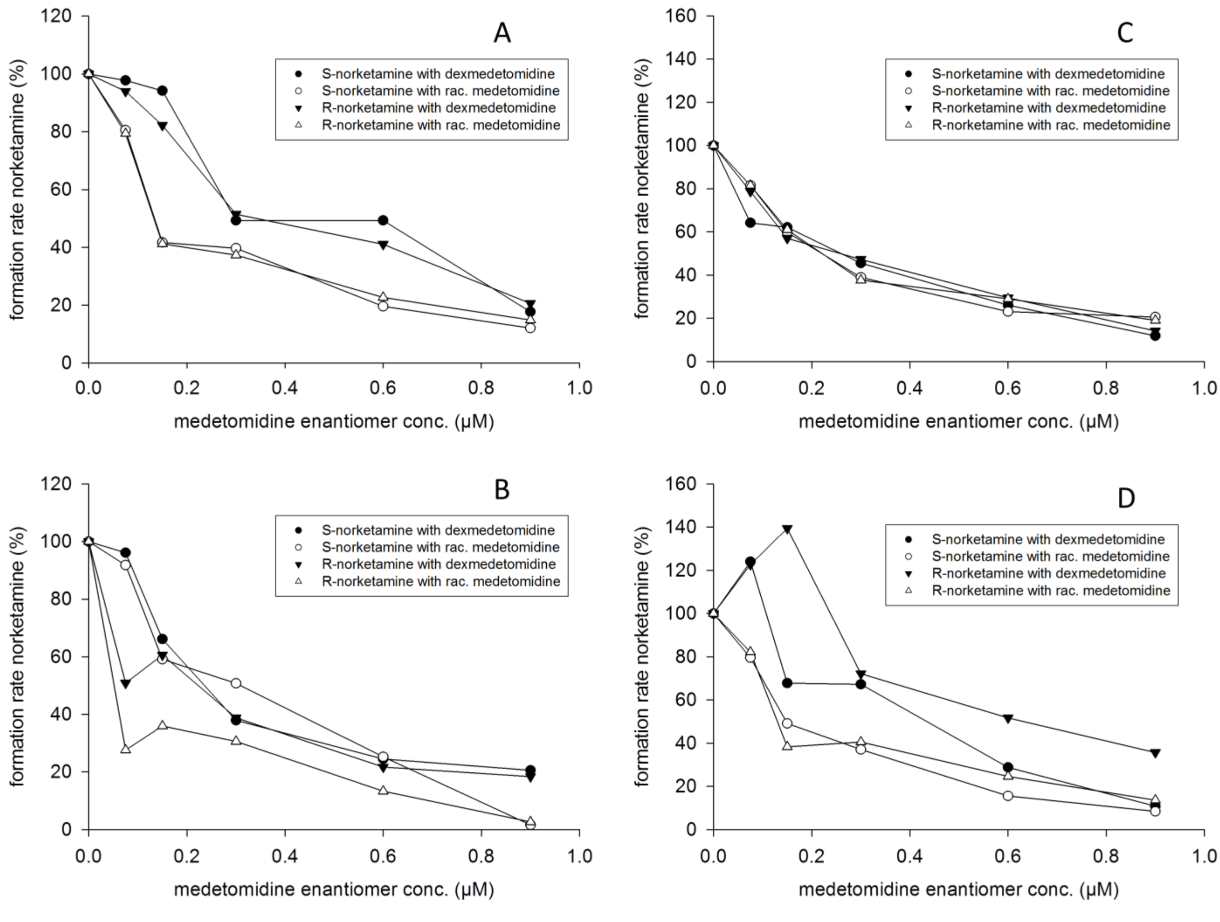

Figure 4. Effect of racemic medetomidine (open symbols) and dexmedetomidine (filled symbols) on ketamine N-demethylation in presence of (A,B) HLM and (C,D) human CYP3A4. Ketamine was added as (A,C) racemate and (B,D) single enantiomers. The formation of S-norketamine (circles) and R-norketamine (triangles) was determined by CE. The symbols denote means of duplicates.

With human CYP3A4, an inhibition was also observed for racemic ketamine as the substrate (Fig. 4C). There was no difference in the effect of racemic medetomidine and dexmedetomidine, as well as no stereoselectivity. Employing single enantiomers as substrates, the inhibition with racemic medetomidine was stronger compared to that of dexmedetomidine (Fig. 4D). Furthermore, an induction was detected at lower concentrations of dexmedetomidine (Fig. 4D). In the European public assessment report of the committee for medicinal products for human use of the European Medicines Agency about dexmedetomidine it is mentioned that it inhibits various CYP enzymes, including CYP2A6, CYP1A2, CYP2E1, CYP2D6 and CYP2C19, and induces CYP3A4, CYP2B6 and CYP2D6 [37]. The clinical relevance of the latter inductive potential of dexmedetomidine in the interplay of all different CYP enzymes is unknown. In the in vitro experiments with HLM, also an environment with various CYP enzymes, the inhibition predominates the metabolism of ketamine.

2.4.4 Inhibition parameters for dexmedetomidine

Inhibition parameters are helpful to characterize the inhibition and to provide a mean for reliable data comparison. The two inhibition parameters, the inhibition constant K_i and the half maximal inhibition concentration IC_{50}, were determined for the inhibitive effect of dexmedetomidine on the N-demethylation reaction of single S- and R-ketamine in presence of CLM and canine CYP3A12. K_i is the equilibrium constant describing the relation between free inhibitor and enzyme on the one side and the inhibitor-enzyme-complex on the other. A low K_i value stands for a high affinity between inhibitor and enzyme and therefore a strong inhibition of the reaction. The inhibitor concentration, which is needed for reducing the formation rate of a product by 50 %, is called IC_{50}. Three different substrate concentrations, 0.5 K_m, 1.0 K_m and 2.0 K_m, were incubated with dexmedetomidine at five concentrations ranged from 0.075 µM to 0.9 µM. The K_m values for CLM were taken from previous studies [22] and for CYP3A12 from the kinetic study described in Section 3.2. The formation rate of norketamine in pmol/min/pmol CYP were plotted against the dexmedetomidine concentration in µM and evaluated by nonlinear regression analysis, based on the four-parameter logistic model $y = \min + (\max - \min) / (1 + (x / IC_{50})^{-n})$ [29]. Obtained graphs are presented in Fig. 5.

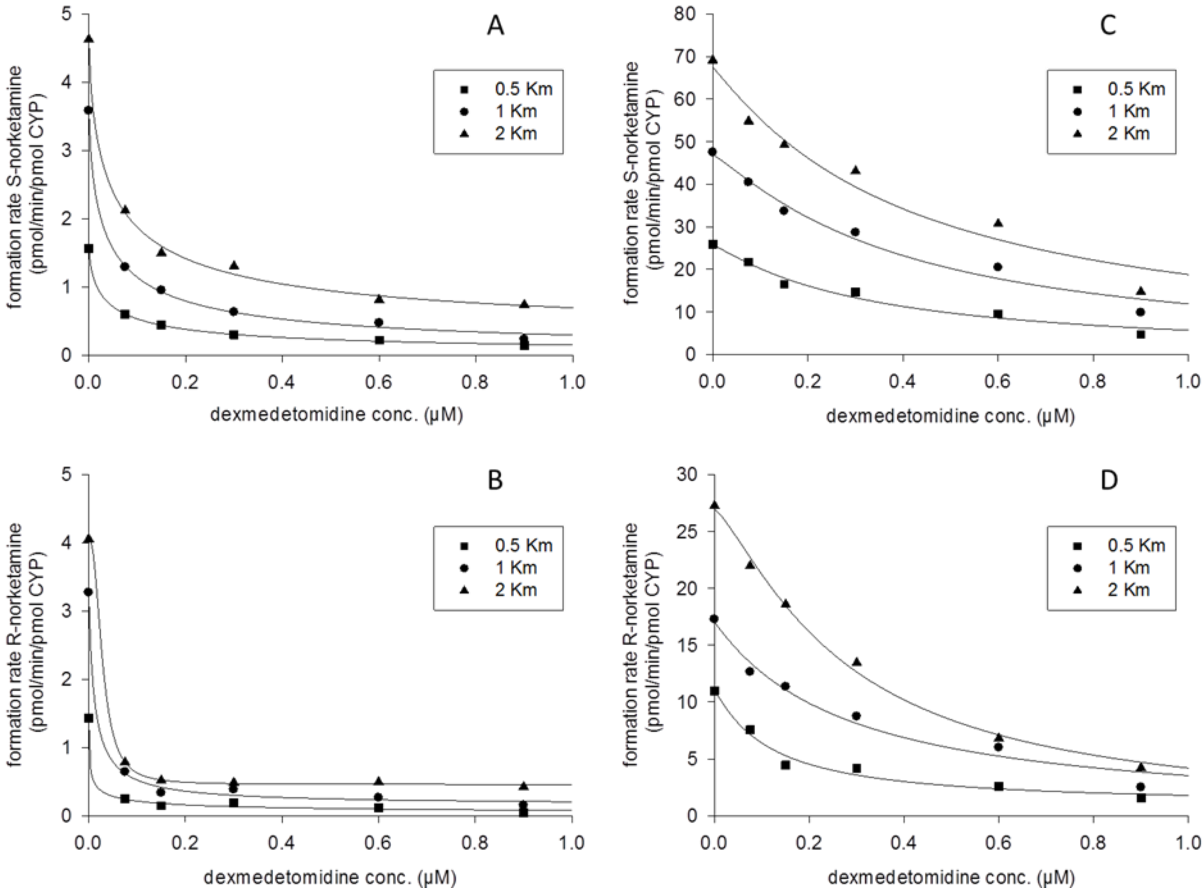

Figure 5. Kinetics of (A,B) CLM and (C,D) CYP3A12 mediated N-demethylation of (A,C) S-ketamine and (B,D) R-ketamine at three substrate concentrations (0.5 Km, 1.0 Km and 2.0 Km) inhibited by dexmedetomidine. Dexmedetomidine concentrations varied from 0.075 to 0.9 µM. Nonlinear regression analysis was performed with the four-parameter logistic model. Km values were from Ref. [22] and Table 2. Symbols denote means of duplicates.

In the used equation y is the norketamine formation rate, x the inhibitor concentration, min and max are the lower and the upper limit of the curve and n the Hill slope. The upper and lower limits of the curves were specified by the formation rate measured with the lowest and highest inhibitor concentration. The values for the Hill slope are in the range of -0.4886 and -2.4154 for CLM and between -1.0232 and -1.5867 for CYP3A12. K_i values were calculated with the Cheng and Prusoff equation [38] under inclusion of the determined IC_{50} values ($K_i = IC_{50} / (1 + ([S] / K_m))$) and obtained K_i and IC_{50} values are presented in Table 4. K_i for CLM is significantly lower than for canine CYP3A12. That means that the inhibition is stronger for the microsomes, what confirms the results of the experiments described in Section 3.3. For both, CLM and CYP3A12, the inhibition is stronger for the R- than for the S-enantiomer of ketamine. This stereoselectivity is not clearly seen in the data of Fig. 3B and 3D. It is interesting to mention that no stereoselectivity was observed with human CYP3A4 and dexmedetomidine as inhibitor [29]. K_i and IC_{50} values, however, were similar to those obtained with CYP3A12.

Table 4. Inhibition parameters for dexmedetomidine for CLM and CYP3A12 mediated N-demethylation of ketamine[a)]

Enzyme	Substrate	IC_{50} (µM)	K_i (µM)
CLM	S-ketamine	0.040 ± 0.007	0.022 ± 0.004
CLM	R-ketamine	0.014 ± 0.008	0.007 ± 0.004
CYP3A12	S-ketamine	0.375 ± 0.049	0.204 ± 0.062
CYP3A12	R-ketamine	0.222 ± 0.091	0.096 ± 0.040

a) Data represent mean values ± SD obtained with three substrate concentrations

2.5 Concluding remarks

The N-demethylation of ketamine mediated by canine CYP3A12 and CLM in absence and presence of medetomidine and dexmedetomidine was investigated and compared to data obtained with human CYP3A4 and HLM. For CYP3A12 and without inhibitor, Michaelis-Menten kinetics was determined for the single enantiomers of ketamine and substrate inhibition kinetics for racemic ketamine. Upon coincubation with medetomidine and dexmedetomidine, drug drug interactions were observed in all experiments. The effect of medetomidine and dexmedetomidine on the ketamine N-demethylation differs from canines to humans and also from liver microsomes to the single enzymes. In most cases an inhibition was found. With CYP3A4, induction was observed at low dexmedetomidine concentrations. With CYP3A12, no induction was noted. For the experiments with liver microsomes, the inhibition of medetomidine was found to be stronger than that of dexmedetomidine. Inhibition parameters, determined for the combination of dexmedetomidine with the single ketamine enantiomers in presence of CLM or CYP3A12, show a stronger inhibition of the formation of

R-norketamine. Thus, these data suggest that comedication of dexmedetomidine and S-ketamine should represent the best option for canines. Further investigations, especially in vivo studies, will provide insight into the relevance of this interaction for daily clinical practice. Enantioselective CE with highly sulfated γ-cyclodextrin as chiral selector is shown to represent an effective tool for determining kinetic and inhibition parameters associated with the N-demethylation of ketamine.

Acknowledgements

This work was supported by the Swiss National Science Foundation.

Conflicts of interest

The authors have declared no conflict of interest.

2.6 References

[1] J. Persson, Ketamine in Pain Management, CNS Neurosci. Ther. 19 (2013) 396–402.

[2] G. Mion, T. Villevieille, Ketamine Pharmacology: An Update (Pharmacodynamics and Molecular Aspects, Recent Findings), CNS Neurosci. Ther. 19 (2013) 370–380.

[3] E.D. Kharasch, R. Labroo, Metabolism of ketamine stereoisomers by human liver microsomes, Anesthesiology 77 (1992) 1201–1207.

[4] R.K. Paul, N.S. Singh, M. Khadeer, R. Moaddel, M. Sanghvi, C.E. Green, K. O'Loughlin, M.C. Torjman, M. Bernier, I.W. Wainer, (R,S)-Ketamine metabolites (R,S)-norketamine and (2S,6S)-hydroxynorketamine increase the mammalian target of rapamycin function, Anesthesiology 121 (2014) 149–159.

[5] X. Zhao, S.L.V. Venkata, R. Moaddel, D.A. Luckenbaugh, N.E. Brutsche, L. Ibrahim, C.A. Zarate, D.E. Mager, I.W. Wainer, Simultaneous population pharmacokinetic modelling of ketamine and three major metabolites in patients with treatment-resistant bipolar depression, Br. J. Clin. Pharmacol. 74 (2012) 304–314.

[6] Y. Hijazi, R. Boulieu, Contribution of CYP3A4, CYP2B6, and CYP2C9 isoforms to N-demethylation of ketamine in human liver microsomes, Drug Metab. Dispos. 30 (2002) 853–858.

[7] J.C. Duque, N. Oleskovicz, E.C.B.P. Guirro, C.A.A. Valadão, V.E. Soares, Relative potency of ketamine and S(+)-ketamine in dogs, J. Vet. Pharmacol. Ther. 31 (2008) 344–348.

[8] M. L. Williams, D. E. Mager, H. Parenteau, G. Gudi, T. S. Tracy, M. Mulheran, I. W. Wainer, Effects of protein calorie malnutrition on the pharmacokinetics of ketamine in rats, Drug Metab. Dispos. 32 (2004) 786–793.

[9] P. F. White, J. Schüttler, A. Shafer, D. R. Stanski, Y. Horai, A. J. Trevor, Comparative pharmacology of the ketamine isomers. Studies in volunteersBr. J. Anaesth. 57 (1985) 197–203.

[10] E.D. Kharasch, S. Herrmann, R. Labroo, Ketamine as a probe for medetomidine stereoisomer inhibition of human liver microsomal drug metabolism, Anesthesiology 77 (1992) 1208–1214.

[11] M.-C. Duhamel, É. Troncy, F. Beaudry, Metabolic stability and determination of cytochrome P450 isoenzymes' contribution to the metabolism of medetomidine in dog liver microsomes, Biomed. Chromatogr. 24 (2010) 868–877.

[12] L. K. Cullen, Medetomidine sedation in dogs and cats: a review of its pharmacology, antagonism and dose, Br. Vet J. 152 (1996) 519–535.

[13] P. Ravipati, P.N. Reddy, C. Kumar, P. Pradeep, R. Pathapati, S.T. Rajashekar, Dexmedetomidine decreases the requirement of ketamine and propofol during burns debridement and dressings, Indian J. Anaesth. 58 (2014) 138–142.

[14] A. Ülgey, R. Aksu, C. Bicer, A. Akin, R. Altuntaş, A. Esmaoğlu, A. Baykan, A. Boyaci, Is the addition of dexmedetomidine to a ketamine-propofol combination in pediatric cardiac catheterization sedation useful?, Pediatr. Cardiol. 33 (2012) 770–774.

[15] Y. Yanagihara, S. Kariya, M. Ohtani, K. Uchino, T. Aoyama, Y. Yamamura, T. Iga, Involvement of CYP2B6 in n-demethylation of ketamine in human liver microsomes, Drug Metab. Dispos. 29 (2001) 887–890.

[16] S. Portmann, H.Y. Kwan, R. Theurillat, A. Schmitz, M. Mevissen, W. Thormann, Enantioselective capillary electrophoresis for identification and characterization of human cytochrome P450 enzymes which metabolize ketamine and norketamine in vitro, J. Chromatogr. A 1217 (2010) 7942–7948.

[17] Z. Desta, R. Moaddel, E.T. Ogburn, C. Xu, A. Ramamoorthy, S. L. V. Venkata, M. Sanghvi, M.E. Goldberg, M.C. Torjman, I.W. Wainer, Stereoselective and regiospecific hydroxylation of ketamine and norketamine, Xenobiotica 42 (2012) 1076–1087.

[18] A. Schmitz, R. Theurillat, P.-G. Lassahn, M. Mevissen, W. Thormann, CE provides evidence of the stereoselective hydroxylation of norketamine in equines, Electrophoresis 30 (2009) 2912–2921.

[19] L. Capponi, A. Schmitz, W. Thormann, R. Theurillat, M. Mevissen, In vitro evaluation of differences in phase 1 metabolism of ketamine and other analgesics among humans, horses, and dogs, Am. J. Vet. Res. res. 70 (2009), 777–786.

[20] A. Schmitz, C. J. Portier, W. Thormann, R. Theurillat, M. Mevissen, Stereoselective biotransformation of ketamine in equine liver and lung microsomes, J. Vet. Pharmacol. Ther. 31 (2008), 446–455.

[21] J. S. Salonen, M. Eloranta, Biotransformation of medetomidine in the rat, Xenobiotica 20 (1990) 471–480.

[22] A. Schmitz, W. Thormann, L. Moessner, R. Theurillat, K. Helmja, M. Mevissen, Enantioselective CE analysis of hepatic ketamine metabolism in different species in vitro, Electrophoresis 31 (2010) 1506–1516.

[23] R. Theurillat, M. Knobloch, O. Levionnois, P. Larenza, M. Mevissen, W. Thormann, Characterization of the stereoselective biotransformation of ketamine to norketamine *via* determination of their enantiomers in equine plasma by capillary electrophoresis, Electrophoresis 26 (2005) 3942–3951.

[24] L. D. Mössner, A. Schmitz, R. Theurillat, W. Thormann, M. Mevissen, Inhibition of cytochrome P450 enzymes involved in ketamine metabolism by use of liver microsomes and specific cytochrome P450 enzymes from horses, dogs and humans, Am. J. Vet. Res. 72 (2011) 1505–1513.

[25] A. Bergadano, O. K. Andersen, L. Arendt-Nielsen, R. Theurillat, W. Thormann, C. Spadavecchia, Plasma levels of a low-dose constant-rate-infusion of ketamine and its effect on single and repeated nociceptive stimuli in conscious dogs, Vet. J. 182 (2009) 252–260.

[26] M. P. Larenza, C. Peterbauer, M. F. Landoni, O. L. Levionnois, U. Schatzmann, C. Spadavecchia, W. Thormann, Stereoselective pharmacokinetics of ketamine and norketamine after constant rate infusion of a subanesthetic dose of racemic ketamine or S-ketamine in Shetland ponies, Am. J. Vet. Res. 70 (2009), 831–839.

[27] H. Y. Kwan, W. Thormann, Enantioselective capillary electrophoresis for the assessment of CYP3A4-mediated ketamine demethylation and inhibition in vitro, Electrophoresis 32 (2011) 2738–2745.

[28] H. Y. Kwan, W. Thormann, Electrophoretically mediated microanalysis for characterization of the enantioselective CYP3A4 catalyzed N-demetylation of ketamine, Electrophoresis, 33 (2012) 3299–3305.

[29] R. Řemínek, Z. Glatz, W. Thormann, Optimized on-line enantioselective capillary electrophoretic method for kinetic and inhibition studies of drug metabolism mediated by cytochrome P450 enzymes, Electrophoresis 36 (2015) 1349–1357.

[30] B. H. Pypendop, J. E. Ilkiw, Pharmacokinetics of ketamine and its metabolite, norketamine, after intravenous administration of a bolus of ketamine to isoflurane-anesthetized dogs, Am. J. Vet. Res. 66 (2005) 2034–2038.

[31] E. Kuusela, M. Raekallio, M. Anttila, I. Falck, S. Mölsä, O. Vainio, Clinical effects and pharmacokinetics of medetomidine and its enantiomers in dogs, J. Vet. Pharmacol. Ther. 23 (2000) 15–20.

[32] M. Afshar, W. Thormann, Capillary electrophoretic investigation of the enantioselective metabolism of propafenone by human cytochrome P-450 SUPERSOMES: Evidence for atypical kinetics by CYP2D6 and CYP3A4, Electrophoresis 27 (2006) 1526–1536.

[33] W. M. Atkins, Non-Michaelis-Menten kinetics in cytochrome P450-catalyzed reactions, Annu. Rev. Pharmacol. Toxicol. 45 (2005) 291–310.

[34] J. M. Hutzler, T. S. Tracy, Atypical kinetic profiles in drug metabolism reactions, Drug Metab. Dispos. 30 (2002) 355–362.

[35] Y. Lin, P. Lu, C. Tang, Q. Mei, G. Sandig, A. D. Rodrigues, T. H. Rushmore, M. Shou, Substrate inhibition kinetics for cytochrome P450-catalyzed reactions, Drug Metab. Dispos. 29 (2001) 368–374.

[36] S. W. J. Wang, K. Abdul-Hadi, L. Cohen, C. Q. Xia, Mechanistic evaluation of substrate inhibition kinetics observed from aldehyd oxidase-catalyzed reactions, Drug Metab. Lett. 7 (2013) 2–14.

[37] European Medicines Agency, Committee for Medicinal Products for Human Use, *Assessment report Dexdor® (Procedure No. EMEA/ H/ C/ 002268/ II/ 0003).* London, UK, 2013, p. 22.

[38] Y. Cheng, W.H. Prusoff, Relationship between the inhibition constant (K1) and the concentration of inhibitor which causes 50 per cent inhibition (I50) of an enzymatic reaction, Biochem. Pharmacol. 22 (1973) 3099–3108.

3. Microassay for ketamine and metabolites in plasma and serum based on enantioselective capillary electrophoresis with highly sulfated γ-cyclodextrin and electrokinetic analyte injection (Electrophoresis 37 (2016) 1129-1138)

Regula Theurillat[1], Friederike A. Sandbaumhüter[1], Regula Bettschart-Wolfensberger[2], Wolfgang Thormann[1]

[1] Clinical Pharmacology Laboratory, University of Bern, Bern, Switzerland
[2] Section of Anaesthesiology, Equine Department, Vetsuisse Faculty, University of Zürich, Zürich, Switzerland

3.1 Abstract

For the assessment of stereoselective aspects of the metabolism of ketamine, an enantioselective CE-based microassay for determination of the stereoisomers of ketamine and three of its major metabolites in plasma and serum was developed. The assay is based on liquid/liquid extraction of the analytes of interest at alkaline pH from 0.05 mL plasma or serum followed by electrokinetic sample injection of the analytes from the extract across a buffer plug without chiral selector. Separation occurs cationically at normal polarity in a pH 3.0 phosphate buffer containing 0.66 % of highly sulfated γ-cyclodextrin (HS-γ-CD). Key parameters for optimization are identified as being the amount of HS-γ-CD in the BGE, the length of the buffer plug and its concentration, the duration of electrokinetic injection, and the extraction medium. Diluted buffer in the plug is employed to ascertain sufficient analyte stacking due to a combination of field amplification and complexation. The newly developed microassay is robust (intraday and interday RSD < 5% and < 9 %, respectively) and well suited to determine enantiomer levels of ketamine and its metabolites down to 10 ng/mL. It is more sensitive, uses less plasma or serum, organic solvent and analysis time compared to previous CE-based assays and was successfully applied to monitor ketamine, norketamine, 5,6-dehydronorketamine (DHNK) and 6-hydroxynorketamine (6HNK) stereoisomer levels in plasma of a Beagle dog that received a bolus of racemic ketamine or S-ketamine after sevoflurane anesthesia. The data suggest that the formation of DHNK and 6-HNK occur stereoselectively.

3.2 Introduction

In CE detection limits of analytes are not only dependent on the type of detector used, but also on the matrix of the sample and the injection procedure employed. CE with UV-absorbance detection and hydrodynamic injection of sample typically provides ppm (µg/mL) detection limits that are one or two orders of magnitude higher than those encountered in HPLC. Thus, procedures leading to concentration and sensitivity enhancements in CE are of high importance and discussed in many recent reviews [1–5]. Many of the applied methods include electrokinetic sample injection, a process that requires proper control of injection parameters in order to achieve acceptable quantitative repeatability [6,7]. For analysis of drugs and metabolites in microliter amounts of body fluids, the combination of electrokinetic injection from extracts with low conductivity and field-amplified sample stacking at the capillary tip provides the basis for ppb (ng/mL) detection limits and robust assays [8–11].

CE is an important technology for enantioselective analyses, including stereoselective bioanalytical drug and metabolite monitoring [12–15]. The rather poor concentration sensitivity, however, is an inherent limitation and requires proper attention particularly in regard to the charge of the chiral selector employed [5]. For ppb analysis of stereoisomers in body fluids by CE with neutral selectors can be dealt with as without involvement of complexation, i.e. with electrokinetic injection and field-amplified sample stacking. Examples include the analysis of the enantiomers of clenbuterol in urine [16], verapamil and norverapamil in plasma [17], and methylphenidate in plasma [18] and oral fluid [19]. With charged chiral selectors, however, the setup is more demanding as deleterious interferences of the chiral selector occurring during electrokinetic injection have to be avoided. This was previously discussed and taken care of via use of a buffer plug without chiral selector at the capillary tip such that cationic analytes could be properly electroinjected prior to separation and analysis in a setup with MS detection using a partially filled capillary with the BGE containing highly sulfated γ-cyclodextrin (HS-γ-CD) as chiral selector [20]. This assay format was successfully applied to the ppb monitoring of the enantiomers of 3,4-methylenedioxymethamphetamine and methadone from large amounts (0.5 to 1.0 mL) of plasma [21].

Mixtures of charged chiral selectors were found to be highly suitable for analysis of the enantiomers of the parent compound and many different metabolites in one run, including the monitoring of the stereoisomers of ketamine, norketamine, 5,6-dehydronorketamine (DHNK), 6-hydroxynorketamine (6HNK) and various other hydroxylated norketamine metabolites in biosamples [22–24]. Chemical structures of selected compounds are presented in Fig. 1. Ketamine is an intravenous analgesic and anesthetic drug widely used in clinical practice of humans and animals. It is administered as racemate (in most countries) or as S-ketamine. Ketamine and its metabolites are bases and thus cations at low pH. Our efforts focus on the elucidation of stereoselective aspects of the ketamine metabolism in different species both in vivo [24–28] and in vitro [24,29–32]. In the work performed thus far, analytes were extracted at alkaline pH from 100 to 1000 µL of sample and applied hydrodynamically prior to separation of the stereoisomers in a pH 2.5 BGE comprising 10 mg/mL amounts of sulfated β-CD or 2.0 to 3.3 % of HS-γ-CD. The analytes migrated anionically, which required reversed voltage for analysis and detection limits were dependent on the amount of sample used for extraction and the volume in which the extract was dissolved prior to hydrodynamic injection. For extraction from a 500 µL sample and final reconstitution in a volume of 30 µL, ppb detection limits for ketamine and norketamine enantiomers could be reached (2.5 ng/mL, [28]) an approach that pushed instrumental possibilities to the limits of the commercially available CE technology. In all other approaches, detection limits were up to 20 times higher.

For the determination of ketamine and metabolites in ppb amounts from 50 µL plasma or serum, assay conditions with electrokinetic sample injection and cationic migration of the analytes in presence of low amounts (< 1 %) of HS-γ-CD in the BGE were explored. The microassay developed is not restricted to the monitoring of the enantiomers of one compound. It includes compounds which exhibit large differences in complexation with the chiral selector and thus effective electrophoretic mobilities. The concept of using a selector-free preinjection plug of buffer for electrokinetic injection reported by Schappler et al. [20,21] was thereby extended to fulfill optimized analyte stacking conditions from liquid/liquid extracts prepared from 50 µL plasma or serum and to provide applicability to multiple chiral compounds with ppb sensitivity. In this paper, the development of the microassay, assay characteristics, and assay application to the enantioselective monitoring of ketamine and three of its metabolites in plasma samples collected within 900 min after bolus administration of racemic ketamine or S-ketamine to a Beagle dog are described.

3.3 Material and Methods

3.3.1 Chemicals, reagents, and origin of dog samples

Ketamine and norketamine (as hydrochlorides in methanol, 1 mg/mL of the free base) and DHNK (100 µg/mL in ACN) were from Cerilliant (Round Rock, TX, USA). (2S,6S)-hydroxynorketamine (SS-6HNK) and (2R,6R)-hydroxynorketamine (RR-6HNK) were received as a kind gift from Dr. Irving Wainer (Laboratory of Clinical Investigations, National Institute on Aging, National Institutes of Health, Baltimore, MD, USA (for information about their synthesis see [33,34]). D-(+)-norephedrine hydrochloride (internal standard) and bovine serum were from Sigma (St. Louis, Mo, USA). Lamotrigine was from The Welcome Foundation (London, UK) and HS-γ-CD (20 % *w/v* solution) was from Beckman Coulter (Fullerton, CA, USA). Disodium hydrogenphosphate, sodium hydroxide and bromothymol blue were from Merck (Darmstadt, Germany) and methanol and phosphoric acid (85 %) were from Fluka (Buchs, Switzerland). Ethylacetate was from AppliChem (Darmstadt, Germany), dichloromethane (HiPerSolv Chromanorm for HPLC) from VWR (Leuven, Belgium) and hexane (HPLC grade) from Lab-Scan, Gliwice, Poland. Dog plasma samples stemmed from a clinical study executed at Vetsuisse Faculty (Zürich, Switzerland) which was performed with the permission of the Committee for Animal Experimentation, Canton Zürich, Switzerland. Briefly, Beagle dogs under sevoflurane anaesthesia received i.v. boluses of racemic ketamine (4 mg/kg) or S-ketamine (2 mg/kg) and venous blood samples were collected before and at 25 time points between 1 and 900 min after drug administration.

3.3.2 Preparation of samples and controls

An aqueous mixture of standards composed of the enantiomers of ketamine (1000 ng/mL each) and of the enantiomers of the ketamine metabolites norketamine, DHNK and 6HNK (250 ng/mL each) was prepared, stored at -20 °C as aliquots in 0.5 mL Eppendorf vials and the content of one vial was used for assay calibration. Five calibrators with ketamine concentrations between 80 and 2000 ng/mL of each enantiomer and with norketamine, DHNK and 6HNK concentrations between 20 and 500 ng/mL each stereoisomer were prepared in aliquots of 50 µL bovine serum via addition of appropriate aliquots of the standard mixture and water. The calibrators were pretreated for analysis as described in Section 2.3. Two independent control samples in bovine serum were prepared, one comprising 440 ng/mL of each enantiomer of NK, DHNK and 6HNK and 1.76 µg/mL of each ketamine enantiomer, the second having 60 ng/mL of each enantiomer of NK, DHNK and 6HNK and 240 ng/mL of each ketamine enantiomer. 50 µL aliquots of the controls were mixed with 200 µL water and stored at -80 °C until analysis.

3.3.3 Sample preparation

For the liquid/liquid extraction, 50 µL of plasma or serum, 200 µL water, 15 µL of IST solution (4 µg/mL D-(+)-norephedrine hydrochloride, solution stored at 4 °C), 50 µL indicator solution (1.25 mM bromothymol blue in 0.5 M NaOH, solution stored at 4 °C) and 1300 µL dichloromethane were pipetted into a 2 mL Eppendorf vial. The closed vials were shaken for 5 min on a horizontal shaker LS 20 (Gerhardt, Königswinter, Germany) and centrifuged at 13000 rpm for 3 min. After removing the upper blue aqueous phase with vacuum suction, the organic phase was transferred to a new vial, acidified with 10 µL of 1 mM phosphoric acid (to avoid the loss of analytes during evaporation and provide increased injection efficiency) and dried at 45 °C in a Speed-Vac Concentrator 5301 (Vaudaux-Eppendorf, Schönenbuch, Switzerland). The residue was reconstituted in 110 µL water, vortexed and transferred to a CE-insert vial (Beckman Coulter, Fullerton, CA, USA) for analysis. Defrosted control samples were treated the same way except that no water was added prior to the addition of the IST solution.

3.3.4 CE instrumentation and analytical conditions

A Proteome Lab PA 800 enhanced instrument (Beckman Coulter, Fullerton, CA, USA) equipped with a 50 µm I.D. fused-silica capillary (Polymicro Technologies, Phoenix, AZ, USA) of 45 cm total length (effective length 35 cm) was used. The phosphate buffer was prepared by addition of 0.5 M phosphoric acid to a 0.5 M disodium hydrogenphosphate solution until a pH of 3.0 was reached. If not stated otherwise, the running buffer was daily diluted and comprised 100 mM phosphate buffer (pH 3.0) to which 0.66 % HS-γ-CD was added. Before each experiment, the capillary was rinsed with bidistilled water (1 min; 20 psi; 1 psi = 6894.8 Pa) and running buffer (1 min; 20 psi). Thereafter, a plug composed of 50 mM phosphate buffer (pH 3.0) without chiral selector was pressure injected at 1 psi for 20 s. Samples were injected electrokinetically via applying 6 kV for 15 s. A voltage of 20 kV (normal polarity) was applied. The current was about 64 µA. Sample storage and capillary cartridge temperatures were set to 25 °C and analyte detection was effected at 200 nm (PDA detector). Quantification of ketamine and norketamine enantiomers was based on internal calibration using corrected peak areas.

3.3.5 Additional tools

Buffer plug lengths were estimated with the CE Expert Lite software (Beckman Coulter, Fullerton, CA, USA). The CE Expert Lite calculator is based on the Poiseuille equation which describes how fluid under pressure is flowing through a cylindrical vessel. Microsoft Excel (Microsoft, Redmont, WA, USA) and SigmaPlot software version 12.5 (Systat Software, San Jose, CA, USA) were used for data evaluation and presentation, respectively.

3.4 Results and discussion

3.4.1 Cationic separation of analytes in the presence of HS-γ-CD

In order to explore the use of electrokinetic sample injection with cationic separation of the compounds, a 100 mM phosphate buffer (pH 3.0, prepared with disodium hydrogenphosphate and phosphoric acid) comprising 0.6-0.8 % HS-γ-CD was employed as separation medium. The buffer was the same as used for the monitoring of methylphenidate stereoisomers in oral fluid by capillary electrophoresis with head-column field-amplified sample injection [19]. The pH 3.0 phosphate buffer was found to have a better baseline stability compared to the pH 2.5 BGE composed of Tris and phosphoric acid employed previously with hydrodynamic sample injection and anionic sample separation [22–32]. Both buffers provided comparable separation. Under cationic separation conditions, hydroxylated norketamine stereoisomers are detected before the enantiomers of norketamine and ketamine with the R-isomers of these compounds migrating faster compared to the S-isomers. Furthermore, S-DHNK is detected shortly after S-norketamine whereas R-DHNK reaches the point of detection after S-ketamine (Fig. 1). This order is reversed compared to that under anionic separation conditions used previously. All separations were performed at 20 kV and a test sample comprising about 91 ng/mL of each analyte and 91 µM phosphoric acid was used.

The concentration of the chiral selector and the temperature of the capillary cartridge were found to have an impact of analyte separability. With 0.66 % of HS-γ-CD in the BGE, complete separation of the analytes of interest and the IST was obtained and the detection time of the compounds occurred between 7 and 16 min (graph A of Fig. 1). Having larger amounts of HS-γ-CD resulted in increased detection intervals whereas the use of a lower concentration provided shorter detection times and insufficient separation. Lamotrigine and d-(+)-pseudoephedrine used previously as internal standards could not be used. Lamotrigine was too strongly retarded and detected considerably after R-DHNK and d-(+)-pseudoephedrine interfered with SS-6HNK (data not shown). Many other ephedrine analogs were tested and interfered as well with one of the target compounds. D-(+)-norephedrine finally provided a nice peak which was detected ahead of all targeted stereoisomers and was thus applied as internal standard (Fig. 1).

The temperature of the cooling fluid flowing through the capillary cartridge was varied between 20 and 35 °C at an interval of 5 °C. The separation of S-norketamine and S-DHNK, as well as the two 6HNK stereoisomers, were found to be the critical pairs for separation of all 8 compounds. At the lowest temperature, the first pair did not separate properly and resolution improved with increasing temperature. The opposite was found to be true for the two 6HNK stereoisomers (data not shown). The separation of all other compounds of interest was complete at all investigated temperatures. Overall best data were obtained at 25 °C. Thus, all further experiments were performed at 25 °C with a 100 mM phosphate buffer (pH 3.0) containing 0.66 % of HS-γ-CD.

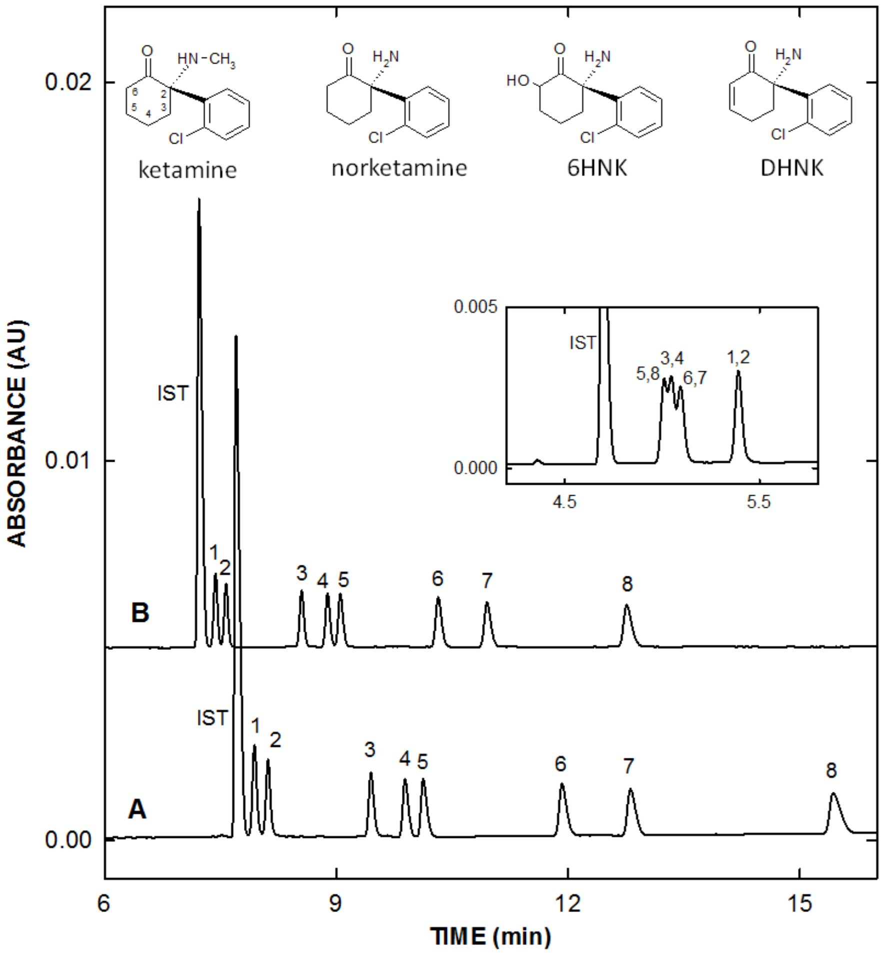

Figure 1. Typical analyte separations and chemical structures of ketamine, norketamine, DHNK and 6HNK. The electropherograms were obtained with standards dissolved in 91 µM phosphoric acid and applied via a 15 s injection at 6 kV across a 50 mM buffer plug generated at 1 psi for (A) 10 s and (B) 40 s. The applied voltage and cartridge temperature were 20 kV and 25 °C, respectively. The concentration of each analyte in the sample was about 91 ng/mL. IST refers to the internal standard. The insert depicts data obtained without the chiral selector in the BGE and having a 50 mM buffer plug generated at 1 psi for 20 s. Key: 1) RR-6HNK, 2) SS-6HNK, 3) R-NK, 4) S-NK, 5) S-DHNK, 6) R-K, 7) S-K, 8) R-DHNK.

Finally, the impact of complexation on analyte migration was assessed by comparing data obtained without and with the chiral selector in the BGE. In absence of the chiral selector, the four compounds could not be completely separated and were detected much earlier compared to the case with the chiral selector (insert in Fig. 1). D-(+)-norephedrine was again detected first. DHNK, NK and K could not be separated completely, and 6HNK was detected last. The electroosmotic mobility was estimated as being 0.70 x 10^{-8} m^2/Vs. Thus, effective electrophoretic mobilities for the five compounds were calculated as being around 2.10 x 10^{-8},

1.93×10^{-8}, 1.90×10^{-8}, 1.88×10^{-8} and 1.74×10^{-8} m^2/Vs, respectively. Effective mobilities in presence of complexation with 0.66 % HS-γ-CD were estimated to be in the range between 1.03×10^{-8} m^2/Vs (IST) and 0.27×10^{-8} m^2/Vs (R-DHNK), indicating that all compounds are being strongly retarded by complexation. These mobility data refer to configurations with a 50 mM buffer plug without chiral selector that was inserted at 1 psi for 20 s prior to electrokinetic injection of the analytes. The reasons for the necessity of this buffer plug are discussed in Section 3.2. The current for the achiral experiment was about 55 µA (power level of 2.44 W/m). With addition of 0.66 % HS-γ-CD to the BGE, the current became about 64 µA (power level of 2.85 W/m). This indicates that HS-γ-CD is considerably increasing the conductivity of the BGE.

3.4.2 Electrokinetic plug injection

Electroinjection of cations directly into the BGE is possible for fast migrating and weakly complexing compounds only. During electroinjection, HS-γ-CD is migrating from the BGE towards and into the sample vial which results in complexation of the cationic sample components and increase of conductivity of the sample solution. Both effects decrease injection efficiency. Thus a short plug of buffer without the chiral selector was introduced after insertion of the BGE, thereby producing a temporary barrier for the migration of HS-γ-CD into the sample vial. For optimization of electrokinetic analyte injection across the plug, the impact of buffer concentration in the plug, the plug length, the applied voltage and the duration of electrokinetic injection were assessed. A test sample comprising about 91 ng/mL of each analyte and 91 µM phosphoric acid was used.

The effect of the plug buffer concentration on analyte peaks was studied using a 2.68 cm (5.96 % of column length, estimated with CE Expert Lite calculator) plug formed at 1 psi for 20 s together with electrokinetic injection at 6 kV for 15 s. Experiments were performed having the same phosphate buffer concentration as in the BGE (100 mM), 50 mM, 25 mM and 10 mM (Fig. 2). For presentation purposes, the four electropherograms were aligned for equal detection of the IST. Shifts used were ≤ 0.2 min. The smallest peaks were detected with 100 mM buffer in the plug (Fig. 2A). In this configuration, analyte stacking is primarily based upon field amplification due to electroinjection from a solution of low conductivity into the buffer plug.

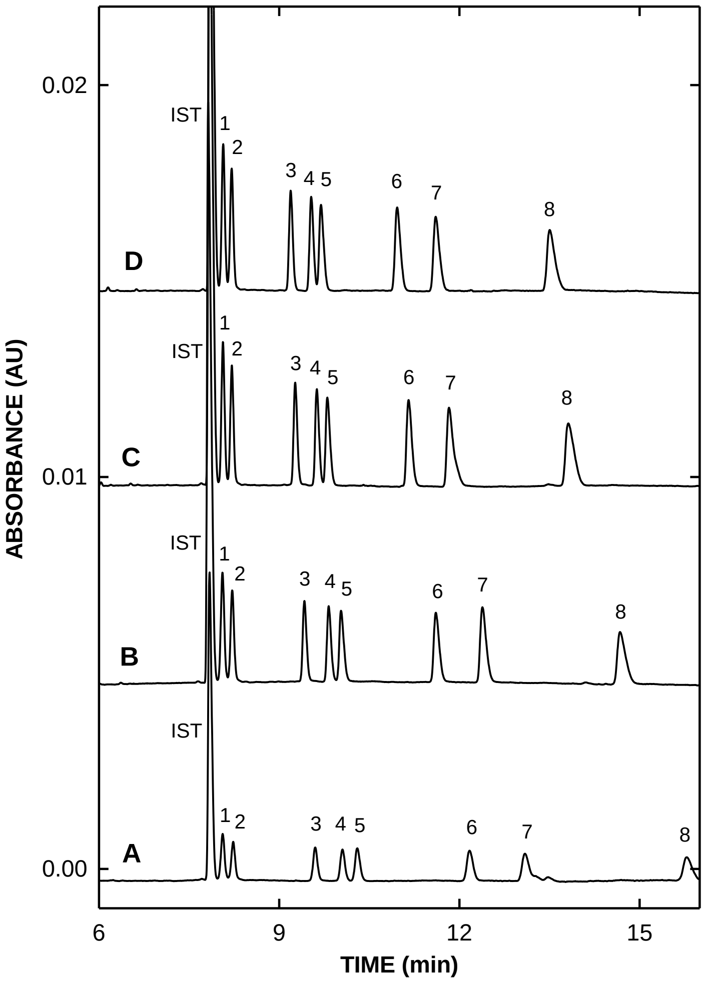

Figure 2. Electropherograms illustrating the impact of plug buffer concentration obtained with a plug formed at 1 psi for 20 s having (A) 100 mM, (B) 50 mM, (C) 25 mM and (D) 10 mM phosphate buffer without chiral selector. For presentation purposes, electropherograms were aligned for equal detection time of the IST. Other conditions and key as for Fig. 1.

Complexation of analytes with HS-γ-CD and a modest field amplification effect occurring at the end of the buffer plug (conductivity change which originates due to the addition of the chiral selector to the BGE (see Section 3.1) might also have an impact on peak enhancement. Increased sensitivity was reached through decrease of the plug buffer concentration to 25 mM (Figs. 2B and 2C). No improvement was observed between 25 and 10 mM (Figs. 2C and 2D). Buffer dilution provides a reduction of the conductivity in the plug and thus increased field amplified stacking of analytes at the transition between plug and BGE. The buffer concentration was also found to have an impact on detection times and resolution of analytes. Both parameters became lower as the buffer concentration was decreased (Fig. 2). 50 mM phosphate buffer provided sufficient sensitivity for the purpose of the anticipated pharmacokinetic project and was used in the assay reported below. It is important to mention that the use of water instead of buffer at the used plug length did not reveal any useful data. A water plug provides a region of very low conductivity. For analyte stacking, it length should be 8-10 times shorter [8,19]. However, a short water plug does not provide the required barrier for HS-γ-CD. Its use was thus not investigated in our work.

The effect of plug length was assessed with plug injections occurring at 1 psi for 10 to 40 s and having a 50 mM plug buffer concentration together with an analyte injection for at 6 kV for 15 s. Using the CE Expert Lite software for a temperature of 25 °C, plug lengths were calculated to be between 1.34 cm (2.98 % of total column length) and 5.36 cm (11.92 % of total column length). Electropherograms obtained for the shortest and longest plugs are presented as graphs A and B, respectively, in Fig. 1. The plug length was found to have an impact on the detection time and resolution of analytes. An increase in plug length resulted in earlier detection of the analytes and reduced resolution (Fig. 1). The latter effect can have an impact on evaluation of the firstly detected peaks (IST, 6HNK stereoisomers) and S-norketamine and R-DHNK. A plug length of 2.68 cm (5.96 % of column length) effected at 1 psi for 20 s was considered as ideal and was thus employed in our project (electropherogram B in Fig. 2). This buffer plug length compares well with that employed by Schappler et al. [20,21].

The last important parameters, whose impact had to be assessed, were the injection voltage and the injection time. With a plug generated at 1 psi for 20 s, voltages applied were 6, 8 and 10 kV and the time was varied between 10 and 70 s (6 kV) and 10 and 50 s (8 and 10 kV). It was interesting to find that there was a gradual loss of the slowest migrating analytes when the injection time became too long. This is illustrated with the data obtained with 6 kV presented in Fig. 3. Increased sensitivity was noted for all analytes when the injection time was increased from 10 s to 30 s (Fig. 3A and 3B). A further increase of the injection time resulted in decreased peak heights for the slowest migrating analytes (see e.g. analytes 6 to 8 in Fig. 3C at an injection time of 50 s) or even a complete loss of analyte 8 at 70 s (Fig. 3D). The opposite behavior was observed for the faster migration analytes (see analytes 1 and 2 in Fig. 3). Similar data were obtained at 8 and 10 kV (data not shown).

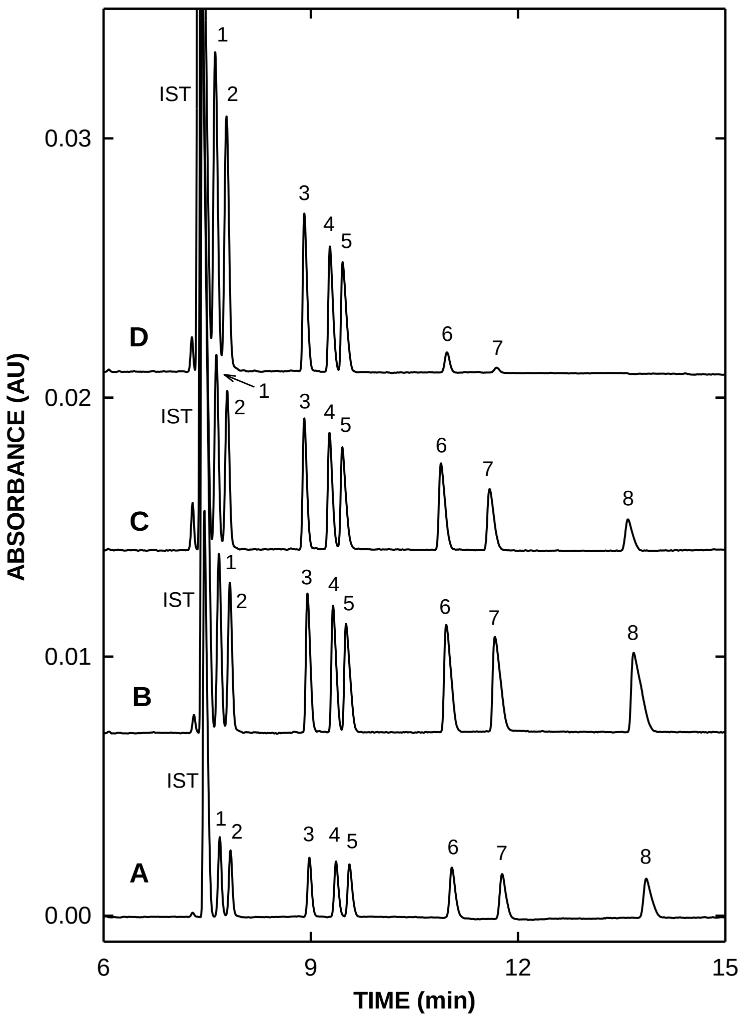

Figure 3. Electropherograms illustrating the impact of the duration of electrokinetic injection at 6 kV across a 50 mM buffer plug formed at 1 psi for 20 s having injection times of (A) 10 s, (B) 30 s, (C) 50 s and (D) 70 s. For presentation purposes, electropherograms were aligned for equal detection time of the IST. Other conditions and key as for Fig. 1.

The penetration of HS-γ-CD from the BGE through the buffer plug into the sample vial during electrokinetic injection is believed to be the reason for this behavior. Electrokinetic injection at 6 kV for 15 s was considered suitable for the purpose of the undertaken project (Fig. 4).

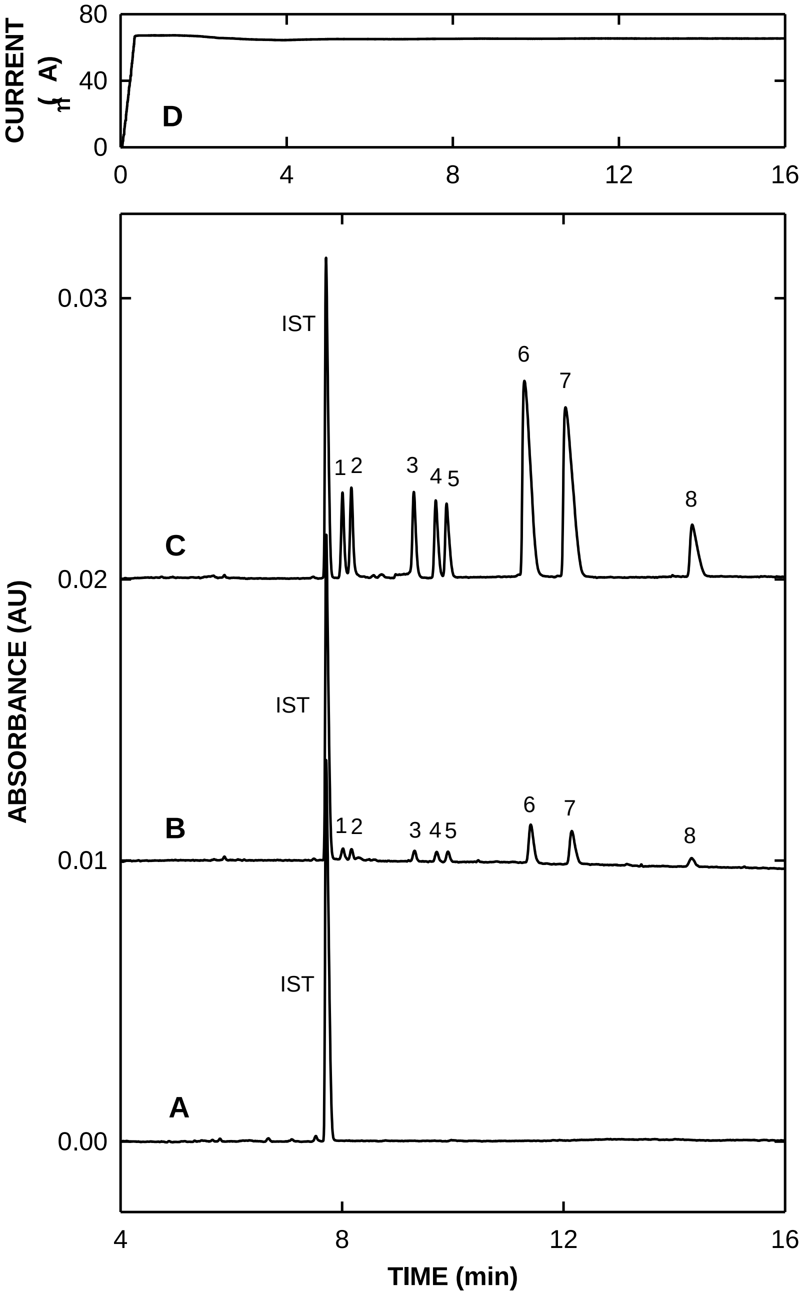

Figure 4 Enantioselective electropherograms of (A) a blank serum extract, (B) an extract of a calibration sample containing 80 ng/mL ketamine and 20 ng/mL of each metabolite and enantiomer, and (C) an extract of a calibration sample containing 800 ng/mL ketamine and 200 ng/mL of each metabolite and enantiomer. The graph in panel D depicts the temporal behavior of the current recorded during analysis of the extracted calibration sample of panel C. Extracts were prepared as described in Section 2.3. Samples were applied via a 15 s injection at 6 kV across a 50 mM buffer plug generated at 1 psi for 20 s. For presentation purposes, electropherograms were aligned for equal detection time of the IST. Key as for Fig. 1.

3.4.3 Impact of sample composition and electrode assembly on electrokinetic injection

Efficiency of electrokinetic injection of cations is dependent on sample composition, particularly conductivity and pH, properties which should both be low [8–11,19]. Thus, addition of 45.5, 90.9, 228 and 455 µM of phosphoric acid to the sample was assessed for the analytes of interest using the configuration with a 50 mM plug buffer concentration, a 1 psi 20 s plug and analyte injection at 6 kV for 15 s. Small amounts of phosphoric acid provided increased sensitivity. Largest peaks were monitored with 90.9 µM phosphoric acid in the sample solution, with the peak magnitudes being twice compared to the case without phosphoric acid. A further increase in phosphoric acid resulted in peaks that became smaller as function of the phosphoric acid concentration. With 228 µM, analyte peaks were smaller compared to those without acid in the sample. Comparable data were obtained after extraction of the analytes from aqueous solutions using dichloromethane according to the description given in Section 2.3. Based on these data, 90.9 µM was used in all samples.

In order to find the best liquid/liquid extraction procedure for electrokinetic analyte injection, bovine serum samples were extracted at alkaline pH with three organic solvents, hexane, ethylacetate and dichloromethane, or mixtures of two of these solvents. Ketamine, norketamine and DHNK can be extracted with all three solvents or their binary mixtures. However, hexane and mixtures with hexane were found to insufficiently extract the hydroxylated norketamine metabolites. Somewhat better results were obtained with ethylacetate and good data were obtained with the previously employed mixture of ethylacetate/dichloromethane (25:75 %, *v/v*). Extracts prepared with dichloromethane alone resulted in the largest analyte peaks. Thus, extraction recovery was measured in triplicates by using samples with up to 8.6 µg/mL amounts of each compound and hydrodynamic sample injection (1 psi for 5 s) in order to exclude any bias associated with electrokinetic injection. For all compounds involved, ketamine, norketamine, DHNK, 6HNK and the internal standard, recoveries were between 51 and 65 % with the lowest values obtained for the enantiomers of DHNK. These values are lower compared to those found for the ethylacetate/dichloromethane (25:75 %, *v/v*) system (between 71-82 % [31,32]). It is assumed that extracts prepared with dichloromethane have a lower conductivity compared to those obtained with the ethylacetate/dichloromethane mixture. Despite the lower recovery obtained with dichloromethane, this solvent was used to prepare the samples as it provided larger peaks in the electropherograms. Typical electropherograms obtained with blank bovine serum, an extract of a calibration sample containing 80 ng/mL ketamine and 20 ng/mL of each metabolite and enantiomer, and an extract of a calibration sample containing 800 ng/mL ketamine and 200 ng/mL of each metabolite and enantiomer are presented in panels A, B and C, respectively, of Fig. 4. It is important to note that evaporation of the solvent under a stream of air at 37 °C as used previously with 100 to 1000 µL samples did not provide sufficient reproducibility. Dichloromethane evaporation at 45 °C in a Speed-Vac Concentrator, however, resulted in reproducible data (for procedure and data see Sections 2.3 and 3.2, respectively).

Finally, the efficiency of electrokinetic injection is known to be affected by the distance between the capillary end and the electrode [6,7]. With the instrument used, capillary and electrode are arranged in parallel, the distance between them is about 2 mm and the positions of their ends cannot be varied much. Experiments executed with the capillary end positioned about 2 mm longer compared to the end of the electrode, provided analyte peaks that were slightly larger (about 5 %) compared to those obtained with capillary and electrodes aligned at the same level. On the other hand, retraction of the capillary by about 2 mm compared to the electrode end resulted in about 35 % larger analyte peaks. Thus, this latter configuration was employed in this work.

3.4.4 Assay characterization

For the purpose of this work with dog plasma samples collected after administration of a bolus of racemic ketamine or S-ketamine, a calibration range of 80 to 2000 ng/mL was employed for the two ketamine enantiomers whereas that of the stereoisomers of norketamine, DHNK and 6HNK were four-fold lower (Section 2.2). Typical calibration data obtained with dichloromethane extracts are presented in Fig. 4. Assay control was performed with two independent bovine serum control samples (Section 2.2), one comprising 240 ng/mL of each ketamine enantiomer and 60 ng/mL of each enantiomer of NK, DHNK and 6HNK, the second with 1.76 µg/mL of each ketamine enantiomer and 440 ng/mL of each enantiomer of the three metabolites. Detection time variation was assessed with analysis of these two control samples. Intraday (n=8) data revealed RSD values that were dependent on analyte detection time and increased between the first (internal standard) and last (R-DHNK) detected compounds from 1.17 % to 2.47 % for the control sample with the lower concentrations. Corresponding values for the sample with higher concentrations were between 1.22 and 2.75 %. All 8 samples of the two groups were analyzed alternatively the same day within a 6 h period. Close inspection of the data revealed a continuous small decrease of detection time which was more pronounced for analytes with higher detection times. As example, for the sample with the lower concentrations, the detection times of the internal standard decreased from 8.26 to 7.98 min first and 8th sample whereas corresponding data for R-DHNK changed between 17.11 and 15.90 min. Similar values were obtained with the sample comprising higher concentrations. Reasons for these drifts were not investigated and the drifts had no deleterious impact on quantification of analytes (see below). Interday (n=8) RSD values of detection times also found to be dependent on the analyte detection time interval and increased between 5.31 and 10.97 % for the sample with lower concentrations and between 6.22 and 13.68 % for the other sample. These values are higher compared to those observed for analyses of ketamine and norketamine enantiomers with hydrodynamic sample injection. In the assay of Sandbaumhüter et al. [32] intraday and interday RSD values of the enantiomers of ketamine and norketamine were around 1 % and 3 %, respectively, and were not observed to be detection time dependent. The rather large interday RSD values for detection times in the microassay did not prohibit quantification of plasma samples as assay calibration and analysis of sets of dog samples were performed under the same conditions. Unidentified aging processes of the chiral selector used are believed to contribute to changes in detection times. Within a few months with the same reagent bottle, the amount of HS-γ-CD in the BGE had to be slightly changed (e.g. from 0.66 to 0.64 %) in order to obtain comparable separations. This change had an impact on detection times.

For assay calibration five bovine serum calibrators as described in Section 2.2 were prepared and extracted as described in Section 2.3. The calibration curves (n=8) were found to be linear with the mean values of the determination coefficient R^2 being between 0.9961 and 0.9979 (Table 1, RSD range: 0.13 to 0.26%). RSD values of the slopes ranged between 2.97 and 5.34 % (Table 1). The interday and intraday repeatability of quantitative results was analyzed with the two control samples. Electropherograms used for this evaluation were the same as those whose detection times are presented above. Typical intraday RSD values (n=8) for the expected amounts were between 2.05 and 4.63 % and for the interday data (n=8) between 4.56 and 8.99 % (Table 1). These data indicate that the developed microassay with electrokinetic sample injection is robust. For each enantiomer, the LOQ with the performed calibration was 10 ng/mL. Compared to the anionic assays with hydrodynamic sample injection and reconstitution of the extract in the same sample volume, a 50-fold sensitivity enhancement was reached.

Table 1. Typical calibration, intraday and interday data [a)]

Enantiomer	Slope of calibration graph [b)]		Correlation coefficient R^2		Target concen-tration level (ng/mL)	Intraday data		Interday data	
	Mean	RSD (%)	Mean	RSD (%)		Mean (ng/mL)	RSD (%)	Mean (ng/mL)	RSD (%)
R-ketamine	0.0306	3.11	0.9967	0.26	240.0	270.8	2.10	244.6	6.49
					1760	1796	2.32	1898	6.14
S-ketamine	0.0280	3.57	0.9969	0.24	240.0	264.8	2.05	245.0	5.71
					1760	1824	2.10	1912	5.07
R-norketamine	0.0263	2.98	0.9972	0.16	60.00	69.06	3.15	63.30	8.82
					440.0	464.3	2.57	476.6	7.80
S-norketamine	0.0246	3.25	0.9974	0.22	60.00	68.36	2.60	62.62	7.40
					440.0	480.5	2.57	491.8	8.99
R-DHNK	0.0205	5.34	0.9975	0.13	60.00	64.32	3.35	55.88	6.50
					440.0	463.7	2.77	447.7	5.11
S-DHNK	0.0234	3.67	0.9979	0.15	60.00	64.80	4.39	58.60	4.94
					440.0	457.7	2.79	444.4	6.24
RR-6HNK	0.0287	2.97	0.9961	0.20	60.00	69.80	4.63	68.08	8.13
					440.0	435.1	2.33	474.3	7.00
SS-6HNK	0.0309	4.00	0.9966	0.16	60.00	68.20	3.53	65.22	4.56
					440.0	474.2	2.34	488.9	6.27

a) Mean of 8 determinations.
b) Interday data. Calibrations with concentrations and ratios of corrected peak areas taken as x and y values, respectively.

3.4.5 Assay application to dog plasma samples

In the context of a clinical pharmacokinetic study, the described microassay was employed to analyze the 8 compounds in more than 550 plasma samples collected before and after bolus injection of 2 mg/kg S-ketamine or 4 mg/kg racemic ketamine to Beagle dogs that were anesthetized under various conditions. Samples were analyzed over a four month period. Typical electropherograms obtained from dog samples that were collected under sevoflurane anesthesia are presented in Fig. 5.

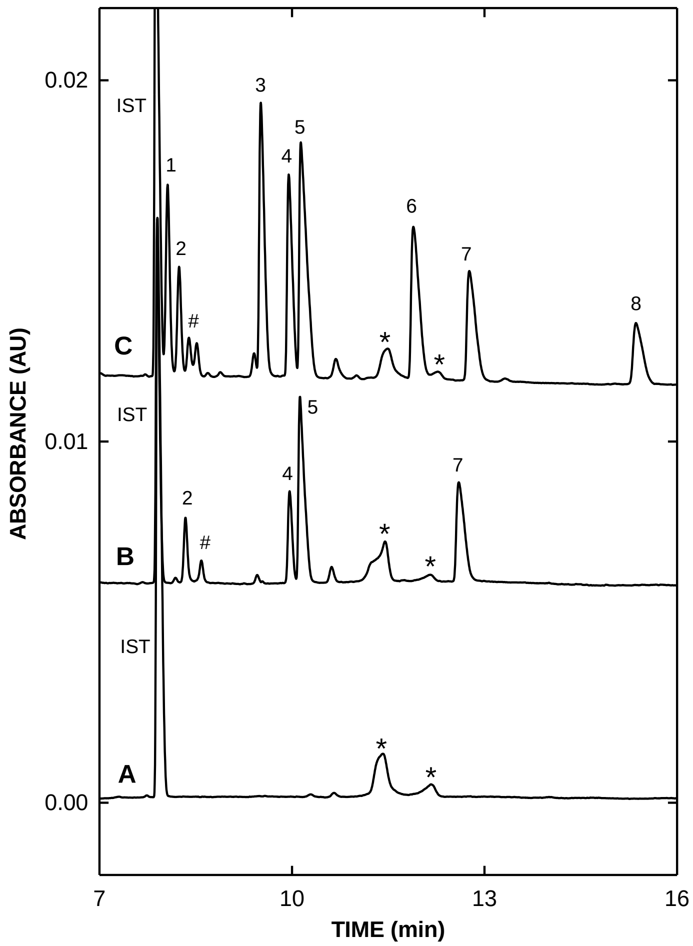

Figure 5. Enantioselective electropherograms of plasma extracts of samples collected (A) before and (B,C) 20 min after bolus administration of (B) 2 mg/kg S-ketamine and (C) 4 mg/kg racemic ketamine to a Beagle dog under sevoflurane anaesthesia. The asterisks mark peaks originating from sevoflurane and # denote peaks of unidentified hydroxylated norketamine metabolites. For presentation purposes, electropherograms were aligned for equal detection of the IST. Procedures and key as for Figs. 4 and 1, respectively.

Analysis of the sample collected prior to ketamine infusion (Fig. 5A) did not reveal any peaks for the compounds of interest. However, peaks originating from sevoflurane that did not interfere with ketamine or its metabolites were detected (marked with asterisks in Fig. 5). Panel B of Fig. 5 depicts data obtained with a sample collected 20 min after infusion of S-ketamine. In this sample, S-ketamine, S-norketamine, S-DHNK and SS-HNK were detected at levels of 326.6, 202.4, 545.6 and 120.6 ng/mL, respectively. Data obtained at the same time point after infusion of racemic ketamine to the same dog after a washout period of several weeks, did reveal both S- and R-stereoisomers of the four compounds (Fig. 5C). The R/S concentrations of ketamine, norketamine, DHNK and HNK were calculated to be 255.4/212.4, 368.6/297.4, 123.4/483.8 and 317.0/116.6 ng/mL, respectively.

Plasma levels for the time periods up to 600 min after drug administration are presented in Fig. 6. The data presented indicate that ketamine is being eliminated in an exponential fashion within about 300 min. After administration of racemic ketamine, the concentrations of both ketamine enantiomers are identical (Fig. 6D). Data evaluation with the Mann-Whitney Rank Sum Test revealed a P value of 0.813 which means there is not a statistically significant difference. The same is true for the comparison of the S-ketamine levels for the cases of racemic and S-ketamine drug administration (P = 0.844).

Norketamine is formed quickly, reaches a maximum concentration at 10 min and becomes eliminated thereafter within about 400 min (Fig. 6C). After administration of racemic ketamine, the concentrations of both norketamine enantiomers do not differ from a statistical point of view (P = 0.430) and the same is true for the comparison of the S-norketamine levels for the cases of racemic and S-ketamine drug administration (P = 0.650).

DHNK is formed more slowly compared to norketamine and reaches maximum concentrations at 45 min. The elimination is also more slowly and completed after about 600 min (Fig. 6B). DHNK is formed in a stereoselective manner with S-DHNK plasma levels being much higher compared to those of R-DHNK (P = 0.003). S-DHNK levels for the cases of racemic and S-ketamine drug administration do not differ significantly (P = 0.969). Finally, there is more RR-6HNK formed compared to SS-6HNK (P = 0.018) and these metabolites are formed and eliminated in time intervals comparable to those of DHNK (Fig. 6A). SS-6HNK levels for the cases of racemic and S-ketamine drug administration do not differ significantly (P = 0.790). These data reveal that there are stereoselectivities involved in the metabolism of ketamine in dogs. These aspects will we further discussed with the data of the whole clinical study which will also include the determinations of pharmacokinetic parameters.

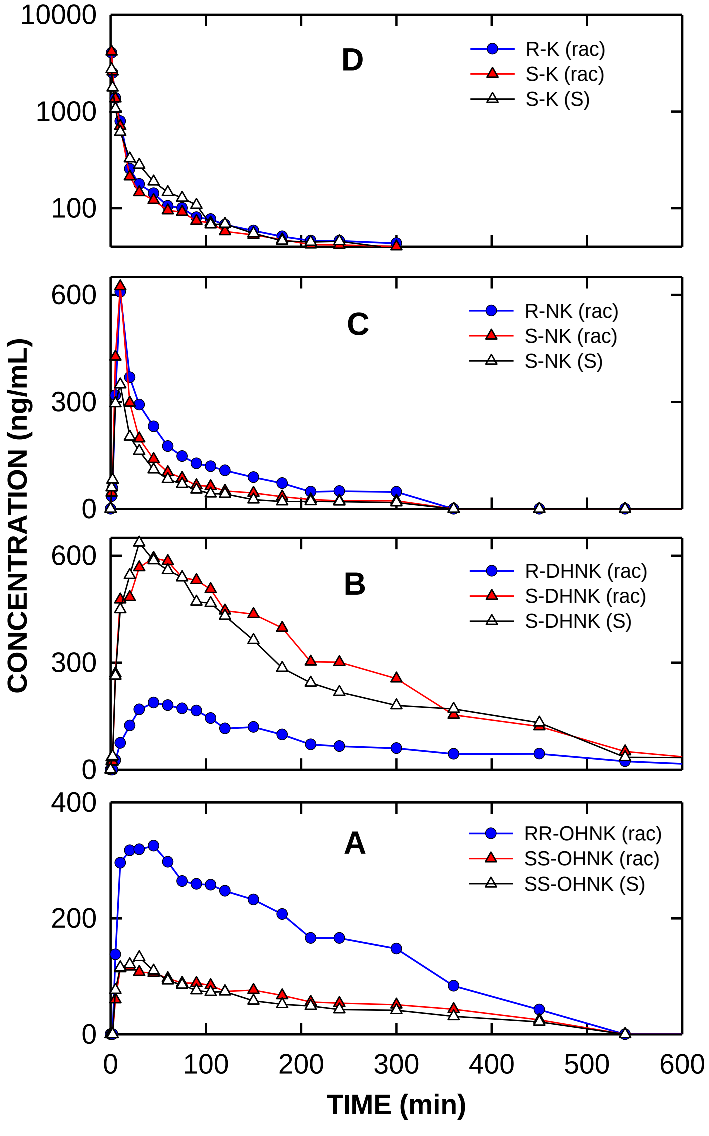

Figure 6. (A) Ketamine, (B) norketamine, (C) DHNK and (D) 6HNK levels monitored after injection of a bolus of 4 mg/kg racemic ketamine (referred to as rac) or 2 mg/kg S-ketamine (referred to as S) to a Beagle dog under sevoflurane anesthesia.

From an analytical point of view, the quantitative data presented for RR-6HNK and SS-6HNK should be considered with caution. First, insufficient amounts of the two standards were available to make multiple independent calibrations. Thus, deviations from the real values of up to 10 % can be expected. Second, SS-6HNK corresponds to the previously unidentified hydroxynorketamine metabolite S-I [24,31]. Under the conditions of the described microassay, this metabolite was found to comigrate with R-IV which is another hydroxynorketamine metabolite [24] (data not shown). Similarly, RR-6HNK represents R-I [24,31] and comigrates under the conditions of the microassay with the S-IV hydroxynorketamine metabolite. According to in vitro work performed with canine liver microsomes, no formation of R-IV and small amounts of S-IV were observed [31]. Furthermore, metabolite IV is known to be conjugated to an appreciable extent [24]. The microassay described, however, does not include hydrolysis of conjugated hydroxylated norketamine metabolites. Thus, the stereoselectivity observed in the data presented in Fig. 6A should not be affected by metabolite IV. Furthermore, it was interesting to find that the peaks in Fig. 5B and 5C detected shortly after those of 6HNK represent those of the unidentified hydroxynorketamine metabolite III of [24,31] with R-III being detected before S-III. The lack of standards still prevents proper identification of metabolites III and IV. More work is required to find experimental conditions to completely separate the stereoisomers of all major hydroxylated norketamine metabolites in a cationic assay format. This is particularly important in view of the recent findings that SS-6HNK has a potent pharmacological activity both in vitro and in vivo [35,36].

3.5 Concluding remarks

With the newly developed microassay which uses electrokinetic sample injection and cationic separation of analytes in presence of small amounts of HS-γ-CD it was possible to determine the enantiomers of ketamine and three of its major metabolites in only 50 µL of plasma or serum and with an LOQ of 10 ng/mL. The microassay is more sensitive, requires less sample, uses less organic solvent and has a lower analysis time compared to our previous assays which were based on anionic separations and hydrodynamic sample injection. LOQs of ≤ 1 ng/mL could be reached with minor modifications, namely by increasing the time interval for electrokinetic analyte injection (e.g. to 20 or 25 s, see Fig. 3), use of 25 mM buffer in the plug instead of the 50 mM used in this assay (see Fig. 2) and/or reconstitution of the extract in a smaller volume. The applicability of the latter aspect is instrument dependent. For the instrument used in this work, nanovials holding about 10-fold smaller volumes should become available soon. Electrokinetic sample injection is effected across a buffer plug without chiral selector. Diluted buffer in the plug provided the combined action of field amplification and complexation used for analyte stacking. The microassay was successfully applied to monitor the enantiomers of ketamine and three of its metabolites in dog plasma. The microassay is robust and reproducible (interday RSD < 9 %). Sets of 30 samples could be analyzed without changing running buffer. For precise quantitative analysis with electrokinetic injection, the use of an internal standard is necessary and sample extracts have to be very clean (low conductivity). Furthermore, injections of buffer for the plug and sample have to be performed with accurate control of time, pressure and voltage. Commercial instrumentation is fulfilling these requirements. CE with electrokinetic sample injection provides ppb sensitivity and is thus an attractive alternative to HPLC.

Acknowledgements

The authors are grateful to Dr. Irving Wainer for receiving the standards of (2S,6S)-hydroxynorketamine and (2R,6R)-hydroxynorketamine. This work was supported by the Swiss National Science Foundation.

Conflicts of interest

The authors have declared no conflict of interest.

3.6 References

[1] Z. Malá, A. Šlampová, L. Křivánková, P. Gebauer, P. Boček, Contemporary sample stacking in analytical electrophoresis, Electrophoresis 36 (2015) 15–35.

[2] M. C. Breadmore, R. M. Tubaon, A. I. Shallan, S. C. Phung, A. S. Abdul Keyon, D. Gstoettenmayr, P. Prapatpong, A. A. Alhusban, L. Ranjbar, H. H. See, M. Dawod, J. P. Quirino, Recent advances in enhancing the sensitivity of electrophoresis and electrochromatography in capillaries and microchips (2012-2014), Electrophoresis 36 (2015) 36–61.

[3] D.-S. Lian, S.-J. Zhao, J. Li, B.-L. Li, Progress in stacking techniques based on field amplification of capillary electrophoresis, Anal. Bioanal. Chem. 406 (2014) 6129–6150.

[4] F. Kitagawa, K. Otsuka, Editorial on "recent applications of on-line sample preconcentration techniques in capillary electrophoresis" by F. Kitagawa and K. Otsuka, J. Chromatogr. A 1335 (2014) 43–60.

[5] L. Sánchez-Hernández, M. Guijarro-Diez, M. L. Marina, A. L. Crego, New approaches in sensitive chiral CE, Electrophoresis 2014, 35, 12–27.

[6] T. Hirokawa, E. Koshimidzu, Z. Xu, Electrokinetic sample injection for high-sensitivity capillary zone electrophoresis (part 1): Effects of electrode configuration and setting, Electrophoresis 29 (2008) 3786–3793.

[7] Z. Xu, E. Koshimidzu, T. Hirokawa, Electrokinetic sample injection for high-sensitivity CZE (part 2): improving the quantitative repeatability and application of electrokinetic supercharging-CZE to the detection of atmospheric electrolytes, Electrophoresis 30 (2009) 3534–3539.

[8] C.-X. Zhang, W. Thormann, Head-column field-amplified sample stacking in binary system capillary electrophoresis: A robust approach providing over 1000-fold sensitivity enhancement, Anal. Chem. 68 (1996) 2523–2532.

[9] C.-X. Zhang, W. Thormann, Head-column field-amplified sample stacking in binary system capillary electrophoresis. 2. Optimization with a preinjection plug and application to micellar electrokinetic chromatography, Anal. Chem. 70 (1998) 540–548.

[10] C.-X. Zhang, Y. Aebi, W. Thormann, Microassay of amiodarone and desethylamiodarone in serum by capillary electrophoresis with head-column field-amplified sample stacking, Clin. Chem. 42 (1996) 1805–1811.

[11] A. B. Wey, C.-X. Zhang, W. Thormann, Head-column field-amplified sample stacking in binary system capillary electrophoresis. Preparation of extracts for determination of opioids in microliter amounts of body fluids, J. Chromatogr. A 853 (1999) 95–106.

[12] S. Zaugg, W. Thormann, Enantioselective determination of drugs in body fluids by capillary electrophoresis, J. Chromatogr. A 875 (2000) 27–41.

[13] P. S. Bonato, Recent advances in the determination of enantiomeric drugs and their metabolites in biological fluids by capillary electrophoresis-mediated microanalysis, Electrophoresis 24 (2003) 4078–4094.

[14] P. Mikuš, K. Maráková, Advanced CE for chiral analysis of drugs, metabolites, and biomarkers in biological samples, Electrophoresis 30 (2009) 2773–2802.

[15] J. Caslavska, W. Thormann, Stereoselective determination of drugs and metabolites in body fluids, tissues and microsomal preparations by capillary electrophoresis (2000–2010), J. Chromatogr. A 1218 (2011) 588–601.

[16] C. Gausepohl, G. Blaschke, Stereoselective determination of clenbuterol in human urine by capillary electrophoresis, J. Chromatogr. B 713 (1998) 443–446.

[17] J.-M. Dethy, S. De Broux, M. Lesne, J. Longstreth, P. Gilbert, Stereoselective determination of verapamil and norverapamil by capillary electrophoresis, J. Chromatogr. B 654 (1994) 121–127.

[18] S.-C. Lee, C.-C. Wang, P.-C. Yang, S.-M., Wu, Enantioseparation of (±)-threo-methylphenidate in human plasma by cyclodextrin-modified sample stacking capillary electrophoresis, J. Chromatogr. A 1232 (2012) 302–305.

[19] R. Theurillat, W. Thormann, Monitoring of threo-methylphenidate enantiomers in oral fluid by capillary electrophoresis with head-column field-amplified sample injection, Electrophoresis 35 (2014) 986–992.

[20] J. Schappler, D. Guillarme, J. Prat, J.-L. Veuthey, S. Rudaz, Enhanced method performances for conventional and chiral CE-ESI/MS analyses in plasma, Electrophoresis 27 (2006) 1537–1546.

[21] J. Schappler, D. Guillarme, J. Prat, J.-L. Veuthey, S. Rudaz, Validation of chiral capillary electrophoresis-electrospray ionization-mass spectrometry methods for ecstasy and methadone in plasma, Electrophoresis 29 (2008) 2193–2202.

[22] R. Theurillat, M. Knobloch, O. Levionnois, P. Larenza, M. Mevissen, W. Thormann, Characterization of the stereoselective biotransformation of ketamine to norketamine via determination of their enantiomers in equine plasma by capillary electrophoresis, Electrophoresis 26 (2005) 3942–3951.

[23] R. Theurillat, M. Knobloch, A. Schmitz, P. G. Lassahn, M. Mevissen, W. Thormann, Enantioselective analysis of ketamine and its metabolites in equine plasma and urine by CE with multiple isomer sulfated beta-CD, Electrophoresis 25 (2007), 2748–2757.

[24] A. Schmitz, R. Theurillat, P.-G. Lassahn, M. Mevissen, W. Thormann, CE provides evidence of the stereoselective hydroxylation of norketamine in equines, Electrophoresis 30 (2009) 2912–2921.

[25] M. Knobloch, C. J. Portier, O. L. Levionnois, R. Theurillat, W. Thormann, C. Spadavecchia, M. Mevissen, Antinociceptive effects, metabolism and disposition of

ketamine in ponies under target-controlled drug infusion, Toxicol. Applied Pharmacol. 216 (2006), 373–386.

[26] M.P. Larenza, M.F. Landoni, O.L. Levionnois, M. Knobloch, P.W. Kronen, R. Theurillat, U. Schatzmann, W. Thormann, Stereoselective pharmacokinetics of ketamine and norketamine after racemic ketamine or S-ketamine administration during isoflurane anaesthesia in Shetland ponies, Br. J. Anaesth. 98 (2007) 204–212.

[27] M.P. Larenza, M. Knobloch, M.F. Landoni, O.L. Levionnois, P.W. Kronen, R. Theurillat, U. Schatzmann, W. Thormann, Stereoselective pharmacokinetics of ketamine and norketamine after racemic ketamine or S-ketamine administration in Shetland ponies sedated with xylazine, Vet. J. 177 (2008) 432–435.

[28] C. Peterbauer, M. P. Larenza, M. Knobloch, R. Theurillat, W. Thormann, M. Mevissen, C. Spadavecchia, Effects of a low dose infusion of racemic and S-ketamine on the nociceptive withdrawal reflex in standing ponies, Vet. Anaesth. Analg. 35 (2008) 414–423.

[29] A. Schmitz, C. J. Portier, W. Thormann, R. Theurillat, M. Mevissen, Stereoselective biotransformation of ketamine in equine liver and lung microsomes, J. Vet. Pharmacol. Ther. 31 (2008), 446–455.

[30] S. Portmann, H.Y. Kwan, R. Theurillat, A. Schmitz, M. Mevissen, W. Thormann, Enantioselective capillary electrophoresis for identification and characterization of human cytochrome P450 enzymes which metabolize ketamine and norketamine in vitro, J. Chromatogr. A 1217 (2010) 7942–7948.

[31] A. Schmitz, W. Thormann, L. Moessner, R. Theurillat, K. Helmja, M. Mevissen, Enantioselective CE analysis of hepatic ketamine metabolism in different species in vitro, Electrophoresis 31 (2010) 1506–1516.

[32] F.A. Sandbaumhüter, R. Theurillat, W. Thormann, Effects of medetomidine and its active enantiomer dexmedetomidine on N-demethylation of ketamine in canines determined in vitro using enantioselective capillary electrophoresis, Electrophoresis 36 (2015) 2703–2712.

[33] R. Moaddel, S. L. V. Venkata, M.J. Tanga, J.E. Bupp, C.E. Green, L. Iyer, A. Furimsky, M.E. Goldberg, M.C. Torjman, I.W. Wainer, A parallel chiral-achiral liquid chromatographic method for the determination of the stereoisomers of ketamine and ketamine metabolites in the plasma and urine of patients with complex regional pain syndrome, Talanta 82 (2010) 1892–1904.

[34] Z. Desta, R. Moaddel, E.T. Ogburn, C. Xu, A. Ramamoorthy, S. L. V. Venkata, M. Sanghvi, M.E. Goldberg, M.C. Torjman, I.W. Wainer, Stereoselective and regiospecific hydroxylation of ketamine and norketamine, Xenobiotica 42 (2012) 1076–1087.

[35] R.K. Paul, N.S. Singh, M. Khadeer, R. Moaddel, M. Sanghvi, C.E. Green, K. O'Loughlin, M.C. Torjman, M. Bernier, I.W. Wainer, (R,S)-Ketamine metabolites (R,S)-norketamine and (2S,6S)-hydroxynorketamine increase the mammalian target of rapamycin function, Anesthesiology 121 (2014) 149–159.

[36] N. S. Singh, C. A. Zarate, R. Moaddel, M. Bernier, I. W. Wainer, What is hydroxynorketamine and what can it bring to neurotherapeutics?, Expert Rev. Neurother. 14 (2014) 1239–1242.

4. Pharmacokinetics of ketamine and three metabolites in Beagle dogs under sevoflurane vs. medetomidine comedication assessed by enantioselective capillary electrophoresis (J. Chromatogr. A 1467 (2016) 436-444)

Friederike A. Sandbaumhüter[1], Regula Theurillat[1], Rima N. Bektas[2], Annette P. N. Kutter[2], Regula Bettschart-Wolfensberger[2], Wolfgang Thormann[1]

[1] Clinical Pharmacology Laboratory, University of Bern, Bern, Switzerland
[2] Section of Anaesthesiology, Equine Department, Vetsuisse Faculty, University of Zürich, Zürich, Switzerland

4.1 Abstract

Ketamine is often used for anesthesia in veterinary medicine. One possible comedication is the sedative α_2-agonist medetomidine. Advantages of that combination are the compensation of side effects of the two drugs and the anesthetic-sparing effect of medetomidine. In vitro studies showed that medetomidine has an inhibitive effect on the formation of norketamine. Norketamine is the first metabolite of ketamine and is also active. It is followed by others like 6-hydroxynorketamine (6HNK) and 5,6-dehydronorketamine (DHNK). In an in vivo pharmacokinetic study Beagle dogs under sevoflurane anesthesia (mean end-tidal concentration 3.0 ± 0.2 %) or following medetomidine sedation (450 µg/m^2) received 4 mg/kg racemic ketamine or 2 mg/kg S-ketamine. Blood samples were collected between 0 and 900 min after drug injection. 50 µL aliquots of plasma were pretreated by liquid-liquid extraction prior to analysis of the reconstituted extracts with a robust enantioselective capillary electrophoresis assay using highly sulfated γ-cyclodextrin as chiral selector and electrokinetic sample injection of the analytes from the extract across a short buffer plug without chiral selector. Levels of S- and R-ketamine, S- and R-norketamine, SS- and RR-6HNK and S- and R-DHNK were determined. Data were analyzed with compartmental pharmacokinetic models which included two compartments for the ketamine and norketamine enantiomers and a single compartment for the DHNK and 6HNK stereoisomers. Medetomidine showed an effect on the formation and elimination of all metabolites.

Stereoselectivities were detected for 6HNK and DHNK, but not for ketamine and norketamine.

4.2 Introduction

The combination of the anesthetic drug ketamine and the sedative drug medetomidine is often used in veterinary medicine and sometimes also for humans. The benefits of this combination include the compensation of side effects of both drugs and the anesthetic sparing effect of medetomidine. Medetomidine decreases tachycardia, hypertension, salivation or muscular rigidity caused by ketamine whereas ketamine compensates bradycardia or hypotension induced by medetomidine [1–5]. Ketamine, a racemic drug (for chemical structure see Fig. 1A), is a N-methyl-d-aspartate (NMDA) receptor antagonist which is well known in anesthesia but also used in analgesia and in the therapy of depressive disorders [6–9]. The S-enantiomer has a stronger affinity to the receptor [8,10–12] which is the reason that S-ketamine is registered in some countries as a drug for humans and for selected animals. Medetomidine, also a racemate, is an α_2-receptor agonist. It is used for sedation or as an adjuvant in anesthesia. Only the S-enantiomer dexmedetomidine is pharmacologically active [1–4,13]. Both enantiomers are able to inhibit cytochrome P450 (CYP) enzymes whereas levomedetomidine is the stronger inhibitor [1,3,4]. Besides advantages, drug combinations have always the risk of pharmacokinetic or pharmacodynamic interactions. Most of the pharmacokinetic interactions can be handled by dose adaptation. For that purpose, as much as possible about the mechanisms of the interaction has to be known.

In vitro experiments with canine liver microsomes and the single canine enzyme CYP3A12 revealed an inhibitive effect of medetomidine on the N-demethylation of ketamine to norketamine [14]. Norketamine is the first and also an active metabolite of ketamine. Furthermore, hydroxylation of ketamine and norketamine at the cyclohexanone and chlorophenyl rings takes place. All these metabolic steps are catalyzed by CYP enzymes [11,15–18]. Another metabolite is dehydronorketamine (DHNK). Chemical structures of selected ketamine metabolites are presented in Fig. 1A. Enzymes of the CYP family are also involved in the metabolism of medetomidine and the main metabolite is hydroxymedetomidine [1]. Thus, both drugs compete for the active site of the enzyme.

Medetomidine as imidazole derivative is also able to bind at the heme iron in the active site of the enzyme which results in an inactivation of the enzyme [4].

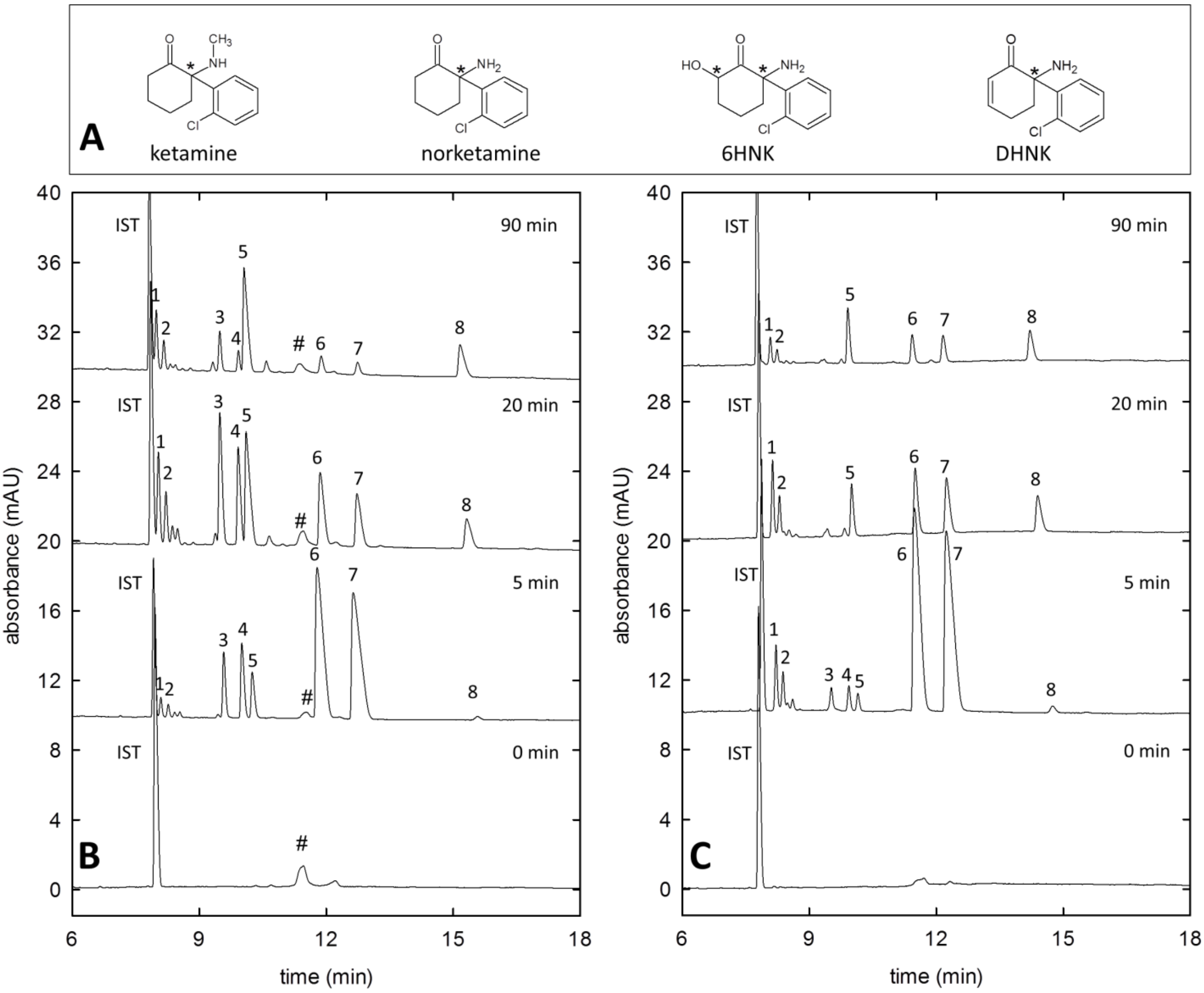

Figure 1. (A) Chemical structures of ketamine, norketamine, 6HNK and DHNK, and electropherograms of plasma extracts of samples collected before and after 5, 20 and 90 min of injection of 4 mg/kg racemic ketamine to (B) a Beagle dog under sevoflurane anesthesia and (C) a Beagle dog under medetomidine sedation. Asterisks mark the chiral centers in the chemical structures and peaks marked with # in the electropherograms stem from sevoflurane. Key: IST, internal standard; 1, RR-6HNK; 2, SS-6HNK; 3, R-norketamine; 4, S-norketamine; 5, S-DHNK; 6, R-ketamine; 7, S-ketamine; 8, R-DHNK.

In vitro experiments performed so far in regard to interactions of ketamine with a second drug like ketoconazole or medetomidine focused on the N-demethylation of ketamine to norketamine only [14,19–21]. The same applies to in vivo pharmacokinetics work performed in our laboratory [22,23]. Ketamine and norketamine concentrations were determined enantioselectively by capillary electrophoresis based methods using highly sulfated γ- or sulfated β-cyclodextrin as chiral selector. The recent development of a microassay with highly sulfated γ-cyclodextrin as chiral selector permits analysis and quantification of the enantiomers of ketamine, norketamine, 6-hydroxynorketamine (6HNK) and dehydronorketamine (DHNK) [24]. This assay was used to analyze enantiomers of ketamine and the three metabolites in plasma samples of Beagle dogs which received a bolus injection of 4 mg/kg racemic ketamine or 2 mg/kg S-ketamine under sevoflurane anesthesia or following medetomidine sedation. Blood samples were collected up to 15 hours after ketamine administration and determined enantiomer drug and metabolite levels were used to elucidate the pharmacokinetics via compartmental analysis. Most pharmacokinetic studies are focused only on ketamine and the first metabolite norketamine [25,26]. Only a few models include also the following metabolites [12,27–29]. To our knowledge, no pharmacokinetic study which considers the effect of another drug on the pharmacokinetics of ketamine, norketamine, 6HNK and DHNK has been published thus far.

The goals of this work were (i) to demonstrate the usefulness of enantioselective capillary electrophoresis for monitoring the levels of ketamine, norketamine, 6HNK and DHNK in dog plasma after bolus drug administration, (ii) to create a pharmacokinetic model for ketamine and the three metabolites, (iii) to calculate the pharmacokinetic parameters for the dogs of the sevoflurane and of the medetomidine groups and (iv) to elucidate enantioselective effects of medetomidine on the pharmacokinetics of ketamine, norketamine, 6HNK and DHNK.

4.3 Material and methods

4.3.1 Chemicals and reagents

Analytical standards for ketamine and norketamine (as hydrochlorides in methanol, 1 mg/mL of the free base), and DHNK (as hydrochloride 100 µg/mL in acetonitrile), were from Cerilliant (Round Rock, TX, USA). (2S,6S)-6-hydroxynorketamine (SS-6HNK) and (2R,6R)-6-hydroxynorketamine (RR-6HNK) were received from Dr. Irving Wainer (Laboratory of Clinical Investigations, National Institute on Aging, National Institutes of Health, Baltimore, MD, USA (synthesis described by Moaddel et al. and Desta et al. [30,31]). Highly sulfated γ-cyclodextrin (20 % *w/v* solution) was purchased from Beckman Coulter (Fullerton, CA, USA). D-(+)-norephedrine hydrochloride and bovine serum were from Sigma (St. Louis, Mo, USA). Disodium hydrogenphosphate, sodium hydroxide and bromothymol blue were from Merck (Darmstadt, Germany), phosphoric acid (85 %) was from Fluka (Buchs, Switzerland) and dichloromethane (HiPerSolv Chromanorm for HPLC) was from VWR (Leuven, Belgium). Ketamine injection solutions Ketasol-100 (racemic ketamine) and Keta-S (S-ketamine) used for the dog trials were from Dr. E. Graeub AG (Bern, Switzerland).

4.3.2 Pharmacokinetic animal study

Dog plasma samples were collected in clinical trials at Vetsuisse Faculty (Zürich, Switzerland) which were performed as prospective randomized crossover studies with the permission of the Committee for Animal Experimentation, Canton Zürich, Switzerland. In both trials the washing-out period was one month. Briefly, six Beagle dogs (3 female and 3 male) with a mean age of 39 (± 9) months under sevoflurane anesthesia (mean end-tidal concentration 3.0 ± 0.2 %) received an i.v. bolus injection of 4 mg/kg racemic ketamine (mean body mass was 15.15 ± 0.99 kg) or 2 mg/kg S-ketamine (mean body mass: 15.15 ± 1.01 kg). Another group of five Beagle dogs (2 female and 3 male) with a mean age of 21 (± 11) months was sedated with medetomidine (450 µg/m^2) prior to bolus injection of 4 mg/kg racemic ketamine (mean body mass: 11.68 ± 2.42 kg) or 2 mg/kg S-ketamine (mean body mass: 12.14 ± 2.50 kg). Venous blood samples were collected before ketamine administration and at 25 or 26 selected time intervals up to 900 min thereafter which included the complete elimination phase. The plasma was separated and stored at -80 °C until analysis.

4.3.3 Sample preparation

Sample preparation followed the procedure described in Ref. [24]. Briefly, analytes were extracted with dichloromethane at alkaline pH via addition of 200 µL water, 15 µL of 4 µg/mL d-(+)-norephedrine hydrochloride solution (internal standard), 50 µL of 0.5 M NaOH with 1.25 mM bromothymol blue and 1300 µL dichloromethane to 50 µL plasma. The vials were shacken and centrifuged. The upper aqueous phase was removed and the organic phase was transferred to a new vial and acidified with 10 µL of 1 mM phosphoric acid prior to drying in a Speed-Vac Concentrator (Vaudaux-Eppendorf, Schönenbuch, Switzerland) at 45 °C. After reconstitution with 110 µL water the samples were analyzed by enantioselective capillary electrophoresis.

4.3.4 Capillary electrophoresis instrumentation and analytical conditions

The analyses were performed on a Proteome Lab PA 800 enhanced instrument (Beckman Coulter, Fullerton, CA, USA) equipped with a photodiode array detector as described elsewhere [24]. Briefly, the 50 µm id fused-silica capillary (Polymicro Technologies, Phoenix, AZ, USA) with a total length of 45 cm (effective length 35 cm) was rinsed before each experiment with bidestilled water (1 min; 20 psi) and running buffer (1 min; 20 psi). The running buffer was composed of 100 mM disodium hydrogenphosphate buffer (pH 3.0) and 0.66 % highly-sulfated γ-cyclodextrin (Beckman Coulter, Fullerton, CA, USA). Before electrokinetic sample injection at 6 kV for 15 s, a plug of 50 mM disodium hydrogenphosphate buffer (pH 3.0) was injected by pressure (20 s; 1 psi). A voltage of 20 kV was applied and the current was about 64 µA. The detection was effected at 200 nm. The temperature for all parts was set to 25 °C. Analyte quantification was based on internal calibration using corrected peak areas. Assay calibration and control was performed with fortified bovine serum samples as is described in Ref. [24]. Typical electropherograms obtained with plasma samples of two dogs are presented in Fig. 1B und 1C.

4.3.5 Data analysis

Data were evaluated with Microsoft Excel (Microsoft, Redmont, WA, USA) and SigmaPlot software version 12.5 (Systat Software, San Jose, CA, USA. The Student's t-test and the Mann-Whitney Rank Sum Test were used to evaluate significant differences of two data sets. An overall value of $P < 0.05$ was considered significant. Pharmacokinetic modeling with compartmental analysis and noncompartmental analysis was performed with Phoenix WinNonlin 6.4 software (Certara: Implementing Translational Science, Cary, NC, USA).

4.4 Results and discussion

4.4.1 Chiral assay and data for ketamine and metabolites

With the applied microassay based on electrokinetic sample injection and cationic separation of analytes in presence of a small amount of highly sulfated γ-cyclodextrin it was possible to determine the enantiomers of ketamine and three of its major metabolites in 50 µL of plasma with a limit of quantification of 10 ng/mL of each enantiomer [24]. Electrokinetic sample injection associated with analyte stacking was effected across a buffer plug without chiral selector whose concentration was half that used for analyte separation. The microassay is robust, repeatable (interday RSD < 9 % [24]) and was successfully applied to monitor the enantiomers of ketamine and the three metabolites in about 600 dog plasma samples of this in vivo pharmacokinetic study. Samples were collected before and after bolus injection of 4 mg/kg racemic ketamine or 2 mg/kg S-ketamine to Beagle dogs that were either anesthetized with sevoflurane or sedated with medetomidine as is described in Section 2.2. Typical electropherograms obtained from a dog of both groups treated with racemic ketamine are presented in panels B and C, respectively, of Fig. 1.

For the group of anesthesia with sevoflurane, the sample collected prior to ketamine infusion did not reveal any peaks for the compounds of interest (Fig. 1B). However, peaks originating from sevoflurane that did not interfere with ketamine or its metabolites were detected (marked with #). Plasma samples collected 5, 20 and 90 min after infusion of 4 mg/kg racemic ketamine revealed peaks for all 8 compounds of interest that could be quantitated (Fig.1B). The same is true for the samples of the medetomidine group except that no peaks originating from medetomidine could be detected (Fig. 1C). Administration of 2 mg/kg S-ketamine instead of 4 mg/kg racemic ketamine resulted in electropherograms comprising the S-stereoisomers of ketamine, norketamine, 6HNK and DHNK only (for example see [24]) and drug levels of these S-stereoisomers were comparable to those monitored after administration of 4 mg/kg racemic ketamine. Comparison of the electropherograms between the two groups immediately revealed that medetomidine comedication resulted in the formation of much lower amounts of norketamine stereoisomers (compare e.g. 20 min electropherograms of panels B and C of Fig. 1). This aspect and those associated with stereoselectivities are further discussed in the context of the pharmacokinetic modeling described in Sections 3.2 and 3.3.

As mentioned in [24], the data for RR-6HNK and SS-6HNK should be considered with some caution. First, insufficient amounts of the two standards were available to make multiple independent calibrations. Thus, deviations from the real values of up to 10 % can be expected. Second, SS-6HNK comigrates with R stereoisomer of another hydroxynorketamine metabolite referred to as hydroxynorketamine IV in Refs. [16,24] (data not shown). Similarly, RR-6HNK comigrates with the S stereoisomer of this metabolite IV [24]. According to in vitro work performed with canine liver microsomes, no formation of R-IV and small amounts of S-IV were observed [32]. Furthermore, metabolite IV is known to be conjugated to an appreciable extent [16]. Thus, as the microassay described does not include hydrolysis of conjugated hydroxylated norketamine metabolites, the obtained data for RR-6HNK and SS-6HNK are not much enhanced due to comigration with metabolite IV. Efforts are currently under way to find conditions to resolve all known hydroxynorketamine stereoisomers in the assay format with electrokinetic sample injection from extracts of 50 µl of plasma.

4.4.2 Pharmacokinetic modeling of ketamine and its metabolites

Pharmacokinetic models describe the concentration of a drug which undergoes the processes of liberation, absorption, distribution, metabolism and elimination in the body as function of time. Modeling can be done with the aid of a polyexponential equation for which the coefficients have to be determined step-by-step manually or by comprehensive computer modeling using commercial software packages such as Phoenix WinNonlin [33]. Both approaches were used in our work and reveal the pharmacokinetic parameters for data comparison. For finding the best model for ketamine and the metabolites all concentration-time plots for one dog were analyzed phase by phase and compared to those obtained using Phoenix WinNonlin software. A schematic representation of pharmacokinetic modeling of ketamine and its metabolites is presented in Fig. 2.

Ketamine administered as an i.v. bolus goes immediately into blood circulation which is part of the central compartment as well as highly perfused tissues like the liver and the kidneys. The semilog plot of the determined S- and R-ketamine concentrations (logarithmic y-axis) as function of time (linear x-axis) showed two phases, the distribution and the elimination phases. This is typical for a two-compartment model and for drug application via bolus injection. The number of compartments which can be found for ketamine pharmacokinetic modeling in the literature varied between two and three and are depended on the administration procedure used [6,26,28,29,34]. Ketamine is distributed very fast into a second compartment, the so-called tissue or peripheral compartment, which includes skin and fatty tissues. The distribution is dependent on drug characteristics like lipophilicity and the tendency for protein-binding. Ketamine is eliminated from the central compartment by metabolic reactions mediated by CYP enzymes in the liver and other organs [11,17,18] or excreted unmodified via the kidneys. The data points of the elimination phase can be analyzed by linear regression analysis thereby revealing the slope β and the y-intercept $\ln(B)$. With this linear equation and the time points of the distribution phase concentration values are calculated and subtracted from the experimentally determined concentrations. After logarithmization, these results are plotted against time and subjected to linear regression analysis thereby revealing slope α and y-intercept $\ln(A)$. Finally the pharmacokinetics of ketamine can be described with the polyexponential equation $c = A*\exp(-\alpha*t)+B*\exp(-\beta*t)$ where c and t are the concentration and time, respectively.

Norketamine is always the first metabolite found after in vitro incubations and also in blood samples after ketamine administration in different species [16,32]. Hydroxylation of ketamine to hydroxyketamines is possible as well and it can take place on different positions on the rings in the molecule [8,15,16]. Norketamine is also an antagonist at the NMDA-receptor but its affinity is only one third of that of ketamine [6]. In contrast to the behavior of ketamine, there is first a phase in which the concentration of norketamine is rising from 0 to a maximum concentration, a fact that must be included in the kinetic model. The calculation starts as described above for ketamine, i.e. the elimination and distribution phases. Then the time points of the increasing concentration phase are inserted into the linear equation of the distribution phase. From the thereby calculated concentration the difference of the experimentally determined concentration and the concentration calculated with the linear equation of the elimination phase is subtracted. After logarithmization, results are plotted against time and analyzed with linear regression revealing the slope γ and the y-intercept $\ln(C)$. The kinetics of norketamine can thereby be described with a two-compartment model using $c=A*\exp(-\alpha*t)+B*\exp(-\beta*t)-C*\exp(-\gamma*t)$.

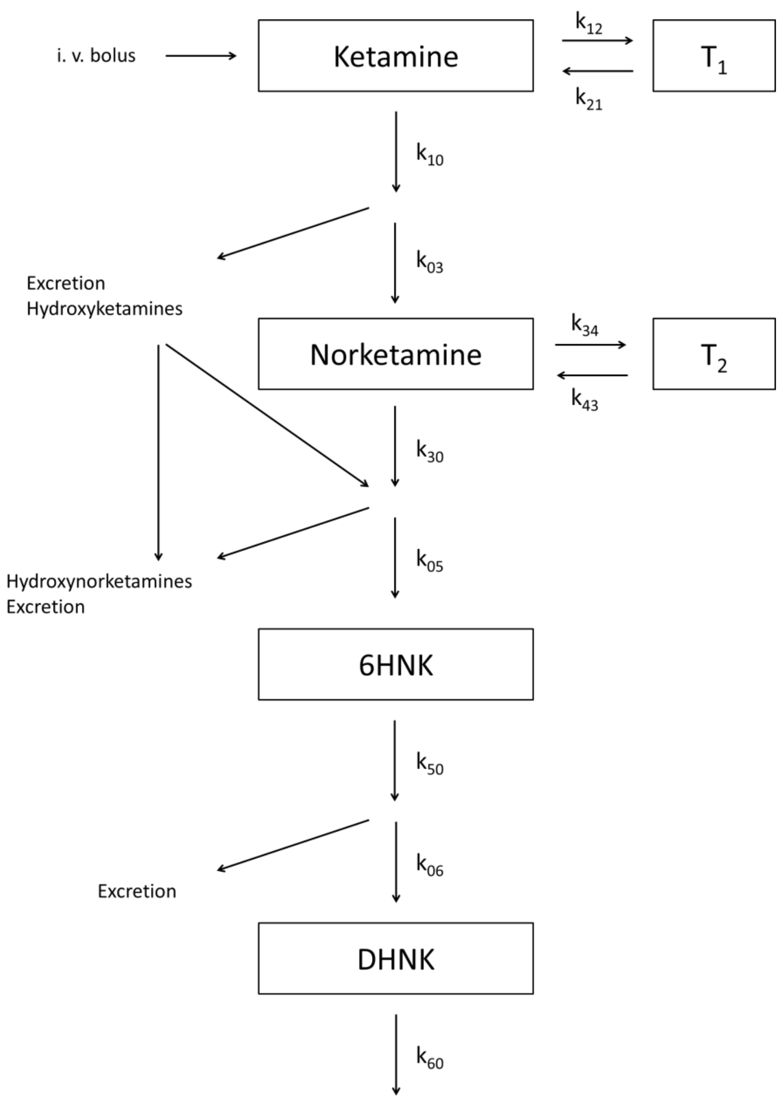

Figure 2. Schematic representation of pharmacokinetic modeling of ketamine and its metabolites based on two-compartment models for ketamine and norketamine and one-compartment models for 6HNK and DHNK enantiomers. The central compartments are labelled with ketamine, norketamine, 6HNK and DHNK. T1 and T2 are the tissue compartments for ketamine and norketamine, respectively. The k values represent inter-compartmental transfer constants.

Elimination of norketamine proceeds via hydroxylation at different positions and unmodified excretion via the kidneys. Although the possibility of direct formation of DHNK from norketamine is discussed in the literature [12,35], DHNK is more likely formed via loss of water from hydroxynorketamine, especially 6HNK and 5HNK [16]. It is not known whether DHNK is formed enzymatically or via a chemical reaction [16,36]. Urine of a pony which received ketamine was collected and fractionated by HPLC. Two fractions comprising hydroxynorketamine metabolites (one with RR- and SS-6HNK) also contained small amounts of DHNK. The appearance of DHNK in these fractions cannot be an impurity of the fractionation procedure because DHNK eluted more than 10 min after the hydroxynorketamine metabolites [16]. Furthermore, hydroxynorketamine metabolites show up earlier compared to DHNK in time-based experimental settings in vivo and in vitro (Fig. 1; [16,32]). Thus, DHNK follows hydroxynorketamine in the model presented in Fig. 2 and 6HNK was included as it was the only hydroxynorketamine analytical standard available. 6HNK is an interesting metabolite because recent studies showed its antidepressive effects [12,35,37]. 6HNK and DHNK are inhibitors of the α_7-nicotinergic acethylcholine receptor [15]. Norketamine is not the only possible source for 6HNK. It can also be formed by N-demethylation of 6-hydroxyketamine.

Analysis of the experimental data of the 6HNK enantiomers in the semilog format revealed only one phase after the maximum concentration (elimination phase). Thus, 6HNK data can be described with a one-compartment model with first order drug absorption according to $c=(k_a*D_0*F)/(V*(k_a-k))*(\exp(-k*t) - \exp(-k_a*t))$ [33]. The elimination phase in the semilog plot is analyzed by linear regression analysis thereby revealing slope k and y-intercept $\ln((k_a*D_0*F)/(V*(k_a-k)))$. Concentration values were calculated for the remaining time points of the first part of the curve and the measured concentration values were subtracted. After logarithmization, results are plotted against time and analyzed with linear regression to obtain the slope k_a and the y-intercept $\ln((k_a*D_0*F)/(V*(k_a-k)))$. Theoretically, the y-intercept for the initial and elimination phases should be the same. Typically there are not because of the lag-time and the residuals. The regression line of the elimination phase is based on the original values and on more data points. The y-intercept of the elimination phase is assumed to be more accurate and is included as an appropriate term in the equation. The same model was used for the DHNK data (Fig. 2). Good fits were obtained for both metabolites. For 6HNK and DHNK it is more difficult to make statements about the kinetics because it is not exactly known what the initial dose of these metabolites is. Thus, noncompartmental analyses were performed as well. Noncompartmental analysis is a statistical description of the experimental curves. The results were comparable with those obtained with compartmental analysis.

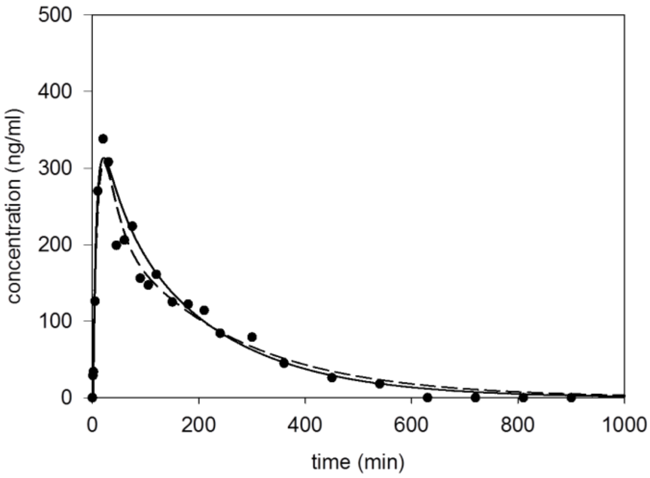

Figure 3. Pharmocokinetic modeling of the R-norketamine data of one dog after administration of racemic ketamine under sevoflurane aneasthesia using a manual step-by-step elucidation of the parameters of the polyexponential function for a two-compartment model (solid line graph graph) and the Phoenix WinNonlin 6.4 software for the same model (broken line graph).

For all compounds there was good agreement of the data calculated stepwise as described above and the data produced by the software. As an example, data obtained for R-norketamine of a dog are presented in Fig. 3. Thus, the data sets of all dogs were analyzed with Phoenix WinNonlin 6.4 software using the same models (Fig. 2). Similarly, concentration – time relationships were calculated for the mean values of each compound and group and are presented in Fig. 4. With the commercial software different variations of the models were also checked and compared according to diagnostic data. The proper choice of the models presented in Fig. 2 was thereby confirmed.

4.4.3 Pharmacokinetic data

The α_2- receptor agonist medetomidine has an effect on the pharmacokinetics of ketamine and the metabolites norketamine, 6HNK and DHNK. Pharmacokinetics can be described with the model shown in Fig. 2. Based on the equations of the model pharmacokinetic parameters can be calculated and compared (Tables 1-4). There is variability in the metabolism of all metabolites among the Beagle dogs which is consistent with the literature [29]. For ketamine, the values of the pharmacokinetic parameter β-half-life and the mean residence time (MRT) are different for the sevoflurane und the medetomidine group (Table 1, $P < 0.05$). Both parameters are connected to the elimination. The half-life is the time in which the concentration of a substance is reduced by 50 %. The MRT is the time a molecule of the substance stays on average in the body. The β-half-life (sevoflurane group: 29.74±25.38 and 28.80±25.35 min for R-and S-ketamine, respectively; medetomidine group: 68.12±10.31 and 66.77±12.81 min, respectively) as well as the MRT (sevoflurane: 34.04±31.34 and 32.02±30.15 min; medetomidine: 71.49±13.12 and 69.38±15.71 min) values for both enantiomers are higher in the medetomidine group (Table 1). The volume of the peripheral compartment (V_{T1}, Table 1) under both conditions is higher than the volume of the central compartment ($V_{central}$). This is typical for lipophilic bases and stands for a high affinity of the drug to all parts of the central compartment. V_{T1}, $V_{central}$ and the volume of distribution at steady state (V_{ss}, Table 1) are higher in the medetomidine group whereas the inter-compartmental transfer constants k_{10}, k_{12}, and k_{21} are higher in the sevoflurane group. For the clearance (Cl, Table 1) and the area under the curve (AUC) no significant differences in relation to the comedication could be found (Table 1; $P > 0.05$). Furthermore, no stereoselectivities were detected (Fig. 4A, $P > 0.05$).

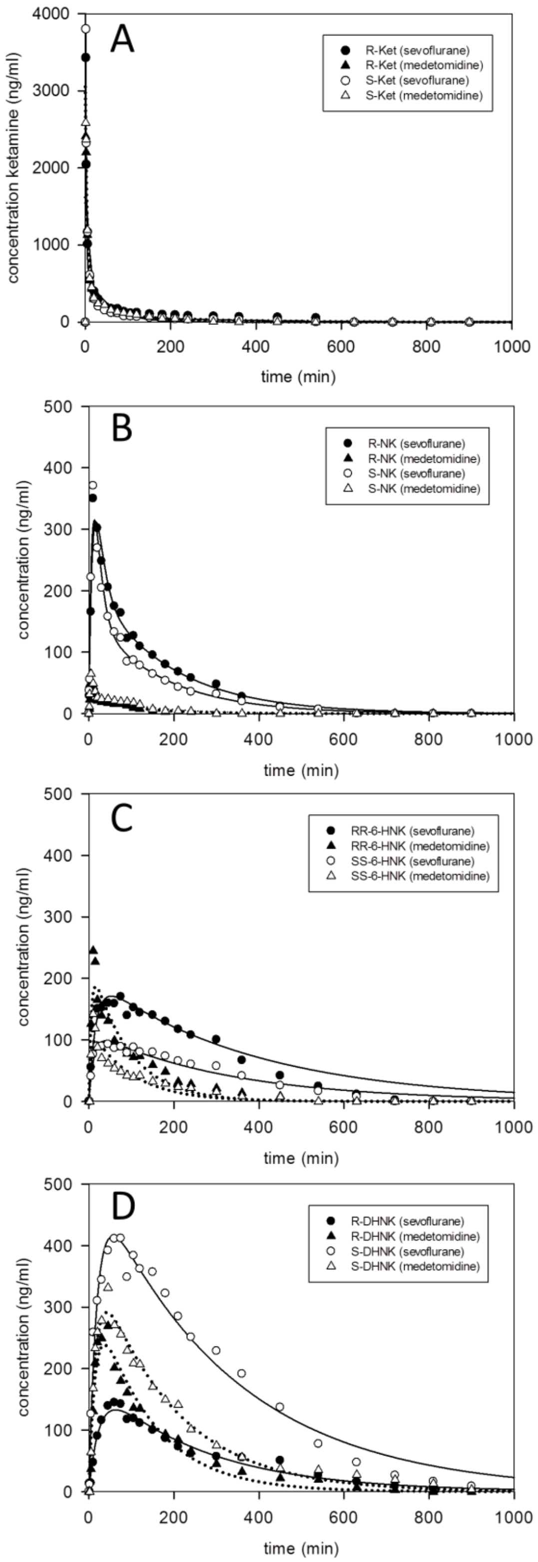

Figure 4. Pharmacokinetics of (A) ketamine, (B) norketamine, (C) 6HNK and (D) DHNK for the mean plasma data of both groups after administration of racemic ketamine and evaluated with the Phoenix WinNonlin 6.4 software using the model of Fig. 2. Key: circles and solid lines, sevoflurane comedication; triangles and dashed lines, medetomidine comedication; filled symbols, R-enantiomers; open symbols, S-enantiomers.

Table 1. Pharmacokinetic parameters of ketamine enantiomers[a)]

Ketamine	Racemic ketamine Sevoflurane (n=6)		Racemic ketamine Medetomidine (n=5)	
	R	S	R	S
AUC (min*ng/L)	37.22 ± 7.97	35.44 ± 6.98	43.13 ± 10.52	44.85 ± 8.02
Cl (mL/min/kg)	55.69 ± 11.07	58.17 ± 10.70	47.41 ± 7.90	45.76 ± 16.61
α-half-life (min)	1.29 ± 0.58	1.35 ± 0.56	3.41 ± 1.20	3.36 ± 1.13
β-half-life (min)	29.74 ± 25.38	28.80 ± 25.35	68.12 ± 10.31	66.77 ± 12.81
A (ng/mL)	6469.47 ± 4820.36	6165.93 ± 3989.23	2845.75 ± 1147.99	3068.43 ± 1225.59
B (ng/mL)	958.39 ± 490.15	939.95 ± 510.94	311.78 ± 27.42	328.28 ± 22.19
$\mathbf{k_{10}}$ (1/min)	0.2231 ± 0.1885	0.2196 ± 0.1654	0.0738 ± 0.0302	0.0760 ± 0.0289
$\mathbf{k_{12}}$ (1/min)	0.3789 ± 0.2333	0.3467 ± 0.2268	0.1339 ± 0.0670	0.1333 ± 0.0659
$\mathbf{k_{21}}$ (1/min)	0.1242 ± 0.0694	0.1209 ± 0.0731	0.0320 ± 0.0042	0.0319 ± 0.0044
MRT (min)	34.04 ± 31.34	32.02 ± 30.15	71.49 ± 13.12	69.38 ± 15.71
$\mathbf{V_{ss}}$ (L/kg)	1.63 ± 1.17	1.62 ± 1.23	3.37 ± 0.66	3.13 ± 0.66
$\mathbf{V_{central}}$ (L/kg)	0.36 ± 0.18	0.35 ± 0.16	0.72 ± 0.34	0.67 ± 0.30
$\mathbf{V_{T1}}$ (L/kg)	1.24 ± 1.00	1.27 ± 1.08	2.64 ± 0.55	2.46 ± 0.61

a) Data represent mean values ± SD and were determined with the Phoenix WinNonlin 6.4 software.

In contrast to ketamine, a large difference between the sevoflurane and the medetomidine group was noted for norketamine. This can be seen in the electropherograms presented in Fig. 1B and 1C, the concentration vs. time plots of Fig. 4B, and the data of Table 2.

Table 2. Pharmacokinetic parameters of norketamine enantiomers[a)]

Norketamine	Racemic ketamine Sevoflurane (n=6)		Racemic ketamine Medetomidine (n=5)	
	R	S	R	S
AUC (min*ng/L)	42.91 ± 12.67	32.32 ± 16.39	3.29 ± 2.21	4.53 ± 2.04
t_{max} (min)	17.68 ± 3.45	13.33 ± 3.53	6.77 ± 2.12	6.38 ± 2.04
c_{max} (ng/mL)	316.12 ± 77.37	322.30 ± 106.50	45.35 ± 9.53	55.38 ± 6.91
α-half-life (min)	8.94 ± 1.52	7.48 ± 1.75	3.72 ± 1.27	3.42 ± 1.11
β-half-life (min)	125.71 ± 26.11	111.28 ± 34.88	78.20 ± 47.83	91.97 ± 43.58
A (ng/mL)	-29713.39 ± 55612	-13691.38 ± 242024	-7251.93 ± 19714	-16470.07 ± 30165
B (ng/mL)	212.18 ± 52.54	160.04 ± 59.10	25.71 ± 4.77	31.95 ± 4.87
k_{03} (1/min)	0.078 ± 0.012	0.097 ± 0.022	0.21 ± 0.07	0.22 ± 0.07
k_{30} (1/min)	0.018 ± 0.008	0.029 ± 0.016	0.039 ± 0.016	0.031 ± 0.009
k_{34} (1/min)	0.039 ± 0.007	0.049 ± 0.008	0.12 ± 0.05	0.14 ± 0.06
k_{43} (1/min)	0.028 ± 0.009	0.026 ± 0.010	0.058 ± 0.023	0.059 ± 0.016

a) Data represent mean values ± SD and were determined with the Phoenix WinNonlin 6.4 software.

Values for the maximum concentration of norketamine (c_{max}) and the AUC are much lower in the medetomidine group. That confirms the previous in vitro experiments in which an inhibition of the N-demethylation of ketamine to norketamine was found in presence of racemic medetomidine or dexmedetomidine [14]. Two mechanisms of inhibition are possible in this drug-drug combination. There is a concurrence on the active site of the enzyme because both drugs are metabolized by CYP enzymes. Medetomidine as an imidazole is able to block the CYP-enzymes by binding to the heme iron in the active site of the CYP enzyme [4]. Norketamine is an active metabolite. Thus, the effect on the NMDA-receptor is expected to be larger in the sevoflurane group. No stereoselectivity for norketamine was detected ($P > 0.05$).

The shorter half-life and MRT of ketamine in the sevoflurane group show that the elimination of ketamine in the sevoflurane group is faster. C_{max} of norketamine is reached earlier but the amounts of norketamine present in the blood are much lower (Fig. 4B, Table 2). The faster formation of norketamine is expressed also in the k_{03} values which are higher after medetomidine administration. The processes between the central and the tissue (T_2) compartments for norketamine are described with k_{34} and k_{43}. These parameters are also higher for the medetomidine group (Fig. 2, Table 2). Thus, the elimination must take another way excluding the formation of norketamine. One possibility is the increased formation of hydroxyketamine metabolites, another is the increased elimination of unmodified ketamine through the kidneys. The α_2-receptor agonist medetomidine causes the inhibition of the release of vasopressin and the increase of the excreted urine volume [38]. Furthermore, hyperglycemia mediated contemporaneously through the α_2-receptor in the β-cells in the endocrine pancreas results in polyuria [39]. No significant difference in the metabolic pattern was found in urines of two dogs which were collected 300 min after administration of 4 mg/kg racemic ketamine under sevoflurane or medetomidine (data not shown). Thus, the second possibility could not be confirmed.

Data for the stereoisomers of 6HNK and DHNK are presented in Tables 3 and 4, respectively. For these metabolites stereoselectivity was observed ($P < 0.05$). This is also nicely seen in the data of panels C and D of Fig. 4. The concentration for RR-6HNK is higher than the concentration of the SS-6HNK in both groups (Table 3). Furthermore, the c_{max} value for RR-6HNK under sevoflurane is the same as that under medetomidine sedation (180.36±52.34 and 188.01±53.99 ng/ mL). The same applies for SS-6HNK (101.67±4.90 and 82.68±23.21 ng/ mL). The maximum concentrations, however, are reached faster under medetomidine comedication (sevoflurane group: 67.57±36.23 min and 48.86±19.25 min; medetomidine: 16.24±1.60 and 16.65±0.79 min). The AUC values are also lower in presence of medetomidine due to the faster elimination.

Table 3. Pharmacokinetic parameters of 6HNK enantiomers[a)]

6HNK	Racemic ketamine Sevoflurane (n=6)		Racemic ketamine Medetomidine (n=3)[b)]	
	RR	SS	RR	SS
AUC (min*ng/L)	60.08 ± 12.67	35.97 ± 7.80	20.37 ± 7.83	10.00 ± 2.27
t_{max} (min)	67.57 ± 36.23	48.86 ± 19.25	16.24 ± 1.60	16.65 ± 0.79
c_{max} (ng/mL)	180.36 ± 52.34	101.67 ± 4.9	188.01 ± 53.99	82.68 ± 23.21
k_{05} (1/min)	0.056 ± 0.037	0.078 ± 0.039	0.18 ± 0.04	0.19 ± 0.04
k_{50} (1/min)	0.0039 ± 0.0011	0.0035 ± 0.0013	0.012 ± 0.004	0.010 ± 0.004

a) Data represent mean values ± SD and were determined with the Phoenix WinNonlin 6.4 software.
b) The 6HNK data of two dogs could not be analyzed with this model.

In contrast to these results with 6HNK, for DHNK under sevoflurane (Table 4) the maximum concentration of S-DHNK is significantly higher compared to that of R-DHNK. For the medetomidine group, the c_{max} value of S-DHNK is also higher than that of R-DHNK. The difference between the enantiomers is much bigger under sevoflurane, not only for c_{max} but also for the AUC. The AUC for R-DHNK in both groups is the same and smaller than the values for S-DHNK (Table 4). The velocity constants k_{05}, k_{50}, k_{06} and k_{60} show that the metabolites HNK and DHNK disperse faster under comedication with medetomidine (Tables 3 and 4). The highest concentration is reached under sevoflurane by S-DHNK (433.97± 152.97 ng/ mL). For both 6HNK and DHNK, pharmacological effects at the α_7-nicotinergic acethylcholine receptor were observed which makes the investigation of these compounds worthwhile [15].

Table 4. Pharmacokinetic parameters of DHNK enantiomers[a)]

DHNK	Racemic ketamine Sevoflurane (n=6)		Racemic ketamine Medetomidine (n=5)	
	R	S	R	S
AUC (min*ng/L)	46.17 ± 13.51	158.55 ± 24.65	45.70 ± 13.96	60.32 ± 15.30
t_{max} (min)	80.25 ± 29.69	37.57 ± 4.79	78.86 ± 37.96	41.12 ± 4.02
c_{max} (ng/mL)	138.55 ± 68.24	433.97 ± 152.74	249.44 ± 42.89	275.50 ± 47.47
k_{06} (1/min)	0.033 ± 0.012	0.045 ± 0.030	0.065 ± 0.013	0.064 ± 0.008
k_{60} (1/min)	0.0044 ± 0.0022	0.0035 ± 0.0010	0.0087 ± 0.0057	0.0062 ± 0.0020

a) Data represent mean values ± SD and were determined with the Phoenix WinNonlin 6.4 software.

For the S-ketamine (2 mg/kg) part of the two dog studies the plasma samples were also analyzed with the enantioselective capillary electrophoresis based microassay. It revealed S-ketamine and all S-metabolites but no R-ketamine and R-metabolites. For the two groups, no significant differences in the results for S-ketamine and the metabolites S-norketamine, SS-6HNK and S-DHNK were found ($P > 0.05$). Typical electropherograms are presented in Ref. [24].

4.5 Concluding remarks

The pharmacokinetics of S- and R-ketamine and its metabolites S- and R-norketamine, SS- and RR-6HNK and S- and R-DHNK were analyzed enantioselectively by using capillary electrophoresis in plasma of Beagle dogs under sevoflurane and under medetomidine comedication. The norketamine levels are significantly lower after administration of medetomidine. Additional experiments revealed that urinary excretion of ketamine and norketamine were unaffected by medetomidine. Stereoselectivities were detected for the 6HNK and DHNK metabolites, but not for ketamine and norketamine. Not all enzymes of the different pathways of the ketamine metabolism are identified and it is not clear which effect medetomidine has on them. It seems that some pathways work under medetomidine better than others. In previous in vitro studies the combination of S-ketamine and dexmedetomidine was found best because the pharmacologically inactive levomedetomidine is the stronger inhibitor of ketamine N-demethylation. It would be of interest to elucidate the impact of dexmedetomidine on the further metabolites in comparison to racemic medetomidine used in this study. Norketamine is also active as a NMDA-receptor antagonist. Thus, it should be investigated whether the effect on that receptor is higher in the sevoflurane group. Highly sulfated γ-cyclodextrin based enantioselective capillary electrophoresis with electrokinetic sample injection of the analytes across a short buffer plug without chiral selector provided the required ppb sensitivity to monitor the stereoisomers of ketamine and the three metabolites in extracts of 50 µL aliquots of plasma in an efficient and repeatable way.

Acknowledgements

The authors are grateful to Dr. Irving Wainer for receiving the standards of (2S,6S)-hydroxynorketamine and (2R,6R)-hydroxynorketamine. This work was supported by the Swiss National Science Foundation and Dr. E. Graeub AG, Bern, Switzerland.

Conflicts of interest
The authors have declared no conflict of interest.

4.6 References

[1] M.-C. Duhamel, Ã. Troncy, F. Beaudry, Metabolic stability and determination of cytochrome P450 isoenzymes' contribution to the metabolism of medetomidine in dog liver microsomes, Biomed. Chromatogr. 24 (2010) 868–877.

[2] W.M. Burnside, P.A. Flecknell, A.I. Cameron, A.A. Thomas, A comparison of medetomidine and its active enantiomer dexmedetomidine when administered with ketamine in mice, BMC Vet. Res. (BMC Veterinary Research) 9 (2013) 48.

[3] E. Kuusela, M. Raekallio, M. Anttila, I. Falck, S. Mölsä, O. Vainio, Clinical effects and pharmacokinetics of medetomidine and its enantiomers in dogs, J. Vet. Pharmacol. Ther. 23 (2000) 15–20.

[4] E.D. Kharasch, S. Herrmann, R. Labroo, Ketamine as a probe for medetomidine stereoisomer inhibition of human liver microsomal drug metabolism, Anesthesiology 77 (1992) 1208–1214.

[5] P. Ravipati, P.N. Reddy, C. Kumar, P. Pradeep, R. Pathapati, S.T. Rajashekar, Dexmedetomidine decreases the requirement of ketamine and propofol during burns debridement and dressings, Indian J. Anaesth. 58 (2014) 138–142.

[6] G. Mion, T. Villevieille, Ketamine Pharmacology: An Update (Pharmacodynamics and Molecular Aspects, Recent Findings), CNS Neurosci. Ther. 19 (2013) 370–380.

[7] J. Persson, Ketamine in Pain Management, CNS Neurosci. Ther. 19 (2013) 396–402.

[8] E.D. Kharasch, R. Labroo, Metabolism of ketamine stereoisomers by human liver microsomes, Anesthesiology 77 (1992) 1201–1207.

[9] R.K. Paul, N.S. Singh, M. Khadeer, R. Moaddel, M. Sanghvi, C.E. Green, K. O'Loughlin, M.C. Torjman, M. Bernier, I.W. Wainer, (R,S)-Ketamine metabolites (R,S)-norketamine and (2S,6S)-hydroxynorketamine increase the mammalian target of rapamycin function, Anesthesiology 121 (2014) 149–159.

[10] J.C. Duque, N. Oleskovicz, E.C.B.P. Guirro, C.A.A. Valadão, V.E. Soares, Relative potency of ketamine and S(+)-ketamine in dogs, J. Vet. Pharmacol. Ther. 31 (2008) 344–348.

[11] Y. Hijazi, R. Boulieu, Contribution of CYP3A4, CYP2B6, and CYP2C9 isoforms to N-demethylation of ketamine in human liver microsomes, Drug Metab. Dispos. 30 (2002) 853–858.

[12] X. Zhao, S.L.V. Venkata, R. Moaddel, D.A. Luckenbaugh, N.E. Brutsche, L. Ibrahim, C.A. Zarate, D.E. Mager, I.W. Wainer, Simultaneous population pharmacokinetic modelling of ketamine and three major metabolites in patients with treatment-resistant bipolar depression, Br. J. Clin. Pharmacol. 74 (2012) 304–314.

[13] F.C. Silva, E. Hatschbach, Y.K. Carvalho, B.W. Minto, F. Massone, P. Nascimento, Hemodynamics and bispectral index (BIS) of dogs anesthetized with midazolam and ketamine associated with medetomidine or dexmedetomidine and submitted to ovariohysterectomy, Acta Cir. Bras. 25 (2010) 181–189.

[14] F.A. Sandbaumhüter, R. Theurillat, W. Thormann, Effects of medetomidine and its active enantiomer dexmedetomidine on N-demethylation of ketamine in canines determined in vitro using enantioselective capillary electrophoresis, Electrophoresis 36 (2015) 2703–2712.

[15] R. Moaddel, G. Abdrakhmanova, J. Kozak, K. Jozwiak, L. Toll, L. Jimenez, A. Rosenberg, T. Tran, Y. Xiao, C.A. Zarate, I.W. Wainer, Sub-anesthetic concentrations of (R,S)-ketamine metabolites inhibit acetylcholine-evoked currents in α7 nicotinic acetylcholine receptors, Eur. J. Pharmacol. 698 (2013) 228–234.

[16] A. Schmitz, R. Theurillat, P.-G. Lassahn, M. Mevissen, W. Thormann, CE provides evidence of the stereoselective hydroxylation of norketamine in equines, Electrophoresis 30 (2009) 2912–2921.

[17] S. Portmann, H.Y. Kwan, R. Theurillat, A. Schmitz, M. Mevissen, W. Thormann, Enantioselective capillary electrophoresis for identification and characterization of human cytochrome P450 enzymes which metabolize ketamine and norketamine in vitro, J. Chromatogr. A 1217 (2010) 7942–7948.

[18] Y. Yanagihara, S. Kariya, M. Ohtani, K. Uchino, T. Aoyama, Y. Yamamura, T. Iga, Involvement of CYP2B6 in n-demethylation of ketamine in human liver microsomes, Drug Metab. Dispos. 29 (2001) 887–890.

[19] R. Remínek, Z. Glatz, W. Thormann, Optimized on-line enantioselective capillary electrophoretic method for kinetic and inhibition studies of drug metabolism mediated by cytochrome P450 enzymes, Electrophoresis 36 (2015) 1349–1557.

[20] H.Y. Kwan, W. Thormann, Enantioselective capillary electrophoresis for the assessment of CYP3A4-mediated ketamine demethylation and inhibition in vitro, Electrophoresis 32 (2011) 2738–2745.

[21] L.D. Mössner, A. Schmitz, R. Theurillat, W. Thormann, M. Mevissen, Inhibition of cytochrome P450 enzymes involved in ketamine metabolism by use of liver microsomes and specific cytochrome P450 enzymes from horses, dogs, and humans, Am. J. Vet. Res. 72 (2011) 1505–1513.

[22] M.P. Larenza, M.F. Landoni, O.L. Levionnois, M. Knobloch, P.W. Kronen, R. Theurillat, U. Schatzmann, W. Thormann, Stereoselective pharmacokinetics of ketamine and norketamine after racemic ketamine or S-ketamine administration during isoflurane anaesthesia in Shetland ponies, Br. J. Anaesth. 98 (2007) 204–212.

[23] M.P. Larenza, M. Knobloch, M.F. Landoni, O.L. Levionnois, P.W. Kronen, R. Theurillat, U. Schatzmann, W. Thormann, Stereoselective pharmacokinetics of ketamine and norketamine after racemic ketamine or S-ketamine administration in Shetland ponies sedated with xylazine, Vet. J. 177 (2008) 432–435.

[24] R. Theurillat, F.A. Sandbaumhüter, R. Bettschart-Wolfensberger, W. Thormann, Microassay for ketamine and metabolites in plasma and serum based on enantioselective capillary electrophoresis with highly sulfated γ-cyclodextrin and electrokinetic analyte injection, Electrophoresis 37 (2016) 1129–1138.

[25] R. Gehring, J.F. Coetzee, J. Tarus-Sang, M.D. Apley, Pharmacokinetics of ketamine and its metabolite norketamine administered at a sub-anesthetic dose together with xylazine to calves prior to castration, J. Vet. Ther. 32 (2009) 124–128.

[26] B.H. Pypendop, J.E. Ilkiw, Pharmacokinetics of ketamine and its metabolite, norketamine, after intravenous administration of a bolus of ketamine to isoflurane-anesthetized dogs, Am. J. Vet. Res. 66 (2005) 2034–2038.

[27] M.L. Williams, D.E. Mager, H. Parenteau, G. Gudi, T.S. Tracy, M. Mulheran, I.W. Wainer, Effects of protein calorie malnutrition on the pharmacokinetics of ketamine in rats, Drug Metab. Dispos. 32 (2004) 786–793.

[28] D. P. K. Lankveld, B. Driessen, L.R. Soma, P.J. Moate, J. Rudy, C.E. Uboh, P. van Dijk, L.J. Hellebrekers, Pharmacodynamic effects and pharmacokinetic profile of a long-term continuous rate infusion of racemic ketamine in healthy conscious horses, J. Vet. Pharmacol. Ther. 29 (2006) 477–488.

[29] Y. Hijazi, C. Bodonian, M. Bolon, F. Salord, R. Boulieu, Pharmacokinetics and haemodynamics of ketamine in intensive care patients with brain or spinal cord injury, Br. J. Anaesth. 90 (2003) 155–160.

[30] R. Moaddel, S.L.V. Venkata, M.J. Tanga, J.E. Bupp, C.E. Green, L. Iyer, A. Furimsky, M.E. Goldberg, M.C. Torjman, I.W. Wainer, A parallel chiral-achiral liquid chromatographic method for the determination of the stereoisomers of ketamine and ketamine metabolites in the plasma and urine of patients with complex regional pain syndrome, Talanta 82 (2010) 1892–1904.

[31] Z. Desta, R. Moaddel, E.T. Ogburn, C. Xu, A. Ramamoorthy, S.L.V. Venkata, M. Sanghvi, M.E. Goldberg, M.C. Torjman, I.W. Wainer, Stereoselective and regiospecific hydroxylation of ketamine and norketamine, Xenobiotica 42 (2012) 1076–1087.

[32] A. Schmitz, W. Thormann, L. Moessner, R. Theurillat, K. Helmja, M. Mevissen, Enantioselective CE analysis of hepatic ketamine metabolism in different species in vitro, Electrophoresis 31 (2010) 1506–1516.

[33] T. Loftsson, Essential pharmacokinetics: A primer for pharmaceutical scientists, Academic Press (Elsevier), London, 2015.

[34] S. Fanta, M. Kinnunen, J.T. Backman, E. Kalso, Population pharmacokinetics of S-ketamine and norketamine in healthy volunteers after intravenous and oral dosing, Eur. J. Pharmacol. 71 (2015) 441–447.

[35] C.A. Zarate, N. Brutsche, G. Laje, D.A. Luckenbaugh, S.L.V. Venkata, A. Ramamoorthy, R. Moaddel, I.W. Wainer, Relationship of ketamine's plasma metabolites with response, diagnosis, and side effects in major depression, Biol. Psychiatry 72 (2012) 331–338.

[36] P. Adamowicz, M. Kala, Urinary excretion rates of ketamine and norketamine following therapeutic ketamine administration: method and detection window considerations, Journal Anal. Toxicol. 29 (2005) 376–382.

[37] N.S. Singh, C.A. Zarate, R. Moaddel, M. Bernier, I.W. Wainer, What is hydroxynorketamine and what can it bring to neurotherapeutics?, Expert Rev. of Neurother. 14 (2014) 1239–1242.

[38] C.M. Creighton, K.A. Lemke, L.A. Lamont, B.S. Horney, A.J. Doyle, Comparison of the effects of xylazine bolus versus medetomidine constant rate infusion on the stress response, urine production, and anesthetic recovery characteristics in horses anesthetized with isoflurane, J.Am. Vet. Med. Assoc. 240 (2012) 998–1002.

[39] B. Ranheim, T.E. Horsberg, N.E. Søli, K.A. Ryeng, J.M. Arnemo, The effects of medetomidine and its reversal with atipamezole on plasma glucose, cortisol and noradrenaline in cattle and sheep, J. Vet. Pharmacol. Ther. 23 (2000) 379–387.

5. Effect of the α_2-receptor agonists medetomidine, detomidine, xylazine and romifidine on the ketamine metabolism in equines assessed with enantioselective capillary electrophoresis (Electrophoresis (2017) doi: 10.1002/elps.201700017)

Friederike A. Sandbaumhüter[1], Regula Theurillat[1], Regula Bettschart-Wolfensberger[2], Wolfgang Thormann[1]

[1] Clinical Pharmacology Laboratory, University of Bern, Bern, Switzerland
[2] Section of Anaesthesiology, Equine Department, Vetsuisse Faculty, University of Zürich, Zürich, Switzerland

5.1 Abstract

The combination of ketamine and an α_2-receptor agonist is often used in veterinary medicine. Four different α_2-receptor agonists, medetomidine, detomidine, xylazine and romifidine, which differ in their chemical structure and thus in selectivity for the α_2-receptor and in the sedative and analgesic potency, are typically employed during surgery of equines. In veterinary practice recovery following anesthesia with ketamine and an α_2-receptor agonist is dependent on the selected α_2-receptor agonist. This prompted us to investigate i) the inhibition characteristics for the N-demethylation of ketamine to norketamine and ii) the formation of the ketamine metabolites norketamine, 6-hydroxynorketamine (6HNK) and 5,6-dehydronorketamine (DHNK) in presence of the four α_2-receptor agonists and equine liver microsomes. Samples were analyzed with enantioselective capillary electrophoresis using highly sulfated γ-cyclodextrin as chiral selector. All four α_2-receptor agonists have an impact on the ketamine metabolism. Medetomidine was found to be the strongest inhibitor, followed by detomidine, whereas xylazine and romifidine showed almost no effect on the ketamine N-demethylation in the inhibition studies with a short incubation period of the reaction mixture. After prolonged incubation, inhibition with xylazine and romifidine was also observed. The formation of 6HNK and DHNK is affected by all selected α_2-receptor agonists. With medetomidine, levels of these metabolites are reduced compared to the case without an α_2-receptor agonist. For detomidine, xylazine and romifidine, the opposite was found.

5.2 Introduction

In equine anesthesia the use of ketamine in combination with α_2-receptor agonists for anesthesia induction and short duration anesthesia is standard practice for a long time. Ketamine has anesthetic, analgesic and antidepressive effects and is administered as racemate or S-ketamine. Most of its effects are mediated by the N-methyl-d-aspartate (NMDA) receptor. Interactions with opioid, monoaminergic, cholinergic, muscarinic and nicotinic receptors are also reported [1–5]. Four different α_2-receptor agonists, medetomidine, detomidine, xylazine and romifidine, which have anesthetic sparing effects, provide muscle relaxation and show analgesic effects, are employed for dose-dependent sedation and anesthesia premedication in veterinary medicine [5–12]. Chemical structures of selected compounds are presented in Fig. 1.

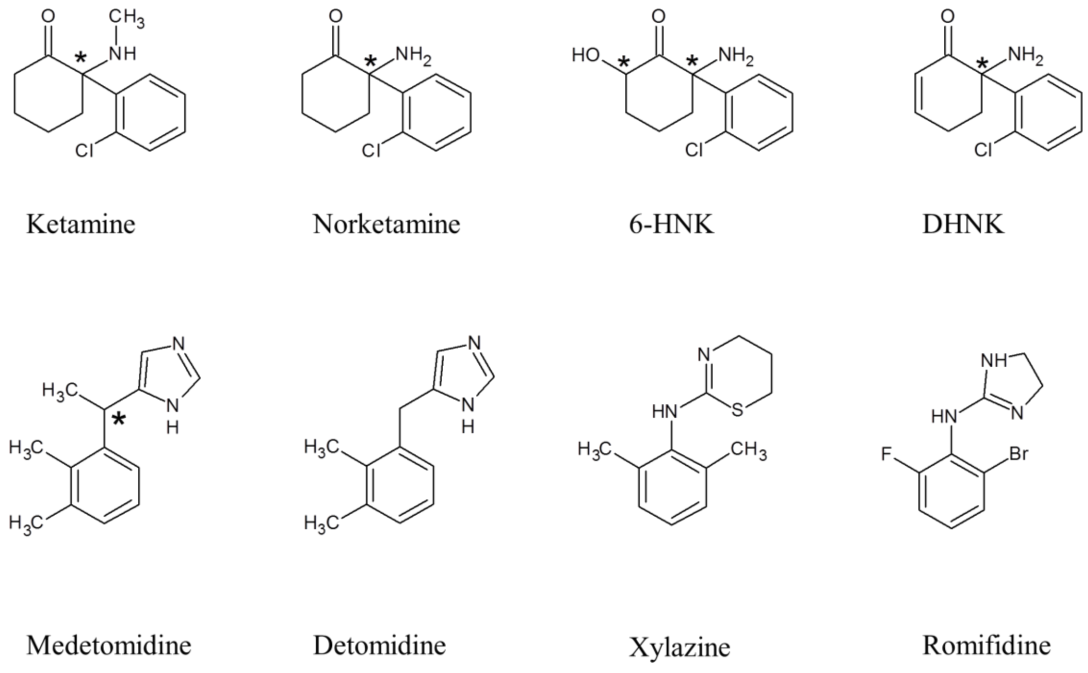

Figure 1. Chemical structures of ketamine, its metabolites norketamine, 6HNK and DHNK and the α_2-receptor agonists medetomidine, detomidine, xylazine and romifidine. Stereocenters are marked with an asterisk.

The first α_2-receptor agonist on the market for animals was xylazine. It was developed at the same time as clonidine which is used in humans. Besides clonidine the α_2-receptor agonists dexmedetomidine and tizanidine play a role in human therapy as sedative and antihypertensive drugs, as anesthesia adjuncts, in the treatment of attention-deficit/hyperactivity disorders and panic disorders, and against the symptoms of opioid, benzodiazepine and alcohol withdrawal [13]. The affinity of xylazine to the α_2-receptor is high but there is also some effect on the α_1-receptor. They all differ in selectivity (Table 1) and their sedative and analgesic potency [5,13,14]. This is also based on the structural differences in the molecules (Fig. 1). Thus, different doses are used in the treatment of animals which is illustrated with the data for horses presented in Table 1 [6,11,15–17]. As reversal agents α_2-receptor antagonists like atipamezole, tolazoline and yohimbine are available [13].

Table 1. Dosing of α_2-agonists and corresponding c_{max} values for horses together with Log(P) and selectivity ratios for the α_2 receptor [a)]

α_2-agonist	Dose (mg/kg)	c_{max} (µM)	Log(P) [b)]	Selectivity ratio (α_2: α_1) [c)]
Medetomidine	0.01 [6]	0.043 [6]	3.1	1620:1 [12]
Detomidine	0.04 [11]	0.55 [11]	2.75	260:1 [12]
Xylazine	0.6 [15]	2.73 [15]	2.37	160:1 [12]
Romifidine	0.08 [9]	0.20 [9]	1.02	340:1 [12]

a) Values from the literature.

b) Log(P) values were taken from the database chemspider.com (calculated with the ACD/ Labs Percepta Platform- PhysChem Module).

c) Affinity for the α_2-receptor compared to the α_1-receptor.

In daily veterinary practice, differences in the behavior of horses under and after anesthesia with ketamine in combination with an α_2-receptor agonist are noted. Observations are dependent on the α_2-receptor agonist used [17–20 and observations at Vetsuisse Zürich]. In in vivo studies with dogs and in vitro studies with human and canine cytochrome P450 (CYP) enzymes and liver microsomes it was shown that the α_2-receptor agonist medetomidine or its single S-enantiomer, dexmedetomidine, has an effect on the ketamine metabolism [21,22]. The CYP enzymes are responsible for the metabolism of ketamine and the α_2-receptor agonists [7,8,10,23–30]. The formation of norketamine in canines was decreased. A stereoselective effect on the formation of further metabolites like 6-hydroxynorketamine (6HNK, Fig. 1) and 5,6-dehydronorketamine (DHNK, Fig. 1) in canines was also detected [31]. Norketamine is active at the NMDA-receptor. Its effect is about one third of that of ketamine [1]. DHNK and 6HNK are active at the α_7-nicotinic acetylcholine receptor and the α-amino-3-hydroxy-5-methyl-4-isoxazolepropionic acid (AMPA) receptors. These activities are connected with the antidepressive effects [32]. The decreased norketamine formation in Beagle dogs and in vitro experiments with canine and human enzymes could be explained with an inhibitive effect of medetomidine on the CYP enzymes [21,31,33].

In this work the effect of the four α_2-receptor agonists medetomidine, detomidine, xylazine and romifidine on the ketamine metabolism, on the N-demethylation of ketamine to norketamine and the formation of the further metabolites 6HNK and DHNK, was analyzed in vitro with equine liver microsomes (ELM) via use of enantioselective capillary electrophoresis. Capillary electrophoresis is an established tool for analyzing samples of in vitro inhibition and drug drug interaction studies. Stereospecific separation becomes possible with the addition of highly sulfated γ-cyclodextrin to the background electrolyte [21,22,24,26,34]. To the best of our knowledge, this is the first study in which the four α_2-receptor agonists used in veterinary practice are compared concerning their effects on the N-demethylation of ketamine to norketamine and on the formation of further metabolites.

5.3 Material and methods

5.3.1 Chemicals and reagents

Analytical standards for ketamine and norketamine (as hydrochlorides in methanol, 1 mg/mL of the free base), and DHNK (as hydrochloride in acetonitrile, 100 µg/mL of the free base), were from Cerilliant (Round Rock, TX, USA). (2S,6S)-6-hydroxynorketamine (SS-6HNK) and (2R,6R)-6-hydroxynorketamine (RR-6HNK) were from Dr. Irving Wainer (Laboratory of Clinical Investigations, National Institute on Aging, National Institutes of Health, Baltimore, MD, USA (synthesis described by Moaddel et al. and Desta et al. [35,36])). Highly sulfated γ-cyclodextrin (20 % *w/v* solution) was purchased from Beckman Coulter (Fullerton, CA, USA). Lamotrigine was from The Welcome Foundation (London, UK). D-(+)-norephedrine hydrochloride, xylazine hydrochloride and bovine serum were from Sigma (St. Louis, Mo, USA). Medetomidine hydrochloride was purchased from Tocris Bioscience, R&D Systems Europe (Abingdon, UK). Romifidine hydrochloride was from LGC (Teddington, UK). Human albumin was from Behringwerke (Marburg, Germany). Disodium hydrogenphosphate, Tris sodium hydroxide and bromothymol blue were from Merck (Darmstadt, Germany), potassium dihydrogen phosphate, di-potassium hydrogen phosphate, detomidine hydrochloride monohydrate, methanol, phosphoric acid (85 %) were from Fluka (Buchs, Switzerland), ethylacetate was from AppliChem (Darmstadt, Germany) and dichloromethane (HiPerSolv Chromanorm for HPLC) was from VWR (Leuven, Belgium). The nicotinamide adenine dinucleotide phosphate (NADPH) regenerating system solutions A and B were from Corning (product of Gentest, Woburn, MA, USA).

5.3.2 Equine liver microsomes

The used ELM were the same as those prepared and characterized by Schmitz et al. [37]. Briefly, liver samples of crossbreeds or Franches-Montagnes horses of both sexes were taken less than 30 min after stunning, placed directly on dry ice and kept at -70 °C until microsomes preparation. After grinding the frozen tissues and homogenization the microsome fraction was isolated through different centrifugation steps. The total protein concentration was determined by using the Biuret method with bovine serum albumin as standard. The total CYP content was measured after the protocol of Omura and Sato [38]. For the current experiments their activity was tested and the results were comparable with the previous data [37].

5.3.3 In vitro reactions for determining inhibition parameters

The substrate ketamine was preincubated in 3 different concentrations (11.5, 23, 46 µM per enantiomer) with NADPH regenerating system consisting of 1.49 mM NADP+, 3.2 mM glucose-6-phosphate, 0.4 U/mL glucose-6-phosphate dehydrogenase, 2.9 mM $MgCl_2$ and 50 µM sodium citrate in 100 mM pH 7.4 potassium phosphate buffer and medetomidine,

detomidine, xylazine or romifidine for 3 min at 37 °C. The ketamine concentrations were based on the K_m value (23 µM per enantiomer) for ELM which was determined in previous work of our laboratory [37]. The concentrations for medetomidine were 0, 0.1, 0.2, 0.4 and 0.6 µM, for detomidine 0, 0.1, 0.2, 0.4, 0.6 and 0.8 µM, for xylazine 0, 8, 12, 15, 30, 80 and 200 µM and for romifidine 0, 75, 90, 93, 96, 100 and 200 µM. The incubation was started by adding ELM (0.5 mg protein/mL) to a final volume of 200 µL. The reaction was stopped after 8 min by adding 50 µL 2 M NaOH. Lamotrigine (2 µg/mL, internal standard) was added before liquid/liquid extraction as described by Sandbaumhüter et al. [21]. Briefly, 1500 µL of ethylacetate/dichloromethane (25:75 %, *v/v*) were added to these samples followed by shaking for 10 min and centrifugation at 12000 rpm for 5 min. The upper aqueous phase was removed and the organic phase was transferred to a new vial. The organic phase was acidified with 10 µL of 50 mM phosphoric acid to avoid the loss of analytes during evaporation under a stream of air at 37 °C. After reconstitution in 150 µL methanol the sample was vortexed and transferred in another vial. Finally the residues were reconstituted in 30 µL of 17.8 mM Tris phosphate buffer (pH 2.5). All experiments were performed in duplicates.

5.3.4 In vitro reactions for analyzing the effect of α_2-receptor agonists on ketamine metabolites

The effect of the α_2-receptor agonists on the different ketamine metabolites was analyzed in incubations under similar conditions as described in Section 2.3. The ketamine concentration was 60 µM per enantiomer and the concentrations for the α_2-receptor agonists were based on the mean of the determined IC_{50} values for the two norketamine enantiomers, namely 0.091 µM for medetomidine, 0.16 µM for detomidine, 19.37 µM for xylazine and 82.88 µM for romifidine. The incubations of a volume of 50 µL were stopped with 15 µL 1M NaOH after 0, 30, 120 and 300 min. To 10 µL of this mixture 240 µL bidestilled water, 20 µL 0.5 M NaOH and 15 µL of a solution of 4 µg/mL d-(+)-norephedrine hydrochloride were added. These samples were analyzed according to Theurillat et al. [22]. Briefly, samples were extracted with 1300 µL dichloromethane, shaken for 5 min and centrifuged for 5 min at 12000 rpm. After removing the aqueous phase the organic phase was transferred to a new vial and acidified with 10 µL of 1 mM phosphoric acid. After evaporation to dryness at 45 °C using the Eppendorf Speed-Vac Concentrator 5301 (Vaudaux-Eppendorf, Schönenbuch, Switzerland) for 30 min, the residues were reconstituted in 110 µL bidestilled water. All experiments were performed in duplicates.

5.3.5 CE instrumentation and analytical conditions

A Proteome Lab PA 800 instrument (Beckman Coulter, Fullerton, CA, USA) equipped with a 50 µm i.d. fused-silica capillary (Polymicro Technologies, Phoenix, AZ, USA) of 45 cm total length (effective length 36 cm) was used. Before each experiment, the capillary was sequentially rinsed with 0.1 M NaOH (1 min; 20 psi), bidistilled water (1 min; 20 psi) and respective running buffer (1 min; 20 psi).

Samples for determining the inhibition parameters were injected by applying a vacuum of 1 psi for 5 s. With an applied voltage of -20 kV (reversed polarity) the current was about -68 µA. For inducing a flow towards the anode a positive pressure of 0.2 psi was applied during the entire experiment. Temperatures for sample storage and capillary cartridge were set to 20 °C. Analyte detection took place with an on-column UV variable wavelength detector at 195 nm. The running buffer was composed of 17.8 mM Tris, phosphoric acid (pH 2.5) and 2 % highly sulfated γ-cyclodextrin. Assay control and quantification of norketamine enantiomers (0.5-30 µM) were based on internal calibration using corrected peak areas as described in Ref. [21]. A typical electropherogram of ketamine, its metabolite norketamine, the internal standard and the α_2-receptor agonists is shown in Fig. 2A.

The other samples were injected electrokinetically with 6 kV for 15 s across a pressure injected (1 psi, 20 s) plug composed of 50 mM phosphate buffer at pH 3 [22]. For separation a voltage of 20 kV (normal polarity) was applied. The current was about 64 µA. All temperatures were set to 25 °C. In this assay a running buffer of 100 mM phosphate buffer (pH 3.0) together with 0.66 % highly sulfated γ-cyclodextrin was used. The quantification of the enantiomers of ketamine, norketamine, DHNK and 6HNK was based on internal calibration using corrected peak areas. The calibration range for all enantiomers was 1-60 µM. Calibration and control solutions were prepared as described elsewhere [22]. The analysis of ketamine, norketamine, 6HNK, DHNK, the internal standard and all α_2-agonists shows that only romifidine is visible in the migration time range of ketamine and its metabolites (Fig. 2D).

5.3.6 Data analysis

Inhibition, kinetic and statistic data were evaluated with SigmaPlot software version 12.5 (Systat Software, San Jose, CA, USA). The statistic paired Student's t-test was employed to evaluate data sets. With a p-value < 0.05 the difference of two data sets was considered to be significant.

5.4 Results and discussion

5.4.1 Inhibition parameter of the N-demethylation of ketamine by α_2-receptor agonists

The inhibition constant K_i and the IC_{50} value help to describe the effect of an inhibitor on a reaction and provide a mean to compare the influence of various substances on the same reaction. K_i describes the equilibrium between free enzyme, inhibitor and the enzyme-inhibitor-complex. IC_{50} is the inhibitor concentration at which the formation rate of a product is reduced by 50 %. Low inhibition parameters mean a strong inhibition. K_i and IC_{50} were determined to compare the effect of the four selected α_2-receptor agonists on the N-demethylation of ketamine to norketamine. Each α_2-receptor agonist was incubated in various concentrations with three different ketamine concentrations (0.5, 1.0, 2.0 K_m). The K_m values were taken from a previous study [37]. The concentrations of the α_2-receptor agonists were chosen depending on their effects on the norketamine formation. Experiments revealed the concentrations which showed the first and the maximum effect on product formation. In that range 5 or 6 concentrations were taken for the incubation (Section 2.3). The electropherogram depicted in Fig. 2C was obtained with medetomidine in the sample and is presented as example. Furthermore control incubations without any α_2-receptor agonist (Fig. 2B) and with the different α_2-receptor agonists but without ketamine were performed. No interferences with the α_2-receptor agonists and the analyzed substances were found (Fig. 2A). The occurrence of metabolites of α_2-receptor agonists was tested with 30 min incubations of 60 µM of the α_2-receptor agonists with ELM under the same conditions as described in Section 2.3. For medetomidine, detomidine and xylazine, no metabolites were detected, whereas a romifidine metabolite comigrated with romifidine (data not shown).

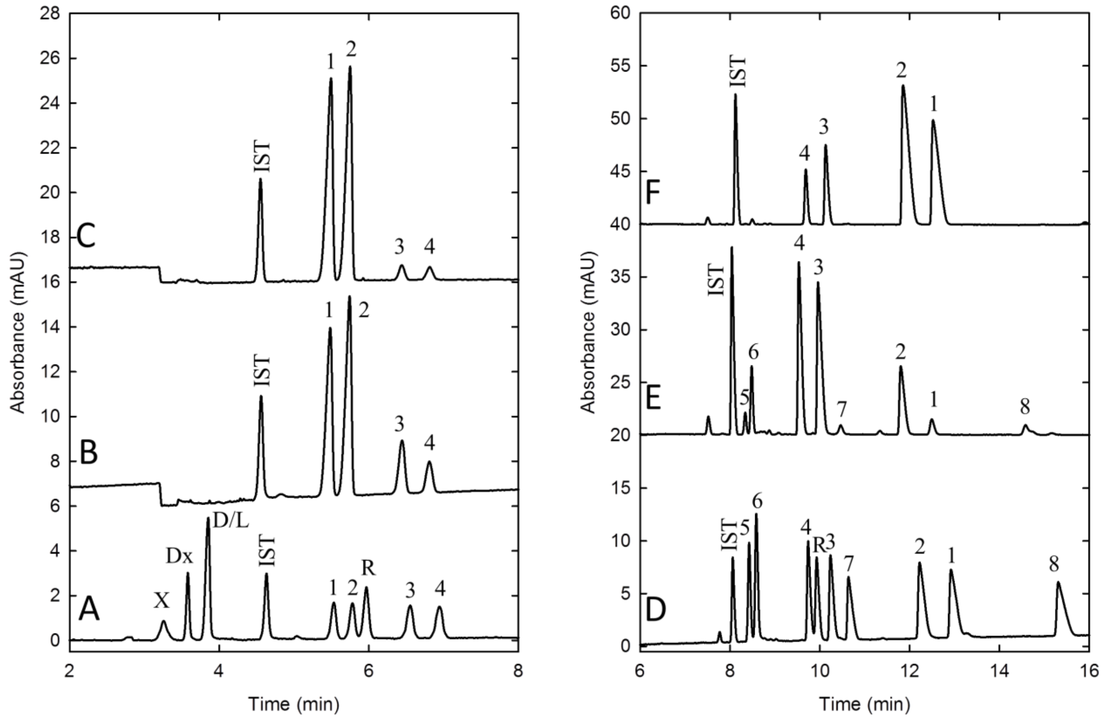

Figure 2. Electropherograms obtained with (A-C) 2 % highly sulfated γ-cyclodextrin in the BGE and reversed polarity and (D-F) 0.66 % highly sulfated γ-cyclodextrin in the BGE and normal polarity. Samples analyzed were (A) a mixture comprising standards of lamotrigine (internal standard), the enantiomers of ketamine, norketamine, and medetomidine (25 µM per enantiomer each), detomidine (25 µM), xylazine (15 µM) and romifidine (25 µM), (B, y-scale shift 6 mAU) an extract prepared after incubation of 46 µM per enantiomer ketamine with ELM for 8 min, (C, y-scale shift 12 mAU) an extract prepared after incubation of 46 µM per enantiomer ketamine and 0.6 µM medetomidine with ELM for 8 min, (D) a sample composed of d-(+)-norephedrine (internal standard), the enantiomers of ketamine, norketamine, 6HNK and DHNK (25 µM per enantiomer each) and the four α_2-agonists (25 µM each), (E, y-scale shift 20 mAU) an extract prepared after incubation of 60 µM per enantiomer ketamine with ELM for 30 min and (F, y-scale shift 40 mAU) an extract after incubation of 60 µM enantiomer ketamine and 0.091 µM medetomidine with ELM for 30 min. Experimental conditions for extract preparation and electrophoretic runs are given in Sections 2.5 and 2.6, respectively. Key: 1: S-ketamine, 2: R-ketamine, 3: S-norketamine, 4: R-norketamine, 5: RR-6HNK, 6: SS-6HNK, 7: S-DHNK, 8: R-DHNK, X: xylazine, Dx: dexmedetomidine, D: detomidine, L: levomedetomidine, R: romifidine, IST: internal standard lamotrigine or d-(+)-norephedrine.

For each α_2-receptor agonist the norketamine formation rates were plotted against their concentrations (Fig. 3). Data were evaluated with nonlinear regression analysis using the four-parameter logistic model $y = \min + (\max - \min) / (1 + (x / IC_{50})^{-n})$ [39]. In this equation y is the norketamine formation rate, x the inhibitor concentration, min and max are the lower and the upper limit of the curve, respectively, and n the Hillslope. From the found IC_{50} value the K_i value can be calculated by using the Cheng-Prusoff equation $K_i = IC_{50} / (1 + ([S] / K_m))$ where

[S] is the substrate concentration [40]. The results are presented in Table 2 and Fig. 3. For medetomidine and detomidine the inhibition parameters are much lower than those observed for xylazine and romifidine. The inhibition with medetomidine (IC_{50} 0.094 µM for S-norketamine and 0.087 µM for R-norketamine, Table 2) is stronger than with detomidine (IC_{50} 0.16 µM for S-norketamine and 0.16 µM for R-norketamine, Table 2). After the application of a usual dose of 0.01 mg/kg medetomidine and 0.04 mg/kg detomidine to horses c_{max} values of 0.043 µM and 0.55 µM, respectively, were measured [6,11, Table 1]. Thus, the inhibition is more important for detomidine although it is stronger for medetomidine.

Table 2. Inhibition parameters

α_2-agonist	**Product**	**IC_{50} (µM)**	**K_i (µM)**
Medetomidine	S-norketamine	0.094 ± 0.034	0.043 ± 0.023
	R-norketamine	0.087 ± 0.059	0.038 ± 0.013
Detomidine	S-norketamine	0.16 ± 0.02	0.079 ± 0.018
	R-norketamine	0.16 ± 0.03	0.077 ± 0.017
Xylazine	S-norketamine	29.11 ± 21.34	27.11 ± 8.95
	R-norketamine	9.62 ± 1.83	13.54 ± 8.42
Romifidine	S-norketamine	89.45 ± 4.69	58.67 ± 14.38
	R-norketamine	76.30 ± 15.31	49.04 ± 9.45

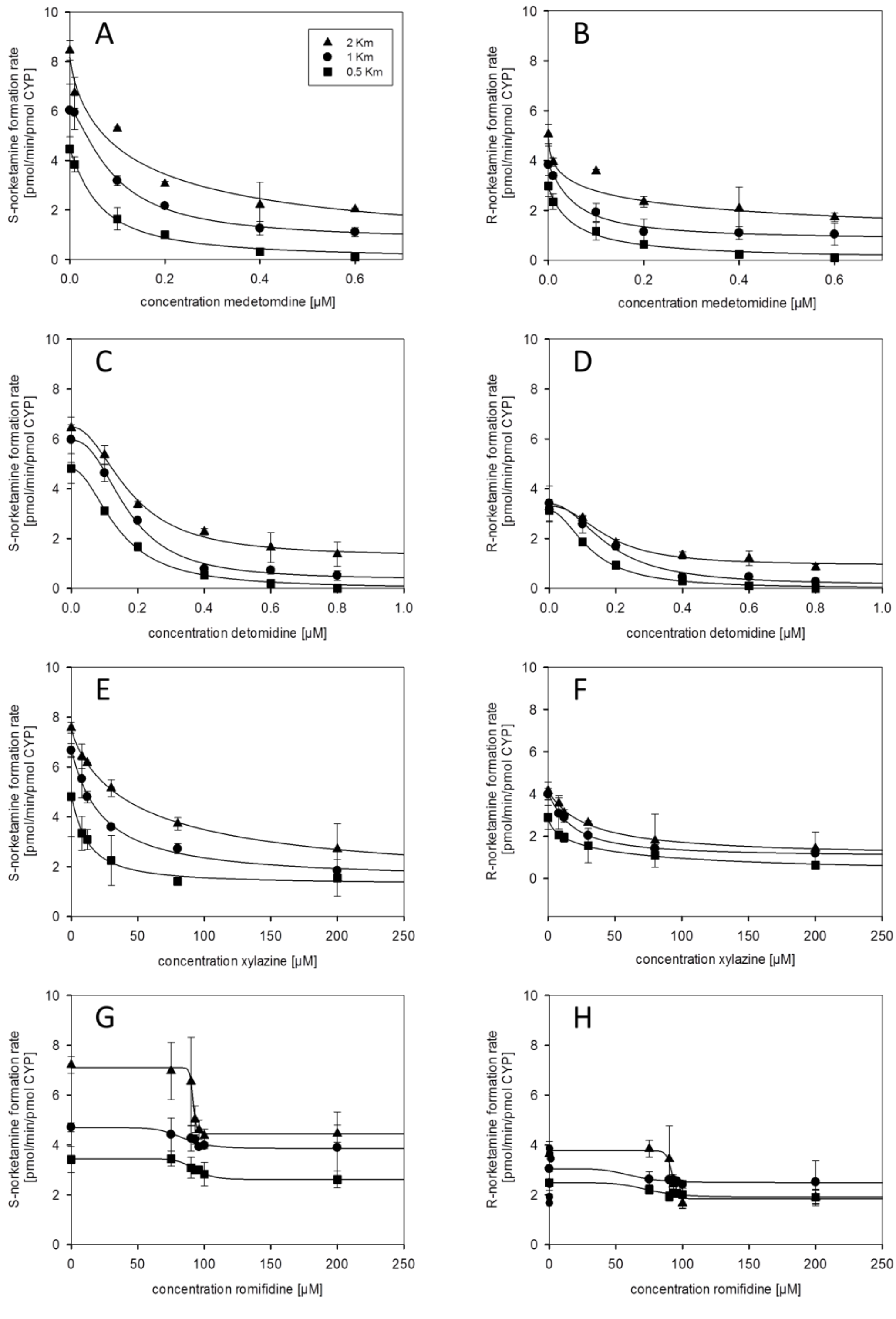

Figure 3. Kinetics of ELM mediated N-demethylation of (A,C,E,G) S-ketamine and (B,D,F,H) R-ketamine at three substrate concentrations (0.5 K_m, 1.0 K_m and 2.0 K_m) effected by (A,B) medetomidine, (C,D) detomidine, (E,F) xylazine and (G,H) romifidine. Concentrations for medetomidine varied between 0.1 and 0.6 µM, for detomidine between 0.1 and 0.8 µM, for xylazine between 8 and 200 µM and for romifidine between 75 and 200 µM. Nonlinear regression analysis was performed with the four-parameter logistic model described in the text. K_m values were from Ref. [37] Symbols denote means ± SD of duplicates.

The usual dose of 0.6 mg/kg for xylazine is considerably higher than for the other α_2-receptor agonists. After i. v. application of xylazine a c_{max} value of 2.73 µM was found [15, Table 1]. The values of inhibition constant and IC_{50} are higher than for medetomidine and detomidine. Furthermore, a difference between the effect on the formation of S-norketamine (IC_{50} 29.11 µM, Table 2) and R-norketamine (IC_{50} 9.62 µM, Table 2) was observed. The inhibition is stronger for the formation of R-norketamine whereas no stereoselectivity was determined for medetomidine and detomidine. It was also tested if the plastic walls adsorb xylazine. To investigate a possible loss of xylazine, the incubation was repeated in glass vials. No difference between glass and plastic vials was found.

For romifidine no inhibition could be detected. Using small ketamine concentrations there was no significant difference ($p>0.05$) between the determined norketamine levels in presence and absence of romifidine. With increasing ketamine concentrations the formation rate of norketamine was found to decrease abruptly at one point (Fig 3G and 4H). This does not look like a typical inhibition. It rather represents a sudden occurrence of a supersaturation.

The four substances have different molecular structures (Fig. 1) and thus differ in their affinity and selectivity to the α_2-receptor (Table 1) and the interaction with the CYP enzymes as a substrate and as a modulator as well. CYP enzymes are involved in the metabolism of all analyzed α_2-receptor agonists [7,8,10,28–30]. There are two characteristics which are important for an inhibitive CYP interaction. There must be a nitrogen-containing function which can bind to the heme iron and the inhibitor should have a hydrophobic part which can interact with the protein part of the CYP enzyme [14,41]. The inhibition will be stronger, if both mechanisms work well. Medetomidine and detomidine have both an imidazole group in the molecule which can fulfill the first condition. Imidazole derivates are known to be strong CYP inhibitors. Xylazine and romifidine have nitrogen for interaction as well. They are, however, not predestined to bind to the iron. Mesomeric and steric effects have also an influence. The various α_2-receptor agonists have the same basic structure but they differ in their substituents and in heteroatoms (Fig. 1). The lipophilicity of the α_2-receptor agonists can be compared with the partition coefficients, the log(P) values (Table 1). These are ratios of the drug concentrations in a two-phase system at equilibrium. High log(P) values stand for a higher lipophilicity and can therefore more strongly interact with CYP enzymes. The log (P) value of medetomidine is almost as high as that of the strong CYP inhibitor ketoconazole which has a log(P) value of 3.7 [14]. For the four α_2-receptor agonists the log(P) values decrease in the order of the decrease of the observed inhibition. Medetomidine has the highest log(P) value whereas romifidine the lowest (Table 1).

5.4.2 Effect of the α_2-receptor agonists on the ketamine metabolism

In the first part of this work the effects of different α_2-receptor agonists on the N-demethylation of ketamine to norketamine were analyzed and described with the inhibition parameters K_i and IC_{50}. This represents only the first step of the ketamine metabolism. Further reactions include the hydroxylation of ketamine and especially norketamine on different positions of the rings in the molecules. Furthermore, selected hydroxylated norketamine metabolites can then be dehydroxylated to DHNK. In previous studies with Beagle dogs it was shown that the impact of medetomidine comedication on the formation of 6HNK and DHNK is not the same as that found for norketamine [31]. Thus, the influence of different α_2-receptor agonists on the concentrations of ketamine and its metabolites norketamine, RR-6HNK, SS-6HNK and DHNK was analyzed with incubations that lasted up to 300 min. This is much longer compared to the 8 min time interval used in the experiments discussed in Section 3.1. Data obtained with concentrations of the α_2-receptor agonists representing the mean of the determined IC_{50} values for the two norketamine enantiomers (Table 2) are presented in Fig. 4. Electropherograms of 30 min incubations without and with medetomidine are shown as examples in Fig. 2E and 2F, respectively.

Furthermore, specific experiments were performed in order to be able to exclude any interference produced by metabolites of the α_2-receptor agonists. For each α_2-receptor agonist the same incubation procedure was followed without having ketamine in the incubation mixture. In the analysis of these samples, a metabolite peak could only be detected in the case of romifidine. This peak did not interfere with ketamine or one of its metabolites. Data without addition of an α_2-receptor agonist were also produced and used as control data to which the data obtained with α_2-receptor agonists were compared to.

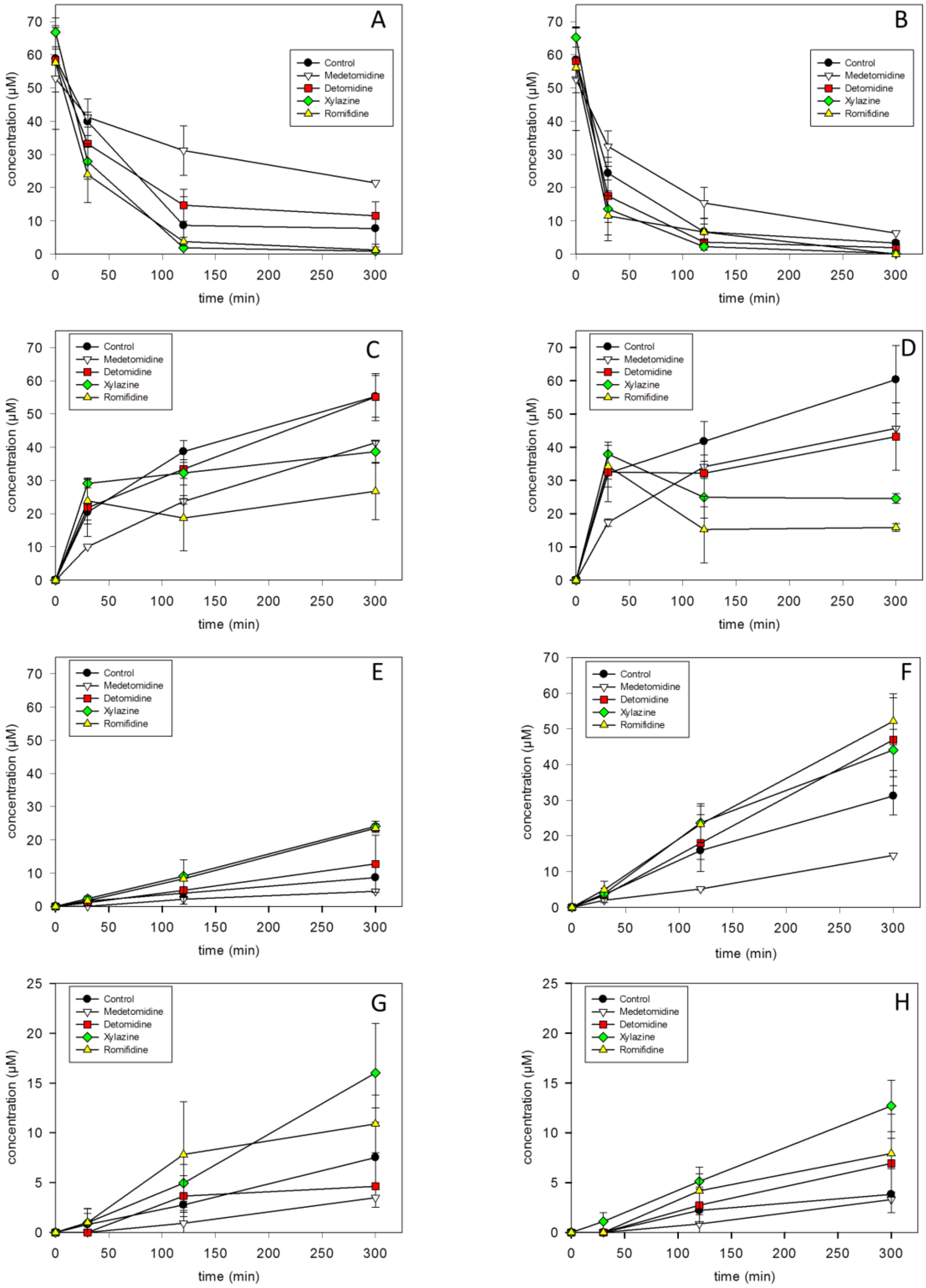

Figure 4. Effect of α_2-receptor agonists on (A) R-ketamine, (B) S-ketamine, (C) R-norketamine, (D) S-norketamine, (E) RR-6HNK, (F) SS-6HNK, (G) R-DHNK and (H) S-DHNK measured in the incubation mixtures as function of time. Concentrations of the applied ketamine enantiomers were 60 µM, whereas those of medetomidine, detomidine, xylazine and romifidine were 0.091 µM, 0.16 µM, 19.37 µM and 82.88 µM, respectively. The control data are those obtained without comedication. All experiments were performed in duplicates. Symbols denote mean values ± SD.

The ketamine enantiomer concentrations decrease with time and the decline was observed to be faster for S-ketamine than for R-ketamine (Fig. 4A and B). For both enantiomers this process is slower under medetomidine than under all other conditions, including the control which represents data without an α_2-receptor agonist. This finding confirms the results of Section 3.1 in which medetomidine was found to be the strongest inhibitor of the ketamine N-demethylation among the tested α_2-receptor agonists. The norketamine formation was inhibited in presence of medetomidine and the curve for norketamine is lower than that of the control experiment (Fig. 4C and D). Data for detomidine are somewhat in between which was expected because of the determined inhibition parameters (Table 2).

For xylazine and romifidine the inhibition parameters are much higher (Table 2) such that no inhibition was expected. Under the influence of these two drugs the ketamine concentrations are similar to that of the control experiment without an α_2-receptor agonist. The norketamine concentration-time curves, however, have a different profile. Norketamine levels first followed the values of the control experiment and reached a maximum around 30 min before reaching a plateau at about the peak concentration (R-norketamine, Fig. 4C) or at a lower plateau value (S-norketamine, Fig. 4D). The concentrations reached at 300 min are lower compared to those found with medetomidine, detomidine and without an α_2-receptor agonist. Furthermore, the xylazine curve is higher than that of romifidine. These data suggest that xylazine and romifidine inhibit the N-demethylation of ketamine at prolonged exposure only and that processes other than those related to inhibition are taking place.

Hydroxylation of norketamine occurs at different positions of both the cyclohexanone and the aromatic ring [26,35,36,42,43]. Only standard compounds for SS-6HNK and RR-6HNK were available. SS-6HNK was found to comigrate with the R stereoisomer of another hydroxynorketamine referred to as metabolite IV in Refs. [26,37] and RR-6HNK with the S stereoisomer of this norketamine metabolite [22]. In the same work, SS-6HNK and RR-6HNK could be assigned to hydroxylated norketamine metabolites S-I and R-I, respectively, of Refs. [26,37]. Thus, the detected peaks (see Fig. 2E) that were quantified for SS-6HNK and RR-6HNK (Fig. 4E and F) represent the sum of the two comigrating compounds. In previous in vitro work from our laboratory which was qualitatively evaluated with another assay, it was noted that significant amounts of both metabolites are formed which is in contrast to the results with canine liver microsomes for which almost no metabolite IV was observed [37]. More R-IV than S-IV and more S-I than R-I is formed in incubations of ketamine with ELM

[37]. The levels presented in Fig. 4F are much higher than those of Fig. 4E which is in agreement with the previous observations. In each case, the lowest levels were detected for medetomidine. All curves show a nearly linear increase of the concentrations. The curves for detomidine, xylazine and romifidine comedication are all higher than the control curve without addition of an α_2-receptor agonist (Fig. 4E and F). Thus, detomidine, xylazine and romifidine appear to induce the formation of the jointly detected compounds.

DHNK is the metabolite which is formed last (Fig. 4G and H). The courses of the curves are similar but the concentrations are lower than the data of Fig. 4E and F. Under medetomidine, the concentrations of both DHNK enantiomers are lower than those of the control experiment. Except for one value of the detomidine samples (Fig. 4G) all other results with the α_2-receptor agonists used are higher than that of the control without comedication. Thus, these data suggest that detomidine, xylazine and romifidine have an inductive impact on the formation of DHNK.

The data presented in Fig. 4 were analyzed for stereoselectivity using the paired Student's t-test for comparison of the curves of the corresponding R- and S-enantiomers. In all cases, $p > 0.05$ (range: 0.26-0.97) was obtained which does not reveal any stereoselectivity. These data, however, have to be considered with caution because data presented for single time points (see Fig. 4E and F) suggest that there are stereoselectivities in the metabolic steps of ketamine. An assay for complete resolution of the stereoisomers of all hydroxynorketamine metabolites is currently under development and will provide better insight into stereoselective aspects of hydroxylation of norketamine.

5.5 Concluding remarks

All tested α_2-receptor agonists showed an effect on the ketamine metabolism. This is important and should be considered when the drugs are applied repetitively during total intravenous or partial intravenous anesthesia. Medetomidine is the strongest inhibitor which is expressed by the lowest IC_{50} and K_i values of the assessed N-demethylation reaction. Its chemical structure and lipophilicity are good requirements for CYP inhibition. Detomidine inhibits the N-demethylation of ketamine to norketamine as well. Under medetomidine, levels of hydroxylated norketamine metabolites and DHNK become lower compared to the case without an α_2-receptor agonist. The opposite was found for xylazine and romifidine.

Stereoselectivity was found in the inhibition parameters of xylazine only. A possible stereoselective formation of hydroxylated norketamine metabolites will have to be assessed with an assay that is capable of resolving all observed hydroxynorketamine stereoisomers. In vivo investigations under consideration of the different cardiovascular effects of the various α_2-receptor agonists have to be undertaken in order to show the impact of α_2-receptor agonists on the pharmacokinetic and pharmacodynamic aspects of ketamine. The two enantioselective CE-based assays with highly sulfated γ-cyclodextrin as chiral selector are shown to represent effective tools for determining inhibition parameters and metabolic patterns in presence of different drugs as comedication.

Acknowledgements

The authors are grateful to Dr. Irving Wainer for receiving the standards of (2S,6S)-hydroxynorketamine and (2R,6R)-hydroxynorketamine. This work was supported by the Swiss National Science Foundation.

Conflicts of interest

The authors have declared no conflict of interest.

5.6 References

[1] G. Mion, T. Villevieille, Ketamine Pharmacology: An Update (Pharmacodynamics and Molecular Aspects, Recent Findings), CNS Neurosci. Ther. 19 (2013) 370–380.

[2] E.D. Kharasch, R. Labroo, Metabolism of ketamine stereoisomers by human liver microsomes, Anesthesiology 77 (1992) 1201–1207.

[3] R.K. Paul, N.S. Singh, M. Khadeer, R. Moaddel, M. Sanghvi, C.E. Green, K. O'Loughlin, M.C. Torjman, M. Bernier, I.W. Wainer, (R,S)-Ketamine metabolites (R,S)-norketamine and (2S,6S)-hydroxynorketamine increase the mammalian target of rapamycin function, Anesthesiology 121 (2014) 149–159.

[4] J. Persson, Ketamine in Pain Management, CNS Neurosci. Ther. 19 (2013) 396–402.

[5] K.N. Grimsrud, S. Ait-Oudhia, B.P. Durbin-Johnson, D.M. Rocke, K.R. Mama, M.L. Rezende, S.D. Stanley, W.J. Jusko, Pharmacokinetic and pharmacodynamic analysis

comparing diverse effects of detomidine, medetomidine, and dexmedetomidine in the horse: a population analysis, J. Vet. Pharmacol. Ther. 38 (2015) 24–34.

[6] K.N. Grimsrud, K.R. Mama, E.P. Steffey, S.D. Stanley, Pharmacokinetics and pharmacodynamics of intravenous medetomidine in the horse, Vet. Anaesth. Analg. 39 (2012) 38–48.

[7] D.S.-G. Lavoie, F. Pailleux, P. Vachon, F. Beaudry, Characterization of xylazine metabolism in rat liver microsomes using liquid chromatography-hybrid triple quadrupole-linear ion trap-mass spectrometry, Biomed. Chromatogr. 27 (2013) 882–888.

[8] A.E. Mutlib, Y.C. Chui, L.M. Young, F.S. Abbott, Characterization of metabolites of xylazine produced in vivo and in vitro by LC/MS/MS and by GC/MS, Drug Metab. Dispos. 20 (1992) 840–848.

[9] M. Wojtasia-Wypart, L.R. Soma, J.A. Rudy, C.E. Uboh, R.C. Boston, B. Driessen, Pharmacokinetic profile and pharmacodynamic effects of romifidine hydrochloride in the horse, J. Vet. Pharmacol. Ther. 35 (2012) 478–488.

[10] D. Veilleux-Lemieux, A. Castel, D. Carrier, F. Beaudry, P. Vachon, Pharmacokinetics of ketamine and xylazine in young and old Sprague-Dawley rats, J. Am. Assoc. Lab. Anim. Sci. 52 (2013) 567–570.

[11] H. Kaukinen, J. Aspegrén, S. Hyyppä, L. Tamm, J.S. Salonen, Bioavailability of detomidine administered sublingually to horses as an oromucosal gel, J. Vet. Pharmacol. Ther. 34 (2011) 76–81.

[12] M. Gozalo-Marcilla, F. Gasthuys, S. Schauvliege, Partial intravenous anaesthesia in the horse: a review of intravenous agents used to supplement equine inhalation anaesthesia. Part 2: opioids and alpha-2 adrenoceptor agonists, Vet. Anaesth. Analg. 42 (2015) 1–16.

[13] J.A. Giovannitti, S.M. Thoms, J.J. Crawford, Alpha-2 adrenergic receptor agonists: a review of current clinical applications, Anesth. Prog. 62 (2015) 31–39.

[14] A. Kamel, S. Harriman, Inhibition of cytochrome P450 enzymes and biochemical aspects of mechanism-based inactivation (MBI), Drug Discov. Today Technol. 10 (2013) e177.

[15] A. Santonastaso, J. Hardy, N. Cohen, V. Fajt, Pharmacokinetics and pharmacodynamics of xylazine administered by the intravenous or intra-osseous route in adult horses, J. Vet. Pharmacol. Ther. 37 (2014) 565–570.

[16] A. Kullmann, M. Sanz, G.T. Fosgate, M.N. Saulez, P.C. Page, E. Rioja, Effects of xylazine, romifidine, or detomidine on hematology, biochemistry, and splenic thickness in healthy horses, Can. J. Vet. 55 (2014) 334–340.

[17] S. Nannarone, R. Gialletti, I. Veschini, A. Bufalari, F. Moriconi, The Use of Alpha-2 Agonists in the Equine Practice: Comparison between Three Molecules, Vet. Res. Commun. 31 (2007) 309–312.

[18] C. L. Kerr, W. N. McDonell, S. S. Young, A comparison of romifidine and xylazine when used with diazepam/ketamine for short duration anesthesia in the horse, Can. Vet. J. 37 (1996) 601–609.

[19] H. Jaugstetter, R. Jacobi, R. Pellmann, Vergleich der Narkoseprämedikation mit Romifidin und Xylazin in Bezug auf das Aufstehverhalten von Pferden nach Allgemeinanästhesie, Der Praktische Tierarzt 9 (2002) 786–791.

[20] K. W. Clarke, P. M. Taylor, S. B. Watkins, Detomidine/ Ketamine anesthesia in the horse, Acta Vet. Scand. Suppl. 82 (1986) 167–179.

[21] F.A. Sandbaumhüter, R. Theurillat, W. Thormann, Effects of medetomidine and its active enantiomer dexmedetomidine on N-demethylation of ketamine in canines determined in vitro using enantioselective capillary electrophoresis, Electrophoresis 36 (2015) 2703–2712.

[22] R. Theurillat, F.A. Sandbaumhüter, R. Bettschart-Wolfensberger, W. Thormann, Microassay for ketamine and metabolites in plasma and serum based on enantioselective capillary electrophoresis with highly sulfated γ-cyclodextrin and electrokinetic analyte injection, Electrophoresis 37 (2016) 1129–1138.

[23] Y. Hijazi, C. Bodonian, M. Bolon, F. Salord, R. Boulieu, Pharmacokinetics and haemodynamics of ketamine in intensive care patients with brain or spinal cord injury, Br. J. Anaesth. 90 (2003) 155–160.

[24] S. Portmann, H.Y. Kwan, R. Theurillat, A. Schmitz, M. Mevissen, W. Thormann, Enantioselective capillary electrophoresis for identification and characterization of human cytochrome P450 enzymes which metabolize ketamine and norketamine in vitro, J. Chromatogr. A 1217 (2010) 7942–7948.

[25] Y. Yanagihara, S. Kariya, M. Ohtani, K. Uchino, T. Aoyama, Y. Yamamura, T. Iga, Involvement of CYP2B6 in n-demethylation of ketamine in human liver microsomes, Drug Metab. Dispos. 29 (2001) 887–890.

[26] A. Schmitz, R. Theurillat, P.-G. Lassahn, M. Mevissen, W. Thormann, CE provides evidence of the stereoselective hydroxylation of norketamine in equines, Electrophoresis 30 (2009) 2912–2921.

[27] R. Moaddel, G. Abdrakhmanova, J. Kozak, K. Jozwiak, L. Toll, L. Jimenez, A. Rosenberg, T. Tran, Y. Xiao, C.A. Zarate, I.W. Wainer, Sub-anesthetic concentrations of (R,S)-ketamine metabolites inhibit acetylcholine-evoked currents in α7 nicotinic acetylcholine receptors, Eur. J. Pharmacol. 698 (2013) 228–234.

[28] M.-C. Duhamel, É. Troncy, F. Beaudry, Metabolic stability and determination of cytochrome P450 isoenzymes' contribution to the metabolism of medetomidine in dog liver microsomes, Biomed. Chromatogr. 24 (2010) 868–877.

[29] W. H. Hsu (Ed.), Handbook of Veterinary Pharmacology, Wiley-Blackwell, Chichester, 2008.

[30] D. F. Kohn, S. K. Wixcon, W. J. White, G. J. Benson, Anestehesia and Analgesia in Laboratory Animals, Academic Press (Elsevier), London, 1997.

[31] F. A. Sandbaumhüter, R. Theurillat, R. N. Bektas, A. P. Kutter, R. Bettschart-Wolfensberger, W. Thormann, Pharmacokinetics of ketamine and three metabolites in Beagle dogs under sevoflurane vs. medetomidine comedication assessed by enantioselective capillary electrophoresis, J. Chromatogr. A 1467 (2016) 436–444.

[32] P. Zanos, R. Moaddel, P.J. Morris, P. Georgiou, J. Fischell, G.I. Elmer, M. Alkondon, P. Yuan, H.J. Pribut, N.S. Singh, K. S. Dossou, Y. Fang, X.-P. Huang, C.L. Mayo, I.W. Wainer, E.X. Albuquerque, S.M. Thompson, C.J. Thomas, C.A. Zarate, T.D. Gould, NMDAR inhibition-independent antidepressant actions of ketamine metabolites, Nature 533 (2016) 481–486.

[33] E.D. Kharasch, S. Herrmann, R. Labroo, Ketamine as a probe for medetomidine stereoisomer inhibition of human liver microsomal drug metabolism, Anesthesiology 77 (1992) 1208–1214.

[34] J. Caslavska, W. Thormann, Stereoselective determination of drugs and metabolites in body fluids, tissues and microsomal preparations by capillary electrophoresis (2000–2010), J. Chromatogr. A 1218 (2011) 588–601.

[35] Z. Desta, R. Moaddel, E.T. Ogburn, C. Xu, A. Ramamoorthy, S. L. V. Venkata, M. Sanghvi, M.E. Goldberg, M.C. Torjman, I.W. Wainer, Stereoselective and regiospecific hydroxylation of ketamine and norketamine, Xenobiotica 42 (2012) 1076–1087.

[36] R. Moaddel, S. L. V. Venkata, M.J. Tanga, J.E. Bupp, C.E. Green, L. Iyer, A. Furimsky, M.E. Goldberg, M.C. Torjman, I.W. Wainer, A parallel chiral-achiral liquid chromatographic method for the determination of the stereoisomers of ketamine and

ketamine metabolites in the plasma and urine of patients with complex regional pain syndrome, Talanta 82 (2010) 1892–1904.

[37] A. Schmitz, W. Thormann, L. Moessner, R. Theurillat, K. Helmja, M. Mevissen, Enantioselective CE analysis of hepatic ketamine metabolism in different species in vitro, Electrophoresis 31 (2010) 1506–1516.

[38] T. Omura, R. Sato, The carbon monoxide-binding pigment of liver microsomes. II. Solubilization, Purification, and Properties, J. Biol. Chem. 239 (1964) 2379–2385.

[39] R. Remínek, Z. Glatz, W. Thormann, Optimized on-line enantioselective capillary electrophoretic method for kinetic and inhibition studies of drug metabolism mediated by cytochrome P450 enzymes, Electrophoresis 36 (2014) 1349–1357.

[40] Y. Cheng, W.H. Prusoff, Relationship between the inhibition constant (K1) and the concentration of inhibitor which causes 50 per cent inhibition (I50) of an enzymatic reaction, Biochem. Pharmacol. 22 (1973) 3099–3108.

[41] M. A. Correia, P. F. Hollenberg, in P. R. Ortiz de Montellano (Ed.), Cytochrome P450: Structure, mechanism, and biochemistry, Springer International Publishing, Switzerland (2015) 177–260.

[42] X. Zhao, S.L.V. Venkata, R. Moaddel, D.A. Luckenbaugh, N.E. Brutsche, L. Ibrahim, C.A. Zarate, D.E. Mager, I.W. Wainer, Simultaneous population pharmacokinetic modelling of ketamine and three major metabolites in patients with treatment-resistant bipolar depression, Br. J. Clin. Pharmacol. 74 (2012) 304–314.

[43] C.A. Zarate, N. Brutsche, G. Laje, D.A. Luckenbaugh, S.L.V. Venkata, A. Ramamoorthy, R. Moaddel, I.W. Wainer, Relationship of ketamine's plasma metabolites with response, diagnosis, and side effects in major depression, Biol. Psychiatry 72 (2012) 331–338.

6. Enantioselective separation of four different hydroxynorketamines using capillary electrophoresis with sulfated β-cyclodextrin and highly sulfated γ-cyclodextrin as selector (Electrophoresis (2017) doi: 10.1002/elps.201700016)

Friederike A. Sandbaumhüter[1], Regula Theurillat[1], Wolfgang Thormann[1]

[1] Clinical Pharmacology Laboratory, University of Bern, Bern, Switzerland

6.1 Abstract

The racemic N-methyl-d-aspartate (NMDA) receptor antagonist ketamine is used in anesthesia, analgesia and the treatment of depressive disorders. It is known that interactions of hydroxylated norketamine metabolites and 5,6-dehydronorketamine (DHNK) with the α_7-nicotinic acetylcholine receptor and the α-amino-3-hydroxy-5-methyl-4-isoxazolepropionic acid (AMPA) receptor are responsible for the antidepressive effects. Ketamine and its first metabolite norketamine are not active on these receptors. As stereoselectivity plays a role in ketamine metabolism, a cationic capillary electrophoresis based method capable of resolving and analyzing the stereoisomers of four hydroxylated norketamine metabolites, norketamine and DHNK was developed. The assay is based on liquid/liquid extraction of the analytes from the biological matrix, electrokinetic sample injection across a buffer plug and analysis of the stereoisomers in a phosphate BGE at pH 3 comprising a mixture of sulfated β-cyclodextrin (5 mg/mL) and highly sulfated γ-cyclodextrin (0.1 %). The method was used to analyze samples of in vitro study in which ketamine was incubated with equine liver microsomes and in plasma samples of dogs and horses that were collected after an i. v. bolus injection of racemic ketamine.

6.2 Introduction

The racemic drug ketamine (for chemical structure see Fig. 1) is applied in anesthesia, analgesia and the treatment of depressive disorders. The risk of strong side effects and abuse must be considered for application of this drug. In recent years, metabolites of ketamine became the focus of interest and are tested concerning their effects. Norketamine is the first metabolite and is formed by N-demethylation. It is active at the N-methyl-d-aspartate (NMDA) receptor but to a lesser extent than the parent drug ketamine [1–5]. Norketamine is transformed to hydroxynorketamine (HNK). Hydroxylation can take place at different positions on the cylohexanone and the chlorophenyl ring (Fig. 1). Addition of a hydroxy group at the cyclohexanone ring leads to a second chiral center in the molecule and thus different stereoisomers. Hydroxylation of ketamine to hydroxyketamine followed by N-demethylation is also possible and is believed to represent a minor role in the metabolic parthways of ketamine (Fig. 1). The next step is the formation of 5,6-dehydronorketamine (DHNK) [6–10]. Most metabolic steps are known to be catalyzed by cytochrome P450 enzymes [9–13]. For stereoisomers of HNK and DHNK only low activity at the NMDA receptor but inhibition of the α_7-nicotinic acetylcholine receptor was shown [14]. (2R,6R)-6-hydroxynorketamine (RR-6HNK) activates processes at the α-amino-3-hydroxy-5-methyl-4-isoxazolepropionic acid (AMPA) receptor [5]. The interactions with the α_7-nicotinic acetylcholine receptor and AMPA receptor are responsible for antidepressive effects [5,14]. RR-6HNK and (2S,6S)-6-hydroxynorketamine (SS-6HNK) revealed antidepressive effects in experiments with mice [8,15]. For ketamine and the metabolites norketamine, 6-hydroxynorketamine (6HNK) and DHNK a decrease of the intracellular d-serine concentrations was also found. D-serine has neurotoxic and neurodegenerative effects on the NMDA receptor and is associated with central nervous system diseases [16].

Analytical methods which are based on enantioselective capillary electrophoresis were primarily developed to analyze ketamine, norketamine and DHNK [9,12,17–25]. In the microassay of Theurillat et al. which uses 0.6-0.8 % highly sulfated γ-cyclodextrin as chiral selector and normal polarity (analytes are migrating as cations), HNK can be determined as well. A complete separation of the stereoisomers of HNK was not obtained [26]. Stereoisomers of HNK, however, can be resolved under conditions using higher amounts of highly sulfated γ-cyclodextrin (unpublished results, tested with 2.0-3.3%) or sulfated β-cyclodextrin (10 mg/mL [9,22]) and using reversed polarity such that the analytes are migrating as anions. Due to high migration times, detected peaks are broad and their analysis becomes inaccurate. Because of stereoselectivities in metabolism, receptor affinity and antidepressive effects the stereoselective separation of all metabolites is important

[5,7,9,11,12,14,17,22–27]. This prompted us to find conditions to properly analyze the stereoisomers of hydroxylated norketamine metabolites in biological samples by cationic CE.

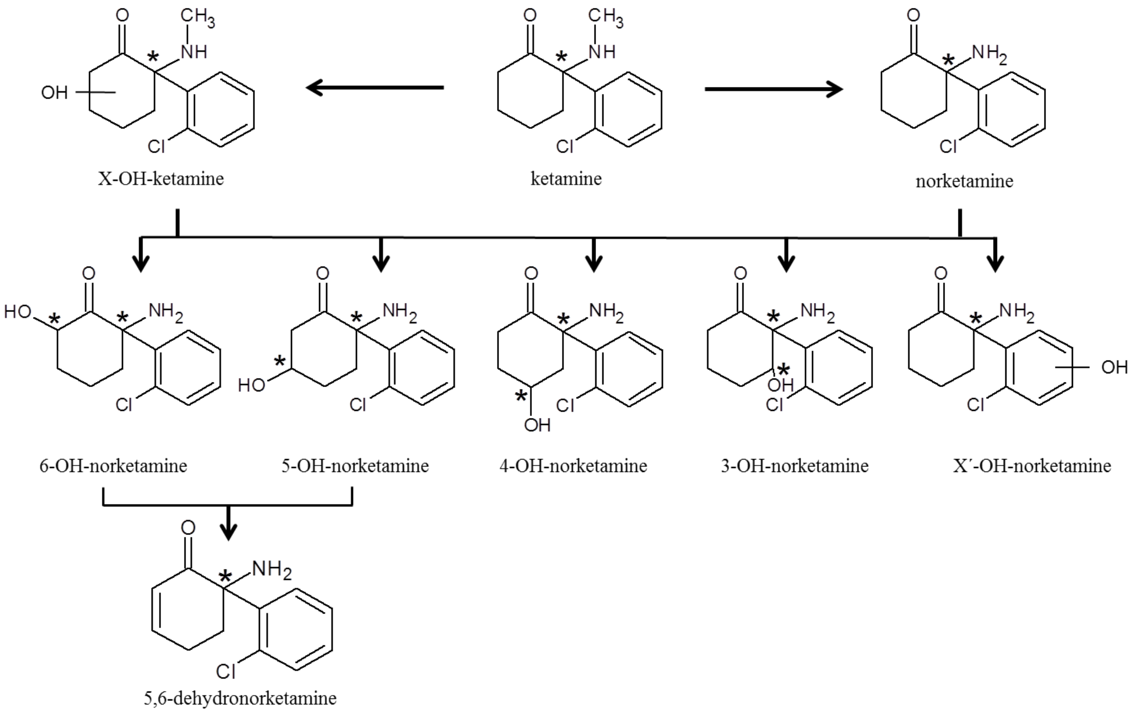

Figure 1. The main metabolic pathways of ketamine. Stereocenters are marked with asterisks. X: 3, 4, 5 or 6; X’: 2’, 3’, 4’ or 5’.

The goal of this work was to develop a stereoselective CE-based assay for four hydroxylated norketamine metabolites that were found in pony urines collected during a ketamine target controlled infusion study [9], in incubations of equine liver microsomes with ketamine [9], and in in vitro experiments with liver microsomes of different species [22]. Data collected during assay development with various sulfated cyclodextrins, the strategy employed for optimization of stereoisomer separation and first results obtained for the analysis of these ketamine metabolites in incubations of ketamine with equine liver microsomes (ELM) and in plasma samples of horses and dogs are reported.

6.3 Material and methods

6.3.1 Chemicals, reagents, and origin of animal samples

(2S,6S)-6-hydroxynorketamine (SS-6HNK), (2R,6R)-6-hydroxynorketamine (RR-6HNK), (2S,6R)-6-hydroxynorketamine (SR-6HNK) and (2R,6S)-6-hydroxynorketamine (RS-6HNK) were from Dr. Irving Wainer (Laboratory of Clinical Investigations, National Institute on Aging, National Institutes of Health, Baltimore, MD, USA). Their synthesis is described by Moaddel et al. and Desta et al. [6,10]. Analytical standards for ketamine and norketamine (as hydrochlorides in methanol, 1 mg/mL of the free base), and DHNK (as hydrochloride 100 µg/mL in acetonitrile) were from Cerilliant (Round Rock, TX, USA). Highly sulfated γ-cyclodextrin (20 % *w/v* solution) was purchased from Beckman Coulter (Fullerton, CA, USA). Sulfated β-cyclodextrin (lot 04426HJ), d-(+)-norephedrine hydrochloride and bovine serum were from Sigma-Aldrich (St. Louis, Mo, USA). Disodium hydrogenphosphate, sodium dihydrogenphosphate, sodium hydroxide, acetic acid, sodium acetate trihydrate were from Merck (Darmstadt, Germany), phosphoric acid (85 %) and detomidine were from Fluka (Buchs, Switzerland) and dichloromethane (HiPerSolv Chromanorm for HPLC) was from VWR (Leuven, Belgium). β-glucuronidase/arylsulfatase from *Helix Pomatia* was from Roche (Mannheim, Germany). ELM were prepared and characterized by Schmitz et al. [22]. Animal plasma samples stemmed from two previously conducted ketamine studies which were executed with the permission of the respective Committee for Animal Experimentations [24,27]. In the first trail, ponies received an i. v. bolus of 2.2 mg/kg racemic ketamine under isoflurane anesthesia [24]. In the other trial, beagle dogs under sevoflurane anesthesia received an i.v. bolus of 4 mg/kg racemic ketamine [27].

6.3.2 Hydroxynorketamine standards

Analytical standards were only available for 6HNK. Thus, hydroxylated norketamine metabolites were fractionated from horse urine using the procedure described in [9]. Before fractionation 1 mL urine in 1 mL 0.2 M sodium acetate buffer pH 5 was treated with 100 µL β-glucuronidase/arylsulfatase over 12 h. The enzymatic reaction was stopped with 200 µL 2 M NaOH and the hydrolyzed urine extracted with 6 mL dichloromethane/ethylacetate

(75:25 %, *v/v*). After evaporation of the organic solvent and reconstitution of the dried extract with 400 µL water, the sample was applied to HPLC. Briefly, the HPLC system comprised a Waters LC-Module I plus equipped with autosampler, absorbance detector and pump (Waters, Milford, MA, USA). The stationary phase was a Purospher RP 18e column (4 mm x 125 mm x 5 µm) (Merck) and the mobile phase was composed of 30 mM ammonium phosphate buffer pH 7.2 (solvent A) and acetonitrile (solvent B). The elution of the hydroxylated norketamine metabolites was performed with 20 % acetonitrile in the mobile phase and the four fractions containing hydroxylated norketamine metabolites were collected manually into glass tubes and referred to as HNK fractions I to IV [9]. Collected fractions were stored at -20 °C until further use.

6.3.3 In vitro reaction with ELM

60 µM per enantiomer ketamine were preincubated with NADPH regenerating system consisting of 1.49 mM NADP+, 3.2 mM glucose-6-phosphate, 0.4 U/mL glucose-6-phosphate dehydrogenase, 2.9 mM $MgCl_2$ and 50 µM sodium citrate in 100 mM pH 7.4 potassium phosphate buffer and 0.16 µM detomidine for 300 min at 37 °C. Detomidine is a sedative α_2-receptor agonist which is often used in combination with ketamine in veterinary medicine. The incubation was started with the addition of ELM (0.5 mg protein/mL) to a final volume of 200 µL. Samples of 50 µL were taken after 0, 30, 120 and 300 min and the reaction was stopped with addition of 15 µL 1 M NaOH.

6.3.4 Sample preparation

10 µL of the incubation samples were mixed with 240 µL of water and 20 µL of 0.5 mM NaOH. Similarly, 50 µL of animal plasma were prepared with 200 µL water and 50 µL 0.5 mM NaOH. After adding 1300 µL of dichloromethane the sample was first shaken for 10 min and then centrifuged (5 min at 12000 rpm). Afterwards the upper aqueous phase was removed and the organic phase was transferred into another vial and acidified with 10 µL 1 mM phosphoric acid. The dichloromethane was evaporated by using the Eppendorf concentrator 5301 (Vaudaux-Eppendorf, Schönenbuch, Switzerland) for 30 min at 45 °C. The residues were reconstituted with 110 µL water and then analyzed by capillary electrophoresis.

6.3.5 CE instrumentation and analytical conditions

A Proteome Lab PA 800 instrument (Beckman Coulter, Fullerton, CA, USA) equipped with a 50 µm i.d. fused-silica capillary (Polymicro Technologies, Phoenix, AZ, USA) of 45 cm total length (effective length 35 cm) was used. The capillary was rinsed before each run with water (20 psi; 3 min) and running buffer (20 psi; 1 min). If not stated otherwise, the background electrolyte (BGE) was composed of 50 mM sodium dihydrogenphosphate solution which was adjusted with phosphoric acid to pH 3, 5 mg/mL sulfated β-cyclodextrin and 0.1 % highly sulfated γ-cyclodextrin. A plug of four times diluted phosphate buffer (pH 3) was injected with pressure (4 psi; 4 s) followed by electrokinetic analyte injection at 7 kV for 10 s. A voltage of 20 kV was applied. The current was about 40 µA. The temperature was set to 20 °C. Detection of the analytes was performed with a PDA detector at 195 nm. Data obtained with this new method were compared to those obtained with the microassay of Theurillat et al. [26]. In this assay, a BGE comprising 100 mM phosphate buffer (pH 3.0) and 0.66 % highly sulfated γ-cyclodextrin was used. The sample was injected at 6 kV for 15 s across a pressure injected plug (1 psi, 20 s) of 50 mM phosphate buffer (pH 3.0). A voltage of 20 kV was applied, the current was about 64 µA, the temperature for all parts was set to 25 °C and the detection was effected at 200 nm. Typical electropherograms of both methods are presented in Fig. 2. Corrected peak areas, i. e. peak areas divided by detection time (units µAU), were used to compare the analyte peaks.

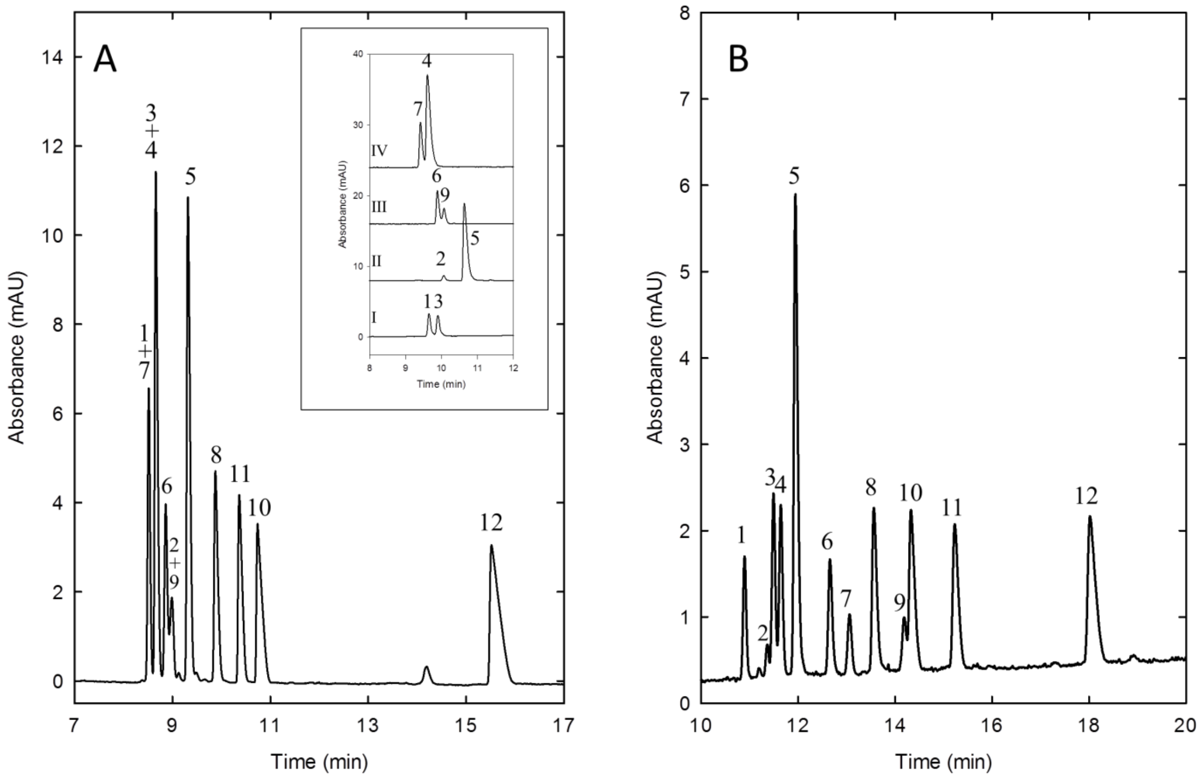

Figure 2. Representative electropherograms of 6HNK (urine fraction I), norketamine, DHNK (100 ng/mL/enantiomer each) and the diluted urine fractions II, III and IV obtained with (A) the microassay of Ref. [16] and (B) the newly developed assay. Data obtained for analysis of urine fractions I to IV with the microassay BGE are presented as insert in panel A (y-scale shift of 8 mAU). The CE conditions were as described in Section 2.5. Key: 1: RR-6HNK (R-I), 2: R-II, 3: SS-6HNK (S-I), 4: R-IV, 5: S-II, 6: R-III, 7: S-IV, 8: R-NK, 9: S-III, 10: S-DHNK, 11: S-NK, 12: R-DHNK.

6.3.6 Data analysis

SigmaPlot software version 12.5 (Systat Software, San Jose, CA, USA) and Microsoft Excel (Microsoft, Redmont, WA, USA) were used for data evaluation. Plug lengths were calculated with the CE Expert Lite calculator software (Beckman Coulter, Fullerton, CA, USA) which is based on the Poiseuille equation and describes the flow of a fluid through a cylindrical vessel.

6.4 Results and discussion

6.4.1 Background and initial attempts for separation

Enantioselective separation conditions comprising 2.0-3.3 % highly sulfated γ-cyclodextrin or 10 mg/mL of sulfated β-cyclodextrin and reversed polarity revealed that migration times were dependent on the lot of the cyclodextrin used and the age of the product [9,17,18,22]. HNK stereoisomers migrated slowly and were detected as broad peaks after those of ketamine, norketamine and DHNK such that they could not be evaluated accurately. Due to lack of standards, the stereochemistry of the four hydroxylated HNK metabolites extracted from equine urine and referred to as metabolites I to IV could not be identified at that time [9,22]. The recent availability of RR-, SS-, RS- and SR-6HNK revealed that R-I and S-I are RR-6HNK and SS-6HNK, respectively. RS-6HNK and SR-6HNK could not be detected in samples of horses and dogs both in vivo and in vitro (data not shown).

With use of a smaller amount of the chiral selector and normal polarity, the detection order becomes reversed. In the microassay format with 0.6-0.8 % highly sulfated γ-cyclodextrin the stereoisomers of ketamine, norketamine, 6HNK and DHNK could be quantitated [26]. Separation of the stereoisomers of the four hydroxylated norketamine metabolites I to IV, however, was not possible (Fig. 2A). RR-6HNK (metabolite R-I of [9,22]) comigrated with metabolite S-IV and SS-6HNK (metabolite S-I of [9,18]) with metabolite R-IV (insert of Fig. 2A). Similarly, S-II and S-III had the same migration time. Small changes of cyclodextrin concentration, buffer concentration (50 instead of 100 mM), plug characteristics and other parameters such as applied voltage or cartridge temperature and otherwise identical assay conditions did not reveal any significant improvements. Thus, efforts with other buffer compositions were investigated namely those based on the use of Tris phosphate [17]. Separation of the four hydroxylated norketamine metabolites could not be obtained with 50 mM, 100 mM or 150 mM Tris phosphate BGEs of pH 2.0 to 4.5 comprising highly sulfated γ-cyclodextrin between 0.1 and 0.6 % and 0 to 20 % of an organic solvent (methanol, ethanol, propanol, acetonitrile, isopropanol and various mixtures of two of these solvents). Varying migration time intervals were observed within one day and between different days such that tests with buffers containing Tris and phosphate were not continued.

6.4.2 Separations with sulfated β-cyclodextrin and highly sulfated γ-cyclodextrin

Further work was geared towards the investigation of various sulfated chiral selectors in a solution of 50 mM sodium dihydrogenphosphate adjusted with phosphoric acid to pH 3, including sulfated β-cyclodextrin that was previously used by Schmitz et al. and others [9,12,18,22–25]. In that work, 10 mg/mL were added to the BGE and the assay was operated in the reversed polarity mode. Rabanes et al. used the same selector for separation of alprenolol enantiomers under conditions of reversed polarity (5 mg/mL) and normal polarity (0.3 mg/mL) [28]. Separation of the stereoisomers of the four hydroxylated norketamine metabolites was assessed under normal polarity with increasing amounts of sulfated β-cyclodextrin in the phosphate buffer (Fig. 3 A-D). With 0.3 mg/mL and 1 mg/mL sulfated β-cyclodextrin in the BGE no resolution was obtained (Fig. 3A and B) whereas with 5 and 6 mg/mL respectable separation of the stereoisomers of HNK, norketamine and DHNK was observed (Fig. 3C and D). In the former case, there was an interference between S-IV and S-DHNK (Fig. 3C) and in the latter configuration the separation between R-IV and S-II as well as between R-NK and S-IV were insufficient (Fig. 3D). Experiments with other available lots of sulfated β-cyclodextrin provided similar results. Finally, mixtures of sulfated β-cyclodextrin and highly sulfated γ-cyclodextrin were applied and found to reveal best resolution when 0.1 % of highly sulfated γ-cyclodextrin was combined with 5 mg/mL sulfated β-cyclodextrin (Fig. 3E). With a higher amount of highly sulfated γ-cyclodextrin (0.2 %) separation of all stereoisomers was not observed (Fig. 3F). These data illustrate how delicate the composition of the chiral selector is for the anticipated task. Thus, a BGE composed of 50 mM sodium dihydrogenphosphate adjusted with phosphoric acid to pH 3.0 together with 5 mg/mL sulfated β-cyclodextrin and 0.1 % highly sulfated γ-cyclodextrin was used for the rest of the work presented in this paper.

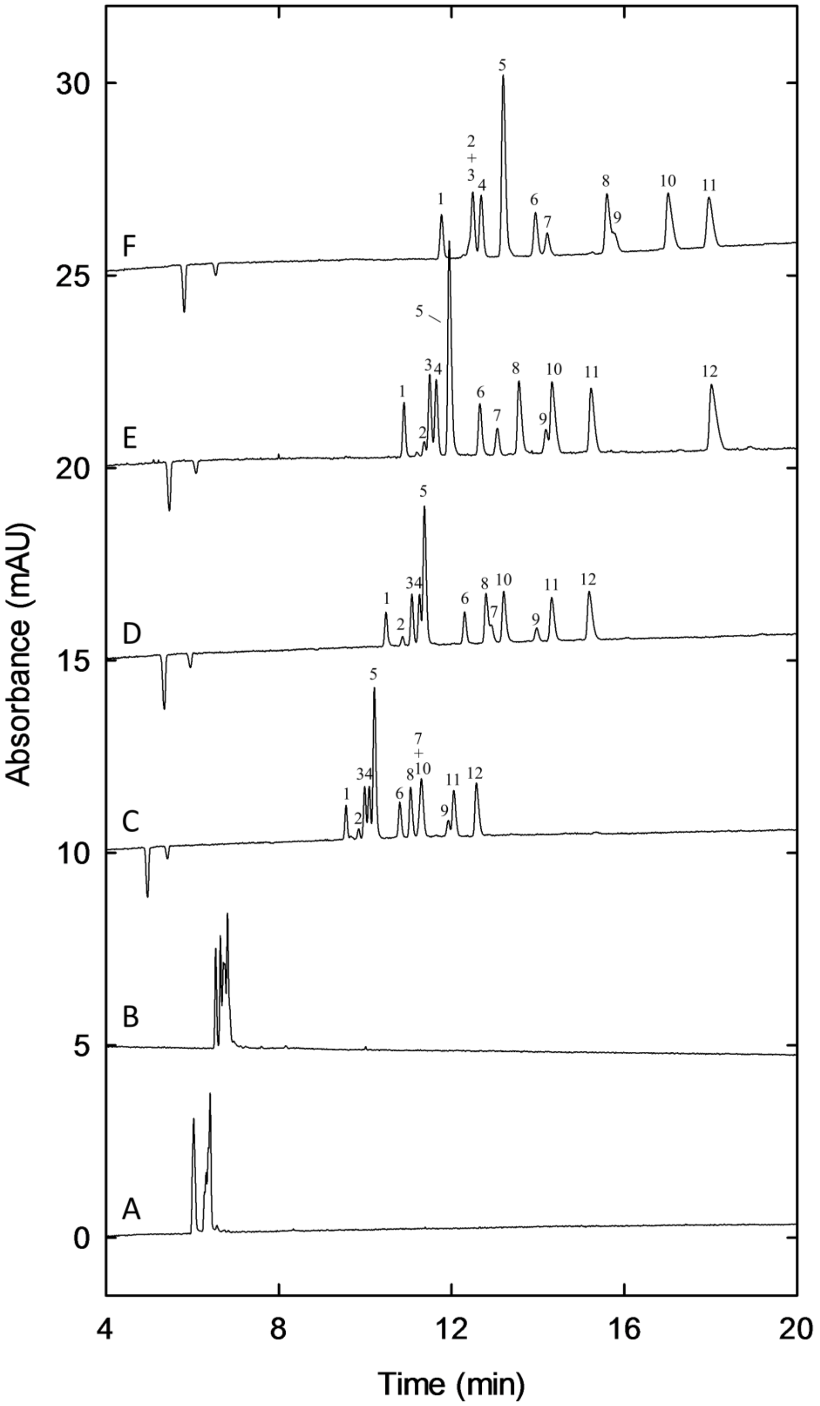

Figure 3. Electropherograms of 6HNK, norketamine, DHNK (100 ng/mL/enantiomer each) and the diluted urine fractions II, III and IV obtained with BGEs containing (A) 0.3 mg/mL sulfated β-cyclodextrin, (B) 1 mg/mL sulfated β-cyclodextrin, (C) 5 mg/mL sulfated β-cyclodextrin, (D) 6 mg/mL sulfated β-cyclodextrin, (E) a mixture of 5 mg/mL sulfated β-cycodextrin and 0.1 % highly sulfated γ-cyclodextrin and (F) 5 mg/mL sulfated β-cyclodextrin and 0.2 % highly sulfated γ-cyclodextrin. Other CE conditions were as described in Section 2.5. Key: 1: RR-6HNK, 2: R-II, 3: SS-6HNK, 4: R-IV, 5: S-II, 6: R-III, 7: S-IV, 8: R-NK, 9: S-III, 10: S-DHNK, 11: S-NK, 12: R-DHNK. Data presented with a y-scale shift of 5 mAU.

6.4.3 Assay development

For electroinjection of analytes as described in [26], a plug of buffer without chiral selector is employed to achieve highest sensitivity and to avoid contamination of the sample with the negatively charged cyclodextrin and phosphate from the BGE. Plug buffer concentrations in the range of 2 to 5 times diluted phosphate buffer were investigated. The separation of analytes and sensitivity improved up to a four-fold dilution. Thus, a plug of four times diluted phosphate buffer was chosen. The length of the buffer plug was another important aspect [26]. Injections at 1 psi for 15 s (17.87 mm plug calculated for 20 °C with CE Expert Lite software), 10 s (11.91 mm) and 8 s (9.53 mm) were tested. Best analyte resolution was obtained for the 15 s plug. Comparable plugs can also be produced by applying 2 psi for 7.5 s, 3 psi for 5 s and 4 psi for 4 s (19.06 mm). The last combination was chosen for the assay as most repeatable results were obtained under these conditions. Electroinjection was investigated with application of 7 kV for time intervals between 5 and 30 s. With a 10 s injection the peaks were twice as high compared to application of power for 5 s. With larger injection times (20 and 30 s) the peak heights of the slower migrating analytes decreased whereas peak heights of the faster migrating analytes increased (20 s) and did not further change (30 s). Thus, an injection time of 10 s with 7 kV was chosen for the final method. Finally, injections from liquid/liquid extracts prepared with a mixture of dichloromethane and ethylacetate (75:25 %, *v/v;* [9,12,17,22,26,27]) or dichloromethane alone [26] were compared. Although best analyte recovery was obtained with the solvent mixture, extraction with dichloromethane provided better peak shapes with electrokinetic sample injection [26]. Using hexane instead of dichloromethane did not provide any better data.

6.4.4 Assay characterization

Repeatability of detection times was assessed with a mixture of the urine fractions I to IV. Interday data (n=7) show RSD values less than 4 % (Table 1). For the same samples the corrected areas were evaluated as well (RSD =14-30 % (Table 1)). Due to lack of standards, calibration could only be performed for RR- and SS-6HNK, the enantiomers of norketamine and the enantiomers of DHNK. The search for an internal standard proved to be difficult. Most of the candidates had too long migration times. Imidazole passes the detector about

6 min earlier than the first hydroxylated norketamine stereoisomer and can be considered as a possible internal standard. The peak of 2,6-xylidine was found to be closer to the HNK peaks. It is, however, a metabolite of lidocaine which is often used as comedication of ketamine.

Samples containing standards of RR- and SS-6HNK and imidazole as internal standard (n=4) were prepared at two different concentration level (12.5 and 25 ng/mL), extracted with dichloromethane and analyzed. The RSD values for the ratio of the corrected areas of analytes and internal standard varied between 5 and 11 %. For RR- and SS-6HNK, the limits of detection and quantification were 5 and 10 ng/mL, respectively.

Table 1. Intraday data (n=7) obtained with a mixture containing the urine fractions I-IV

HNK stereoisomers	Migration time		Corrected peak areas [a)]	
	Mean (min)	RSD (%)	Mean (µAU)	RSD (%)
R-I	11.15	2.40	244	29.61
S-I	11.93	2.34	184	19.23
R-II	11.75	2.53	167	22.75
S-II	12.43	3.72	2268	19.93
R-III	13.51	3.03	817	16.55
S-III	15.45	3.00	234	14.20
R-IV	12.21	3.02	1485	20.90
S-IV	13.80	3.10	643	29.20

a) Peak areas divided by detection time.

6.4.5 Analysis of in vitro and in vivo samples

With the newly developed assay it is now possible to resolve most stereoisomers of hydroxylated norketamine metabolites as cations and to detect them with short analysis times. Electropherograms obtained with extracts of incubations of racemic ketamine and detomidine with ELM are presented in Fig. 4. The samples were analyzed with the microassay (Fig. 4A) and with the new assay for hydroxylated norketamine metabolites (Fig. 4B). Data for incubation of ketamine in the presence of detomidine at time intervals of 0, 30, 120 and 300 min are depicted in panels A and B of Fig. 4. Comparison of the obtained data reveals that the latter assay provides much improved data for the stereoisomers of HNK. With that method metabolites I and IV are now resolved (see peaks labeled 1, 3, 4, and 7 in Fig. 4B in comparison to 4A). The same is true for peaks 2 and 9 (compare with data of Fig. 2). The data nicely show that a significant amount of R-IV metabolite is formed in presence of ELM. Thus, data obtained with the microassay (Fig. 4A) overestimate the formation of SS-6HNK (interference is much larger than 10 %; corrected peak areas of R-IV and SS-6HNK in the 300 min data of Fig. 4B are 964 and 1996 μAU, respectively).

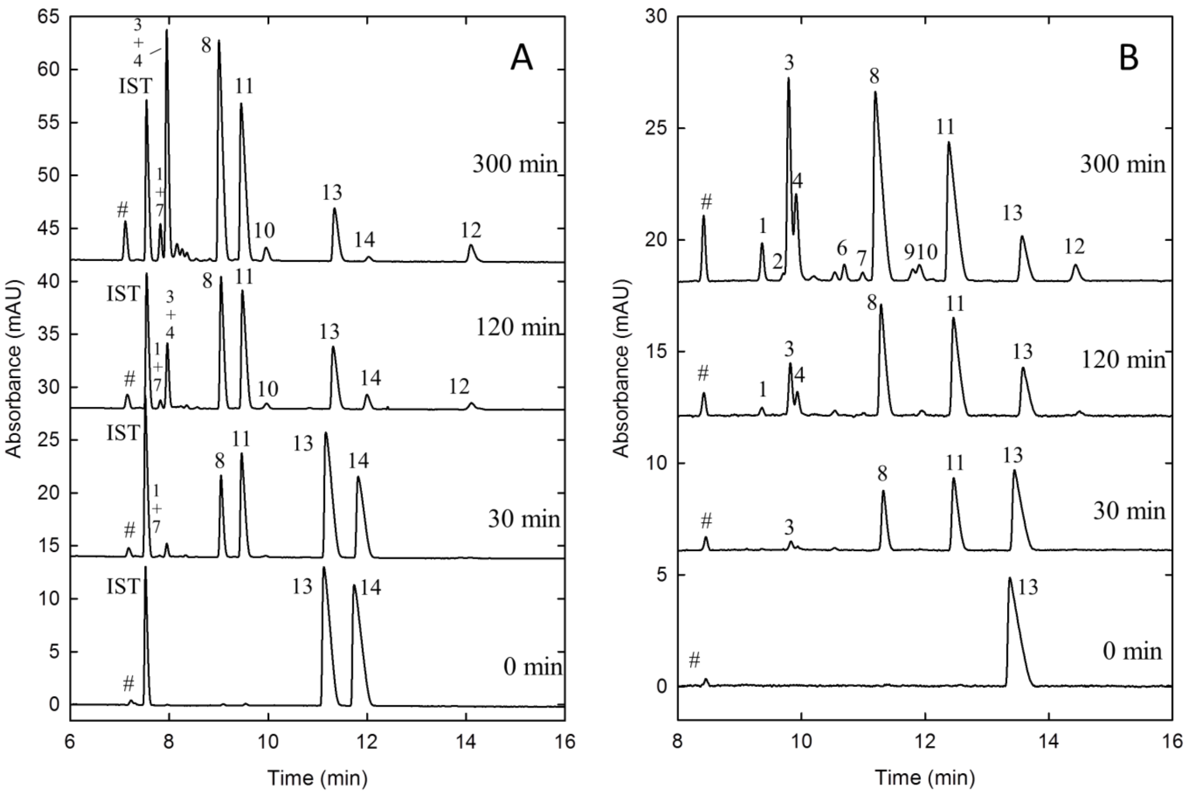

Figure 4. Electropherograms of incubation samples. 60 μM/enantiomer ketamine were incubated with 0.16 μM detomidine and ELM for 0, 30, 120 and 300 min. The samples were analyzed with (A) the microassay and (B) the HNK-method. CE conditions were as described in Section 2.5. Key: 1: RR-6HNK, 2: R-II, 3: SS-6HNK, 4: R-IV, 5: S-II, 6: R-III, 7: S-IV, 8: R-NK, 9: S-III, 10: S-DHNK, 11: S-NK, 12: R-DHNK, 13: R-ketamine, 14: S-ketamine, IST: internal standard d-(+)-norephedrin. An unknown peak is marked with #. Data is presented with a y-scale shift of 14 and 6 mAU, respectively.

For RR-6HNK, the situation is similar (corrected peak areas of 108 and 348 µAU for S-IV and RR-6HNK, respectively). The data obtained with the new assay further reveal that metabolites I and IV are formed stereoselectively. This is in agreement with previous observations using a different assay format [9,22].

Furthermore, metabolites II and III could be detected as well (peaks 2, 6 and 9 representing R-II, R-III and S-III, respectively, in Fig. 4B). The stereoisomer S-II was not detected in these in vitro preparations with ELM. In addition to the hydroxylated norketamine metabolites, the newly developed assay provides also peaks for norketamine (peaks 8 and 11 in Fig. 4B), DHNK (peaks 10 and 12) and R-ketamine (peak 13). S-ketamine migrates much more slowly and was not detected in the analyzed time interval (Fig. 4B). This approach is thus not suitable for the analysis of the ketamine enantiomers. For that purpose the previously published microassay should be used (Fig. 4A). The migration times in Fig. 4B are shorter than those observed in Fig. 2B und 3. Different sample matrices and undefined aging processes of the cyclodextrin preparations used are believed to be responsible for that change. Furthermore, the results of Fig. 4 indicate that some of the HNK peaks appear earlier than those of DHNK. This confirms the pathway presented in Fig. 1 in which DHNK is formed from HNK and not directly from norketamine.

The electropherograms presented in Fig. 5 show the differences in the metabolism between dogs and horses. The levels of metabolite IV are much higher in a sample of a pony that received 2.2 mg/kg racemic ketamine under isoflurane anesthesia (Fig. 5A) than of a dog that received 4 mg/kg racemic ketamine under sevoflurane (Fig. 5B). The samples were collected 64 and 60 min, respectively, after ketamine injection. In both species the 6HNK stereoisomers (peaks 1 and 3 in Fig. 5) are the prevalent hydroxylated norketamine metabolites. They are formed stereoselectively. SS-6HNK (peak 3) is dominant in the pony whereas RR-6HNK (peak 1) in the dog. Furthermore, these data confirm that the newly developed assay is required for equine samples. As discussed above for the in vitro samples, compounds 3 and 4 have lower impact on the results as was assumed in [27]. Formation of HNK stereoisomers is species dependent. This is in agreement with the data of Schmitz et al. [22].

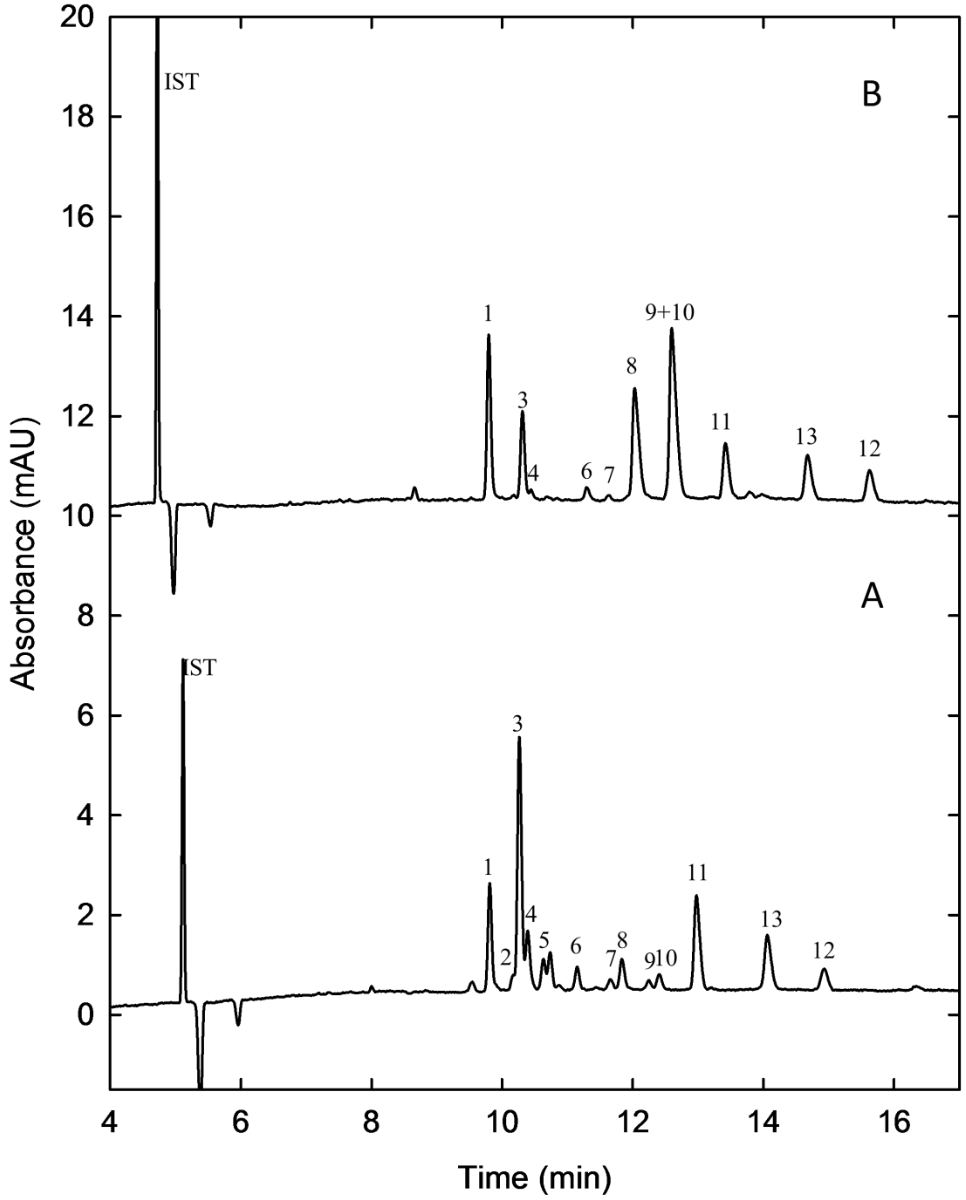

Figure 5. Electropherograms of in vivo samples of (A) a pony that received 2.2 mg/kg racemic ketamine under isoflurane anesthesia and of (B) a dog that was treated with 4 mg/kg racemic ketamine under sevoflurane anesthesia. The samples were taken 64 min and 60 min, respectively, after ketamine injection, were prepared as described in Section 2.4 and were analyzed with the HNK assay under the conditions of section 2.5. Key: 1: RR-6HNK, 2: R-II, 3: SS-6HNK, 4: R-IV, 5: S-II, 6: R-III, 7: S-IV, 8: R-NK, 9: S-III, 10: S-DHNK, 11: S-NK, 12: R-DHNK, 13: R-ketamine. IST: internal standard imidazole. Data is presented with a y-scale shift of 10 mAU.

6.5 Concluding remarks

Ketamine is mainly metabolized to norketamine, various hydroxylated norketamine metabolites and DHNK. The data presented in this paper demonstrate that the newly developed assay is a useful tool for analyzing the stereoisomers of these metabolites in biosamples. The main focus is on the stereoselective separation of four hydroxylated norketamine metabolites that were extracted from equine urine and found in equine, canine and human samples. Hydroxylated norketamine metabolites are believed to play an important option in the therapy of depressive disorders and even central nervous diseases [16]. A mixture of sulfated β-cyclodextrin and highly sulfated γ-cyclodextrin was found to be suitable as chiral selector to completely resolve most of the stereoisomers of the four hydroxylated norketamine metabolites. The assay is based upon electroinjection across a plug of diluted buffer without the chiral selector. Proper adjustment of assay parameters, including plug concentration, plug length and analyte injection conditions, provided the conditions for a sensitive and repeatable assay. The analysis of in vitro and in vivo samples showed that it is important to separate the hydroxylated norketamine metabolites to obtain reliable results for RR- and SS-6HNK concentrations. The identification and quantification of HNK peaks other than those of SS-6HNK and RR-6HNK will be possible when analytical standards become available. The assay will then provide further information about the metabolic pathways of ketamine and the participating enzymes.

Acknowledgements

The authors are grateful to Dr. Irving Wainer for receiving the standards of (2S,6S)-hydroxynorketamine, (2R,6R)-hydroxynorketamine, (2S,6R)-6-hydroxynorketamine and (2R,6S)-6-hydroxynorketamine. This work was supported by the Swiss National Science Foundation.

Conflicts of interest

The authors have declared no conflict of interest.

6.6 References

[1] G. Mion, T. Villevieille, Ketamine Pharmacology: An Update (Pharmacodynamics and Molecular Aspects, Recent Findings), CNS Neurosci. Ther. 19 (2013) 370–380.

[2] J. Persson, Ketamine in Pain Management, CNS Neurosci. Ther. 19 (2013) 396–402.

[3] E.D. Kharasch, R. Labroo, Metabolism of ketamine stereoisomers by human liver microsomes, Anesthesiology 77 (1992) 1201–1207.

[4] R.K. Paul, N.S. Singh, M. Khadeer, R. Moaddel, M. Sanghvi, C.E. Green, K. O'Loughlin, M.C. Torjman, M. Bernier, I.W. Wainer, (R,S)-Ketamine metabolites (R,S)-norketamine and (2S,6S)-hydroxynorketamine increase the mammalian target of rapamycin function, Anesthesiology 121 (2014) 149–159.

[5] P. Zanos, R. Moaddel, P.J. Morris, P. Georgiou, J. Fischell, G.I. Elmer, M. Alkondon, P. Yuan, H.J. Pribut, N.S. Singh, K. S. Dossou, Y. Fang, X.-P. Huang, C.L. Mayo, I.W. Wainer, E.X. Albuquerque, S.M. Thompson, C.J. Thomas, C.A. Zarate, T.D. Gould, NMDAR inhibition-independent antidepressant actions of ketamine metabolites, Nature 533 (2016) 481–486.

[6] R. Moaddel, S. L. V. Venkata, M.J. Tanga, J.E. Bupp, C.E. Green, L. Iyer, A. Furimsky, M.E. Goldberg, M.C. Torjman, I.W. Wainer, A parallel chiral-achiral liquid chromatographic method for the determination of the stereoisomers of ketamine and ketamine metabolites in the plasma and urine of patients with complex regional pain syndrome, Talanta 82 (2010) 1892–1904.

[7] X. Zhao, S.L.V. Venkata, R. Moaddel, D.A. Luckenbaugh, N.E. Brutsche, L. Ibrahim, C.A. Zarate, D.E. Mager, I.W. Wainer, Simultaneous population pharmacokinetic modelling of ketamine and three major metabolites in patients with treatment-resistant bipolar depression, Br. J. Clin. Pharmacol. 74 (2012) 304–314.

[8] C.A. Zarate, N. Brutsche, G. Laje, D.A. Luckenbaugh, S.L.V. Venkata, A. Ramamoorthy, R. Moaddel, I.W. Wainer, Relationship of ketamine's plasma metabolites with response, diagnosis, and side effects in major depression, Biol. Psychiatry 72 (2012) 331–338.

[9] A. Schmitz, R. Theurillat, P.-G. Lassahn, M. Mevissen, W. Thormann, CE provides evidence of the stereoselective hydroxylation of norketamine in equines, Electrophoresis 30 (2009) 2912–2921.

[10] Z. Desta, R. Moaddel, E.T. Ogburn, C. Xu, A. Ramamoorthy, S. L. V. Venkata, M. Sanghvi, M.E. Goldberg, M.C. Torjman, I.W. Wainer, Stereoselective and regiospecific hydroxylation of ketamine and norketamine, Xenobiotica 42 (2012) 1076–1087.

[11] Y. Hijazi, C. Bodonian, M. Bolon, F. Salord, R. Boulieu, Pharmacokinetics and haemodynamics of ketamine in intensive care patients with brain or spinal cord injury, Br. J. Anaesth. 90 (2003) 155–160.

[12] S. Portmann, H.Y. Kwan, R. Theurillat, A. Schmitz, M. Mevissen, W. Thormann, Enantioselective capillary electrophoresis for identification and characterization of human cytochrome P450 enzymes which metabolize ketamine and norketamine in vitro, J. Chromatogr. A 1217 (2010) 7942–7948.

[13] Y. Yanagihara, S. Kariya, M. Ohtani, K. Uchino, T. Aoyama, Y. Yamamura, T. Iga, Involvement of CYP2B6 in n-demethylation of ketamine in human liver microsomes, Drug Metab. Dispos. 29 (2001) 887–890.

[14] R. Moaddel, G. Abdrakhmanova, J. Kozak, K. Jozwiak, L. Toll, L. Jimenez, A. Rosenberg, T. Tran, Y. Xiao, C.A. Zarate, I.W. Wainer, Sub-anesthetic concentrations of (R,S)-ketamine metabolites inhibit acetylcholine-evoked currents in α7 nicotinic acetylcholine receptors, Eur. J. Pharmacol. 698 (2013) 228–234.

[15] N. S. Singh, C. A. Zarate, R. Moaddel, M. Bernier, I. W. Wainer, What is hydroxynorketamine and what can it bring to neurotherapeutics?, Expert Rev. Neurother. 14 (2014) 1239–1242.

[16] N. S. Singh, E. Rutkowska, A. Plazinska, M. Khadeer, R. Moaddel, K. Jozwiak, M. Bernier, I. W. Wainer, Ketamine metabolites enantioselectively decrease intracellular d-serine concentrations in PC-12 cells, PLos One 11 (2016) e0149499.

[17] F.A. Sandbaumhüter, R. Theurillat, W. Thormann, Effects of medetomidine and its active enantiomer dexmedetomidine on N-demethylation of ketamine in canines determined in vitro using enantioselective capillary electrophoresis, Electrophoresis 36 (2015) 2703–2712.

[18] H. Y. Kwan, W. Thormann, Enantioselective capillary electrophoresis for the assessment of CYP3A4-mediated ketamine demethylation and inhibition in vitro, Electrophoresis 32 (2011) 2738–2745.

[19] R. Theurillat, M. Knobloch, A. Schmitz, P. G. Lassahn, M. Mevissen, W. Thormann, Enantioselective analysis of ketamine and its metabolites in equine plasma and urine by CE with multiple isomer sulfated beta-CD, Electrophoresis 25 (2007), 2748–2757.

[20] N. Porpiglia, G. Musile, F. Bortolotti, E. F. De Palo, F. Tagliaro, Chiral separation and determination of ketamine and norketamine in hair by capillary electrophoresis. Forensic Sci. Int. 266 (2016) 304–310.

[21] A. Rousseau, F. Gillotin, P. Chiap, E. Bodoki, J. Crommen, M. Fillet, A. Servais, Generic systems for the enantioseparation of basic drugs in NACE using single-isomer anionic CDs, J. Pharm. Biomed. Anal. 54 (2011) 154–159

[22] A. Schmitz, W. Thormann, L. Moessner, R. Theurillat, K. Helmja, M. Mevissen, Enantioselective CE analysis of hepatic ketamine metabolism in different species in vitro, Electrophoresis 31 (2010) 1506–1516.

[23] A. Schmitz, C. J. Portier, W. Thormann, R. Theurillat, M. Mevissen, Stereoselective biotransformation of ketamine in equine liver and lung microsomes, J. Vet. Pharmacol. Ther. 31 (2008), 446–455.

[24] M.P. Larenza, M.F. Landoni, O.L. Levionnois, M. Knobloch, P.W. Kronen, R. Theurillat, U. Schatzmann, W. Thormann, Stereoselective pharmacokinetics of ketamine and norketamine after racemic ketamine or S-ketamine administration during isoflurane anaesthesia in Shetland ponies, Br. J. Anaesth. 98 (2007) 204–212.

[25] M.P. Larenza, M. Knobloch, M.F. Landoni, O.L. Levionnois, P.W. Kronen, R. Theurillat, U. Schatzmann, W. Thormann, Stereoselective pharmacokinetics of ketamine and norketamine after racemic ketamine or S-ketamine administration in Shetland ponies sedated with xylazine, Vet. J. 177 (2008) 432–435.

[26] R. Theurillat, F.A. Sandbaumhüter, R. Bettschart-Wolfensberger, W. Thormann, Microassay for ketamine and metabolites in plasma and serum based on enantioselective capillary electrophoresis with highly sulfated γ-cyclodextrin and electrokinetic analyte injection, Electrophoresis 37 (2016) 1129–1138.

[27]F. A. Sandbaumhüter, R. Theurillat, R. N. Bektas, A. P. Kutter, R. Bettschart-Wolfensberger, W. Thormann, Pharmacokinetics of ketamine and three metabolites in Beagle dogs under sevoflurane vs. medetomidine comedication assessed by enantioselective capillary electrophoresis, J. Chromatogr. A 1467 (2016) 436–444.

[28] H. R. Rabanes, J. P. Quirino, Sweeping of alprenolol enantiomers with an organic solvent and sulfated β-cyclodextrin in capillary electrophoresis, Electrophoresis 34 (2013) 1319–132.

7. Conclusions

The α_2-receptor agonists medetomidine, its active enantiomer dexmedetomidine, detomidine, xylazine and romifidine have an effect on the ketamine metabolism. In vitro and in vivo they influence the formation and/or elimination of ketamine and its metabolites norketamine, HNK and DHNK. In vitro studies with canine and human liver mircrosomes and the single human CYP3A4 and the canine ortholog CYP3A12 showed that medetomidine is a strong inhibitor of the N-demethylation of ketamine to norketamine. The racemic medetomidine inhibits the norketamine formation more than the single S-enantiomer dexmedetomidine. Differences between the species and liver microsomes and single enzymes were found. The calculated inhibition parameters assessed with the single ketamine enantiomers as substrates revealed that the inhibition of the R-norketamine formation is stronger (Chapter 2).

Reduced norketamine levels under medetomidine sedation in comparison to sevoflurane application were determined in in vivo experiments with Beagle dogs. Concentrations of ketamine, norketamine, 6HNK and DHNK were measured in plasma samples which were collected between 0 and 900 min after ketamine injection. Pharmacokinetics were described by using compartmental analysis with two compartment models for ketamine and norketamine and single compartment models for 6HNK and DHNK. The calculated pharmacokinetic parameters show that medetomidine has an impact on the pharmacokinetics of all analyzed compounds. The half-life of ketamine was decreased as well as AUC, t_{max} and c_{max} of norketamine. Smaller AUC values were also found for 6HNK and S-DHNK. The elimination of the metabolites was faster under medetomidine comedication. Stereoselectivities were detected for 6HNK (RR-6HNK > SS-6HNK) and DHNK (R-DHNK < S-DHNK) (Chapter 4).

Medetomidine and also detomidine as imidazole derivates have good structural requirements for binding to the heme iron of CYP enzymes. This leads to an inactivation of the enzymes and was assessed with incubations of ketamine with ELM in presence and absence of α_2-receptor agonists. Detomidine is less hydrophobic and has higher inhibition parameters in comparison to medetomidine whereas the inhibition parameters for xylazine and romifidine indicate almost no inhibition potential. For extended incubation time intervals xylazine and romifidine show an impact on the formation of the ketamine metabolites as well (Chapter 5).

Further investigations under consideration of the various cardiovascular effects will have to be undertaken in vivo in order to elucidate the impact of the comedication on the plasma levels of ketamine and its metabolites.

Enantioselective CE with cyclodextrin as chiral selector was found to be a good technique to determine ppb to ppm amounts of ketamine, norketamine, HNK and DHNK in biosamples. For analyzing the N-demethylation of ketamine to norketamine an existing assay was optimized and validated. Highly sulfated γ-cyclodextrin could be employed as chiral selector and lamotrigine as internal standard. The robust assay (interday RSD < 7 %) requires less reagents and less preparation time (Chapter 2). Due to the fact that additional metabolites should be considered, a microassay for the stereoisomers of ketamine, norketamine, 6HNK and DHNK was developed. The consumption of sample and reagents could be further reduced and the assay was determined to be repeatable (interday RSD < 9 %). Furthermore, electrokinetic sample injection across a buffer plug provided increased sensitivity. The limit of quantification was decreased by a factor of 12 (Chapter 3).

For a detailed assessment of hydroxylated norketamine metabolites another method had to be found. Chiral separation of four hydroxylated norketamine metabolites, norketamine and DHNK was obtained by using a mixture of sulfated β-cyclodextrin and highly sulfated γ-cyclodextrin as chiral selector. This method is also based on electrokinetic sample injection. After optimization of a range of parameters, including the composition of the BGE, the composition and length of the buffer plug, the injection time and voltage and sample preparation, this method could be applied for studying the differences in the formation of hydroxylated norketamine metabolites between dogs and horses (Chapter 6). At the moment only analytical standards for RR- and SS-6HNK are available. The other hydroxylated norketamine metabolites will have to be identified in the future.

The pathways in the ketamine metabolism and the involved enzymes must be further elucidated also with regard to the discussion about hydroxylated norketamine metabolites and their role in human therapy. The presented methods can play a role in the determination of ketamine and its metabolites in in vitro experiments and in blood, urine or tissue samples of clinical trials. Investigations of the effects of the different α_2-receptor agonists on the ketamine metabolism in vitro were only the first step to improve safety in veterinary anesthesia. In vivo studies must follow. Such investigations are also important for human medicine in which the combination of dexmedetomidine and ketamine is applied as well.

8. References

[1] G. Mion, T. Villevieille, Ketamine Pharmacology: An Update (Pharmacodynamics and Molecular Aspects, Recent Findings), CNS Neurosci. Ther. 19 (2013) 370–380.

[2] J. Persson, Ketamine in Pain Management, CNS Neurosci. Ther. 19 (2013) 396–402.

[3] E.D. Kharasch, R. Labroo, Metabolism of ketamine stereoisomers by human liver microsomes, Anesthesiology 77 (1992) 1201–1207.

[4] R.K. Paul, N.S. Singh, M. Khadeer, R. Moaddel, M. Sanghvi, C.E. Green, K. O'Loughlin, M.C. Torjman, M. Bernier, I.W. Wainer, (R,S)-Ketamine metabolites (R,S)-norketamine and (2S,6S)-hydroxynorketamine increase the mammalian target of rapamycin function, Anesthesiology 121 (2014) 149–159.

[5] L. Degenhardt, J. Copeland, P. Dillon, Recent Trends in the Use of "Club drugs": An Australian Review, Subst. Use Misuse 40 (2005) 1241–1256.

[6] J.C. Duque, N. Oleskovicz, E.C.B.P. Guirro, C.A.A. Valadão, V.E. Soares, Relative potency of ketamine and S(+)-ketamine in dogs, J. Vet. Pharmacol. Ther. 31 (2008) 344–348.

[7] Y. Hijazi, R. Boulieu, Contribution of CYP3A4, CYP2B6, and CYP2C9 isoforms to N-demethylation of ketamine in human liver microsomes, Drug Metab. Dispos. 30 (2002) 853–858.

[8] X. Zhao, S.L.V. Venkata, R. Moaddel, D.A. Luckenbaugh, N.E. Brutsche, L. Ibrahim, C.A. Zarate, D.E. Mager, I.W. Wainer, Simultaneous population pharmacokinetic modelling of ketamine and three major metabolites in patients with treatment-resistant bipolar depression, Br. J. Clin. Pharmacol. 74 (2012) 304–314.

[9] P. Zanos, R. Moaddel, P.J. Morris, P. Georgiou, J. Fischell, G.I. Elmer, M. Alkondon, P. Yuan, H.J. Pribut, N.S. Singh, K. S. Dossou, Y. Fang, X.-P. Huang, C.L. Mayo, I.W. Wainer, E.X. Albuquerque, S.M. Thompson, C.J. Thomas, C.A. Zarate, T.D. Gould, NMDAR inhibition-independent antidepressant actions of ketamine metabolites, Nature 533 (2016) 481–486.

[10] R. Moaddel, G. Abdrakhmanova, J. Kozak, K. Jozwiak, L. Toll, L. Jimenez, A. Rosenberg, T. Tran, Y. Xiao, C.A. Zarate, I.W. Wainer, Sub-anesthetic concentrations of (R,S)-ketamine metabolites inhibit acetylcholine-evoked currents in α7 nicotinic acetylcholine receptors, Eur. J. Pharmacol. 698 (2013) 228–234.

[11] A. Schmitz, R. Theurillat, P.-G. Lassahn, M. Mevissen, W. Thormann, CE provides evidence of the stereoselective hydroxylation of norketamine in equines, Electrophoresis 30 (2009) 2912–2921.

[12] M. Knobloch, C. J. Portier, O. L. Levionnois, R. Theurillat, W. Thormann, C. Spadavecchia, M. Mevissen, Antinociceptive effects, metabolism and disposition of ketamine in ponies under target-controlled drug infusion, Toxicol. Applied Pharmacol. 216 (2006), 373–386.

[13] M.P. Larenza, M.F. Landoni, O.L. Levionnois, M. Knobloch, P.W. Kronen, R. Theurillat, U. Schatzmann, W. Thormann, Stereoselective pharmacokinetics of ketamine and norketamine after racemic ketamine or S-ketamine administration during isoflurane anaesthesia in Shetland ponies, Br. J. Anaesth. 98 (2007) 204–212.

[14] M.P. Larenza, M. Knobloch, M.F. Landoni, O.L. Levionnois, P.W. Kronen, R. Theurillat, U. Schatzmann, W. Thormann, Stereoselective pharmacokinetics of ketamine and norketamine after racemic ketamine or S-ketamine administration in Shetland ponies sedated with xylazine, Vet. J. 177 (2008) 432–435.

[15] C. Peterbauer, M. P. Larenza, M. Knobloch, R. Theurillat, W. Thormann, M. Mevissen, C. Spadavecchia, Effects of a low dose infusion of racemic and S-ketamine on the nociceptive withdrawal reflex in standing ponies, Vet. Anaesth. Analg. 35 (2008) 414–423.

[16] A. Schmitz, C. J. Portier, W. Thormann, R. Theurillat, M. Mevissen, Stereoselective biotransformation of ketamine in equine liver and lung microsomes, J. Vet. Pharmacol. Ther. 31 (2008), 446–455.

[17] F. A. Sandbaumhüter, R. Theurillat, R. N. Bektas, A. P. Kutter, R. Bettschart-Wolfensberger, W. Thormann, Pharmacokinetics of ketamine and three metabolites in Beagle dogs under sevoflurane vs. medetomidine comedication assessed by enantioselective capillary electrophoresis, J. Chromatogr. A 1467 (2016) 436–444.

[18] A. Schmitz, W. Thormann, L. Moessner, R. Theurillat, K. Helmja, M. Mevissen, Enantioselective CE analysis of hepatic ketamine metabolism in different species in vitro, Electrophoresis 31 (2010) 1506–1516.

[19] S. Portmann, H.Y. Kwan, R. Theurillat, A. Schmitz, M. Mevissen, W. Thormann, Enantioselective capillary electrophoresis for identification and characterization of human cytochrome P450 enzymes which metabolize ketamine and norketamine in vitro, J. Chromatogr. A 1217 (2010) 7942–7948.

[20] F.A. Sandbaumhüter, R. Theurillat, W. Thormann, Effects of medetomidine and its active enantiomer dexmedetomidine on N-demethylation of ketamine in canines determined in vitro using enantioselective capillary electrophoresis, Electrophoresis 36 (2015) 2703–2712.

[21] Y. Yanagihara, S. Kariya, M. Ohtani, K. Uchino, T. Aoyama, Y. Yamamura, T. Iga, Involvement of CYP2B6 in n-demethylation of ketamine in human liver microsomes, Drug Metab. Dispos. 29 (2001) 887–890.

[22] P. Adamowicz, M. Kala, Urinary excretion rates of ketamine and norketamine following therapeutic ketamine administration: method and detection window considerations, Journal Anal. Toxicol. 29 (2005) 376–382.

[23] P. Stenberg, J. Idvall, Does ketamine metabolite II exist in vivo?, Br. J. Anes. 53 (1981) 778.

[24] H. R. Lin, A. C. Lua, Detection of acid-labile conjugates of ketamine and its metabolites in urine samples collected from pub participants, J. Anal Toxicol. 28 (2004) 181–186.

[25] S. A. Savchuk, E. S. Brodskii, B. A. Rudenko, A. A. Formanosvkii, I. V. Mikhura, N. A. Davydova, Determination of biotransformation products of the anesthetic ketamine by chromatography mass-spectrometry, J. Anal. Chem. 52 (1997), 1175–1186.

[26] S. A. Savchuk, B. A. Rudenko, E. S. Brodskii, A. A. Formanovskii, V. V. Erofeev, E. V. Babanova, V. V. Chistyakov, M. L. Rabinovich, O. A. Dolina, Application of gas chromatography with selective detection and gas chromatography-mass spectrometry to identifying ketamine metabolites and to examining the conjugation of ketamine and its metabolites in human and rat organisms, J. Anal. Chem. 53 (1998), 583–589.

[27] S. C. Turfus, M. C. Parkin, D. A. Cowan, J. M. Halket, N. W. Smith, R. A. Braithwaite, S. P. Elliot, G. B. Steventon, A. T. Kicman, Use of human microsomes and deuterated substrates: an alternative approach for the identification of novel metabolites of ketamine by mass spectrometry, Drug Metab. Dispos. 37 (2009) 1769 –1778.

[28] X. Li, P. Martinez-Lozano Sinues, R. Dallmann, L. Bregy, M. Hollmén; S. Proulx, S. A. Brown, M. Detmar, M. Kohler, R. Zenobi, Drug Pharmacokinetics Determined by Real-Time Analysis of Mouse Breath, Angew. Chem. Int. Ed. Engl. 54 (2015) 7815–7818.

[29] J.A. Giovannitti, S.M. Thoms, J.J. Crawford, Alpha-2 adrenergic receptor agonists: a review of current clinical applications, Anesth. Prog. 62 (2015) 31–39.

[30] A. Doozandeh, S. Yazdani, Neuroprotection in Glaucoma, J. Ophthalmic Vis. Res. 11 (2016) 209–20.

[31] E.D. Kharasch, S. Herrmann, R. Labroo, Ketamine as a probe for medetomidine stereoisomer inhibition of human liver microsomal drug metabolism, Anesthesiology 77 (1992) 1208–1214.

[32] M.-C. Duhamel, É. Troncy, F. Beaudry, Metabolic stability and determination of cytochrome P450 isoenzymes' contribution to the metabolism of medetomidine in dog liver microsomes, Biomed. Chromatogr. 24 (2010) 868–877.

[33] P. Ravipati, P.N. Reddy, C. Kumar, P. Pradeep, R. Pathapati, S.T. Rajashekar, Dexmedetomidine decreases the requirement of ketamine and propofol during burns debridement and dressings, Indian J. Anaesth. 58 (2014) 138–142.

[34] L. K. Cullen, Medetomidine sedation in dogs and cats: a review of its pharmacology, antagonism and dose, Br. Vet J. 152 (1996) 519–535.

[35] A. Ülgey, R. Aksu, C. Bicer, A. Akin, R. Altuntaş, A. Esmaoğlu, A. Baykan, A. Boyaci, Is the addition of dexmedetomidine to a ketamine-propofol combination in pediatric cardiac catheterization sedation useful?, Pediatr. Cardiol. 33 (2012) 770–774.

[36] K.N. Grimsrud, S. Ait-Oudhia, B.P. Durbin-Johnson, D.M. Rocke, K.R. Mama, M.L. Rezende, S.D. Stanley, W.J. Jusko, Pharmacokinetic and pharmacodynamic analysis comparing diverse effects of detomidine, medetomidine, and dexmedetomidine in the horse: a population analysis, J. Vet. Pharmacol. Ther. 38 (2015) 24–34.

[37] W.M. Burnside, P.A. Flecknell, A.I. Cameron, A.A. Thomas, A comparison of medetomidine and its active enantiomer dexmedetomidine when administered with ketamine in mice, BMC Vet. Res. 9 (2013) 48.

[38] E. Kuusela, M. Raekallio, M. Anttila, I. Falck, S. Mölsä, O. Vainio, Clinical effects and pharmacokinetics of medetomidine and its enantiomers in dogs, J. Vet. Pharmacol. Ther. 23 (2000) 15–20.

[39] A. Kamel, S. Harriman, Inhibition of cytochrome P450 enzymes and biochemical aspects of mechanism-based inactivation (MBI), Drug Discov. Today Technol. 10 (2013) e177–e189.

[40] S. Nannarone, R. Gialletti, I. Veschini, A. Bufalari, F. Moriconi, The Use of Alpha-2 Agonists in the Equine Practice: Comparison between Three Molecules, Vet. Res. Commun. 31 (2007) 309–312.

[41] C. L. Kerr, W. N. McDonell, S. S. Young, A comparison of romifidine and xylazine when used with diazepam/ketamine for short duration anesthesia in the horse, Can. Vet. J. 37 (1996) 601–609.

[42] H. Jaugstetter, R. Jacobi, R. Pellmann, Vergleich der Narkoseprämedikation mit Romifidin und Xylazin in Bezug auf das Aufstehverhalten von Pferden nach Allgemeinanästhesie, Der Praktische Tierarzt 9 (2002) 786–791.

[43] K. W. Clarke, P. M. Taylor, S. B. Watkins, Detomidine/ Ketamine anesthesia in the horse, Acta Vet. Scand. Suppl. 82 (1986) 167–179.

[44] K. D. Altira (Ed.), Capillary Electrophoresis Guidebook: Principles, Operation, and Applications, Humana Press, Totowa, New Jersey, 1996.

[45] Y. Xu, Tutorial: Capillary Electrophoresis, in M. Schimpf (Ed.), The Chemical Educator, Springer, New York, 1996.

[46] G. Rücker, M. Neugebauer, G. G. Willems, Instrumentelle pharmazeutische Analytik: Lehrbuch zu spektroskopischen, chromatographischen und thermischen Analysemethoden, Wissenschaftliche Verlagsgesellschaft, Stuttgart, 2007.

[47] J. W. Jorgenson, K. D. Lukacs, Free-Zone Electrophoresis in Glass Capillaries, Clin. Chem. 27 (1981) 1551–1553.

[48] R. Weinberger, Practical Capillary Electrophoresis, Academic Press, London, 1993.

[49] E. Francotte, W. Lindner (Eds.), Chirality in Drug Research, Wiley-VCH, Weinheim, 2006.

[50] G. Gübitz, M. G. Schmid (Eds.), Chiral Separations: Methods and Protocols, Humana Press, Totowa, New Jersey, 2004.

[51] G. K. E. Scriba (Ed.), Chiral Separations: Methods and Protocols, Springer, Luxemburg, 2013.

[52] A. Amini, Recent development in chiral capillary electrophoresis and applications of this technique to pharmaceutical and biomedical analysis, Electrophoresis, 22 (2001), 3107–3130.

[53] G. Gübitz, M. G. Schmid, Recent progress in chiral separation principles in capillary electrophoresis, Electrophoresis 21 (2000), 4112–4135.

[54] J. Caslavska, W. Thormann, Stereoselective determination of drugs and metabolites in body fluids, tissues and microsomal preparations by capillary electrophoresis (2000–2010), J. Chromatogr. A 1218 (2011) 588–601.

[55] Europäisches Arzneibuch, Ausgabe 8, EDQM, Straßburg, 2014.

[56] R. Theurillat, F.A. Sandbaumhüter, R. Bettschart-Wolfensberger, W. Thormann, Microassay for ketamine and metabolites in plasma and serum based on enantioselective capillary electrophoresis with highly sulfated γ-cyclodextrin and electrokinetic analyte injection, Electrophoresis 37 (2016) 1129–1138.

[57] R. Řemínek, Z. Glatz, W. Thormann, Optimized on-line enantioselective capillary electrophoretic method for kinetic and inhibition studies of drug metabolism mediated by cytochrome P450 enzymes, Electrophoresis 36 (2015) 1349–1357.

[58] T. Loftsson, Essential pharmacokinetics: A primer for pharmaceutical scientists, Academic Press (Elsevier), London, 2015.

[59] T. A. Ahmed (Ed.), Basic pharmacokinetic: concepts and some clinical applications, InTech, 2015.

[60] S. A. Peters, Physiologically-based pharmacokinetics (PBPK) modeling and simulations: principles, methods and applications in the pharmaceutical industry, John Wiley & Sons, Hoboken, New Jersey, 2012.

9. Publications

F.A. Sandbaumhüter, R. Theurillat, W. Thormann, Effects of medetomidine and its active enantiomer dexmedetomidine on N-demethylation of ketamine in canines determined in vitro using enantioselective capillary electrophoresis, Electrophoresis 36 (2015) 2703–2712.

R. Theurillat, F.A. Sandbaumhüter, R. Bettschart-Wolfensberger, W. Thormann, Microassay for ketamine and metabolites in plasma and serum based on enantioselective capillary electrophoresis with highly sulfated γ-cyclodextrin and electrokinetic analyte injection, Electrophoresis 37 (2016) 1129–1138.

F. A. Sandbaumhüter, R. Theurillat, R. N. Bektas, A. P. Kutter, R. Bettschart-Wolfensberger, W. Thormann, Pharmacokinetics of ketamine and three metabolites in Beagle dogs under sevoflurane vs. medetomidine comedication assessed by enantioselective capillary electrophoresis, J. Chromatogr. A 1467 (2016) 436–444.

M. Pelcová, R. Řemínek, F. A. Sandbaumhüter, R. A. Mosher, Z. Glatz, W. Thormann, Simulation and experimental study of enzyme and reactant mixing in capillary electrophoresis based on-line methods, J. Chromatogr. A 1471 (2016) 192–200.

F.A. Sandbaumhüter, R. Theurillat, W. Thormann, Separation of hydroxynorketamine stereoisomers using capillary electrophoresis with sulfated β-cyclodextrin and highly sulfated γ-cyclodextrin, Electrophoresis (2017) doi: 10.1002/elps.201700016.

F.A. Sandbaumhüter, R. Theurillat, R. Bettschart-Wolfensberger, W. Thormann, Effect of the α_2-receptor agonists medetomidine, detomidine, xylazine and romifidine on the ketamine metabolism in equines assessed with enantioselective capillary electrophoresis, Electrophoresis (2017) doi: 10.1002/elps.201700017.

10. Congress participations and presentations

7th Swiss Pharma Science Day, Swiss Society of Pharmaceutical Sciences (SSPhS)
20th August 2014 in Bern, Switzerland
"Effect of medetomidine on ketamine N-demethylation in canine liver microsomes analyzed by enantioselective capillary electrophoresis" *(Poster)*

Annual Research Meeting Pharmaceutical Science Basel 2015
13th February 2015 in Basel, Switzerland
"Effect of medetomidine on ketamine N-demethylation in vitro analyzed by enantioselective capillary electrophoresis" *(Poster)*

22nd International Symposium on Electro- and Liquid Phase-Separation techniques
8th Nordic Separation Science Symposium
30th August – 3rd September 2015 in Helsinki, Finland
"Effects of medetomidine on N-demethylation of ketamine determined in vitro using enantioselective capillary electrophoresis" *(Poster)*
"Microassay for ketamine and its metabolites in plasma based on enantioselective capillary electrophoresis with electrokinetic sample injection" *(Poster)*

CE-Forum 2015
5th – 6th October 2015 in Tübingen, Germany
"Effects of medetomidine on N-demethylation of ketamine determined in vitro using enantioselective capillary electrophoresis" *(Poster)*

Annual Research Meeting Pharmaceutical Science Basel 2016
10th February 2016 in Basel, Switzerland
"Pharmacokinetics of ketamine and three metabolites in beagle dogs under sevoflurane vs. medetomidine comedication" *(Poster)*

International PhD student and postdoc meeting, German Pharmaceutical Society (DPhG)

16th – 18th March 2016 in Aachen, Germany

"Pharmacokinetics of ketamine and three metabolites in beagle dogs under sevoflurane vs. medetomidine comedication" *(oral presentation)*

9th Swiss Pharma Science Day, Swiss Society of Pharmaceutical Sciences (SSPhS)

31st August 2016 in Bern, Switzerland

"Effect of different α_2-receptor agonists on the ketamine metabolism assessed with equine liver microsomes" *(Poster)*

Symposium Clinical Pharmacy Switzerland 2016

14th August 2016 in Basel, Switzerland

"Pharmacokinetics of ketamine and three metabolites in beagle dogs under sevoflurane vs. medetomidine comedication" *(Poster)*

CE-Forum 2016

4th – 5th October 2016 in Regensburg, Germany

"Effect of different α_2-receptor agonists on the ketamine metabolism assessed with equine liver microsomes" *(Poster)*

11. Acknowledgement

This thesis was performed in the Clinical Pharmacology Laboratory of the University of Bern under the supervision of Prof. Dr. Wolfgang Thormann.

Hereby, I want to thank all the people who contributed in any way to the completion of this thesis.

First of all, I would like to thank my advisor **Prof. Dr. Wolfgang Thormann** for giving me the opportunity to work on this interesting topic in his laboratory, for being always open to discussion and for teaching and guiding me throughout the thesis.

Prof. Dr. Dr. Stephan Krähenbühl from the Division of Clinical Pharmacology and Toxicology of the University of Basel I would like to thank for taking the responsibitlity as a faculty representive. I appreciate his support as well as our interesting and helpful discussions. I thank **Dr. Manuel Haschke** from the Division of Clinical Pharmacology and Toxicology of the University of Basel for taking the responsibility as a co-referee and **Prof. Dr. Alex Odermatt** from the Division of Molecular and Systems Toxicology of the University of Basel for his commitment to chair the exam of the dissertation.

Many thanks go to **Prof. Dr. Regula Bettschart-Wolfensberger** from the Vetsuisse faculty of the University of Zürich for the the good collaboration, for giving insights into the veterinary practice and for the motivating and inspiring discussions. All work with the dogs and horses were done by her and her team.

I also thank my collegues **Regula Theurillat** and **Jitka Caslavska** who were the whole three years by my side for the good atmosphere in the laboratory, a lot of valuable inputs and help in the laboratory and beyond. Furthermore, I would like to thank **Dr. Roman Řemínek** and **Dr. Christian Lanz** for their help especially at the beginning. For good discussions, fun and adventures in and outside the laboratory I thank **Nadia Porpiglia** and **Mirjam Kummer**.

My thanks go to a lot of people working and worked on floor F of the Maurice E. Müller building in Bern for the time we spent together in that building and on our trips through Switzerland.

Finally, I express my gratitude to my family for their encouragement. My **parents** support me always unconditionally. In discussions with my sister **Viktoria** problems were solved and new ideas were created.